SCIEPublish

Review

Recent Progress in Modification and Preparations of the Promising Biodegradable Plastics: Polylactide and Poly(butylene adipate-co-terephthalate)

Mei Meng [1], Shuanjin Wang [1], Min Xiao [1,*] and Yuezhong Meng [1,2,3,*]

[1] Research Center of Green Catalysts, College of Chemistry, Zhengzhou University, Zhengzhou 450001, China; mengmuyao@163.com (M.M.); wangshj@mail.sysu.edu.cn (S.W.)

[2] Institute of Chemistry, Henan Academy of Sciences, Zhengzhou 450000, China

[3] The Key Laboratory of Low-carbon Chemistry & Energy Conservation of Guangdong Province/State Key Laboratory of Optoelectronic Materials and Technologies, School of Materials Science and Engineering, Sun Yat-sen University, Guangzhou 510275, China

* Corresponding authors. E-mail: stsxm@mail.sysu.edu.cn (M.X.); mengyzh@mail.sysu.edu.cn (Y.M.)

Received: 15 December 2022; Accepted: 27 February 2023; Available online: 12 April 2023

ABSTRACT: The acquisition of high-performance biodegradable plastics is of great significance in addressing the problem of environmental pollution of plastics. Polylactide (PLA) and poly(butylene adipate-co-terephthalate) (PBAT) are the most promising biodegradable polymers and have excellent functional properties. However, low elongation at break and impact strength of PLA and low tensile modulus and flexural strength of PBAT hinder their application. A large number of studies focus on improving the performance of PLA and PBAT and broadening their applications. In terms of polymer modification, this paper summarized recent progresses in both chemical and physical modification methods for PLA and PBAT, respectively. The properties of PLA can be improved by co-polymerization, grafting, cross-linking and blending. The properties of PBAT can be improved mainly through blending with other degradable polymers, natural macromolecules and inorganic materials. This review can provide the reference and ideas for the modification of biomass-based biodegradable plastics like PLA and fossil-based biodegradable plastics like PBAT.

Keywords: Polylactide, PLA, Poly(butylene adipate-co-terephthalate), PBAT, Biodegradable, Modification, Biodegradable plastic

© 2023 by the authors; licensee SCIEPublish, SCISCAN co. Ltd. This article is an open access article distributed under the CC BY license (http://creativecommons.org/licenses/by/4.0/).

1. Introduction

Plastics have brought enormous ease to human life due to their unique functional properties at low-cost and good durability. One of the biggest challenges with plastics is that it becomes waste after a single use. Currently, the treatment methods of plastic waste mainly include: landfill, burning for energy recovery and recycle [1–3]. Plastic recycling is mainly implemented through primary recycling, mechanical/physical recycling and chemical recycling [3–5]. The accumulation of plastic waste may contaminate water and soil, and affect the global carbon cycle, ecological balance and human health. The impact of plastic waste includes the effects of landfilling: plastics degrading into microplastics leads to long-term changes in soil properties, and the effects of the plastics suspended in water through wastewater treatment plants or the release of textile fibers during laundry on the growth environment of bacteria and thus on the food chain before settling on the seafloor [6–8]. The types of microplastics can be pellet, microbead, fragment, fiber, film or foam [9]. The microplastics such as polyethylene (PE), polyamide (PA), polypropylene (PP) fragments, acrylic fabrics, polyester fabrics, polystyrene foam and phenolic foam are ingested frequently by marine, freshwater, and terrestrial wildlife, according to records of plastic ingestion by birds, fish, mammals, reptiles, and invertebrate [5,9–11]. Bioplastics have become a suitable substitute for traditional fossil-based plastics [12,13]. If bioplastics degrade at a very low rate, the environmental accumulation of plastic waste as microplastics still exists [14]. To make more rational use of plastics, various international legislatures have formulated laws and regulations to limit the use of plastics [15], such as the plastic limit order in China [16], Plastic Bags Prohibition Bill in Nigeria [17] and plastic bag ban policy in Chile [18]. During the United Nations Environment Assembly (UNEA-5) in March 2022, the representatives from 175 countries approved and signed a Resolution on

https://doi.org/10.35534/spe.2023.10006

Ending Plastic Pollution (Draft) to end plastic pollution and reach an internationally legally binding agreement covering the entire life cycle of plastic products by 2024 [19].

Bioplastic is bio-based plastic, a big polymer family with the prefix 'bio' referring to its carbon source or biodegradability [13,20]. The monomers or polymers of bioplastics are usually sourced from renewable and biological resources such as biomass and then polymerized through chemical mechanisms or combined through physical processes [21]. Although bioplastics are initially 100% biodegradable, compostable and environment-friendly [22], traditional plastics can also be made from renewable resources or biomass and are commonly referred to as bioplastics, which is not more sustainable and biodegradable than fossil-based plastics and possess the same threat as traditional plastics, such as bio-PE, bio-PP, bio-PA, or bio-PET(polyethylene terephthalate), belonging to non-biodegradable bioplastics [23]. However, biodegradable bioplastics can be biomass-based or fossil-based, which are susceptible to degradation by microorganisms into environmentally acceptable substances, such as water, carbon dioxide (CO_2), methane (CH_4), and biomass [24]. Biomass-based biodegradable bioplastics can be renewable-resource-based bioplastics produced directly from biomass, or by microbial biosynthesis, and chemically synthesized from biobased chemicals, including starch, lignin, cellulose, chitosan, poly(lactic acid) (PLA), polyhydroxybutyrate (PHB), polyhydroxyalkanoates (PHA) [24,25]. Fossil-based biodegradable bioplastics are synthesized from petroleum resources or petrochemicals but are biodegradable at the end of their functionality, including poly(propylene carbonate) (PPC), poly(butylene adipate-co-terephthalate) (PBAT), poly(vinyl alcohol)(PVOH), polycaprolactone (PCL) [22,25]. The classification of bioplastics is shown in Figure 1. Bioplastics attracted great interest not only from the scientific community but from the plastic industry, with global production growing over the past decade to 2.42 million tons in 2021, almost 0.66% of global plastic production [26]. Currently, the global production capacity of degradable plastics is concentrated in PLA and PBAT based bioplastics products, accounting for nearly 59% of the production capacity of biodegradable plastics and more than 38% of the global production capacity of bioplastics. PLA and PBAT are the most promising biodegradable polymer with the greatest research interest and application prospects [27,28].

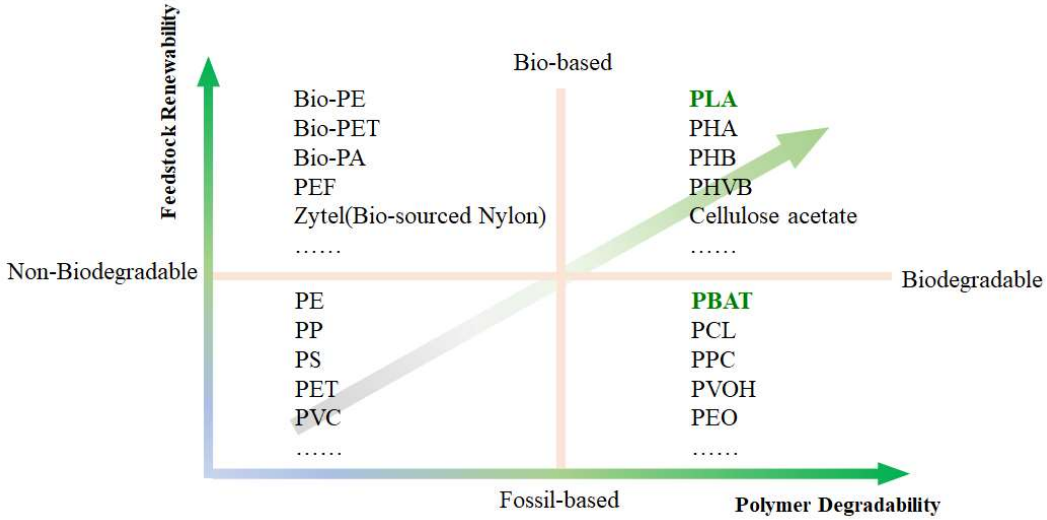

Figure 1. Classification of bioplastics.

Polylactide or poly(lactic acid) (PLA) is a linear thermoplastic aliphatic polyester with good biocompatibility, high strength, non-toxicity, and compostability that makes it attractive as a material with potential usabilities, such as packaging, textiles, electronics, biomedical, construction and automotive [29,30]. According to the statistics of the European Bioplastics Association, in 2020, the global PLA production capacity was about 394,800 tons increasing to 457,000 tons in 2021. From the perspective of production capacity pattern, Nature Works of the United States and Total Corbion of the Netherlands jointly owned 73% of the global PLA production capacity in 2020 decreasing to 50% by 2021, while the market share of China's PLA production capacity has jumped to 37%. The Asia Pacific is most likely to be the fastest-growing market of PLA from 2021 to 2028 due to high market demand by various sectors such as textile, medical, electronics and automobile in emerging economies, primarily driven by inconsistent petroleum prices and initiatives to cut fossil fuels dependence [31]. Formulations containing PLA have been approved for multiple applications by Food and Drug Administration (FDA). PLA shows excellent characteristics daily applications, making it a "polymer in the 21st century" [29].

Poly(butylene adipate-co-terephthalate) (PBAT) is one of the most promising and popular aliphatic-aromatic co-polyester. It can be produced by a polycondensation reaction of terephthalic acid (TPA), butanediol (BBO), and adipic acid (AA). PBAT has good biodegradability due to the aliphatic unit and excellent mechanical properties with flexibility similar to low-density PE(LDPE) because of the aromatic unit in the molecule chain, making PBAT a very promising biodegradable material for a wide range of potential applications [32]. In 2020 global production capacity of PBAT about 279,000 tons increased to 465,000 tons in 2021, with

128,000 tons/year by Xinjiang Blue Ridge Tunhe Polyester Co. Ltd. (Changji, China), 100,000 tons/year by Novamont Spa (Novara, Italy), 74,000 tons/year by Basf SE (Ludwigshafen, Germany), 60,000 tons/year Kingfa Bio (Guangzhou, China) and the remaining capacity provided by other companies [26]. The industrial production of PBAT is still at the embryonic stage. In 2022, Kingfa Bio's production capacity of PBAT resin was about 180,000 tons/year, and the capacity utilization rate was 50%. Many countries and enterprises were orderly promoting the capacity expansion of biodegradable plastics [33].

Both PLA and PBAT have numerous advantages, such as:

(1) Eco-friendly—PLA and PBAT are biodegradable, recyclable, and compostable;
(2) Biocompatibility—PLA and PBAT degradation products are non-toxic [34];
(3) Processibility—PLA and PBAT can be processed by film extrusion, blow molding, injection molding.

Figure 2 shows that the tensile modulus and flexural strength of PLA are better than PBAT, while impact strength and elongation at break of PBAT is better [32,35,36], compared with the mechanical properties of PLA with PBAT (Table 1). Besides, numeric values of properties reported in Table 1 show PLA and PBAT can complement with each other in mechanical performance. PLA and PBAT have drawbacks, which limit their use in certain applications. Less than 10% elongation at break and 10 kJ/m^2 impact strength lead PLA to be a very brittle material with poor toughness, whereas the lower tensile modulus and flexural strength lead PBAT very easy to deform. The Heat Distortion Temperature (HDT) reflects the resistance of plastic materials to heat in the short term, which is used as one of the benchmarks for "heat resistance". The HDT of PLA and PBAT are both below 100 °C, belonging to low heat resistant plastic.

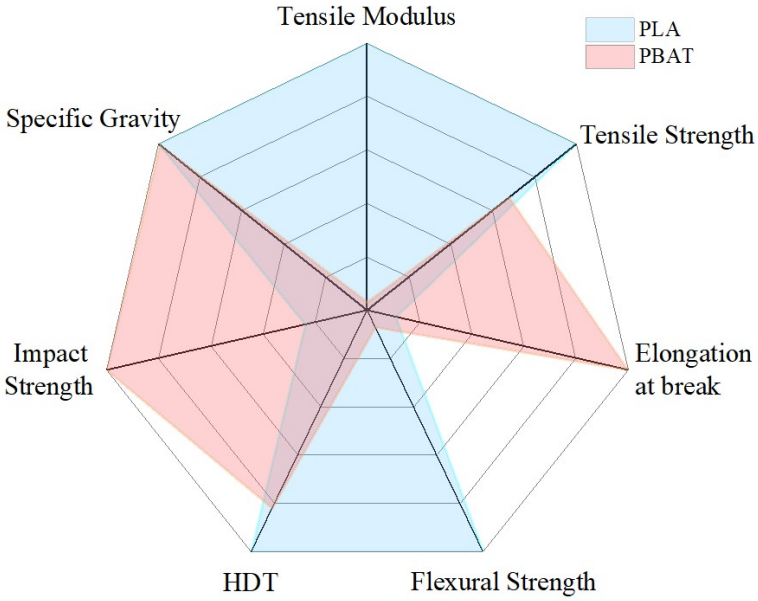

Figure 2. Comparison among the mechanical properties of PLA and PBAT (value expressed in a.u.).

Table 1. The mechanical properties of PLA and PBAT.

Properties	Units	PLA	PBAT
Tensile Modulus	MPa	3500	75–150
Tensile Strength	Mpa	59	35–44
Elongation at break	%	7	560–710
Flexural Strength	Mpa	106	7.5
Heat Distortion Temp.	°C	55 (0.45 Mpa)	45 (1.82 Mpa)
Impact Strength	kJ/m^2	5	21
Specific Gravity	g·cm^{-3}	1.21–1.25	1.22
T_g	°C	45–60	−30
T_m	°C	150–180	115–125

The weaknesses of PLA and PBAT in mechanical properties and low thermal deformation temperature hinder their extensive application in the industrial field. Many studies have been carried out in academic and industrial fields to improve the mechanical properties and thermal stability of PLA and PBAT by physical and chemical modification methods including copolymerization, grafting, crosslinking, blending and compounding. These studies aim that the modification process will not only maintain the biodegradability of PLA or PBAT (Table 2), but also improve the performance of the polymer, so as to prepare a more versatile and high-performance biodegradable polymer material.

Table 2. Summary of biodegradability of PLA and PBAT.

Name	Modification Method	Types of Biodegradation	Conditions	Standards	Biodegradability (%)	Degradation Time (days)	Ref.
PLLA	-	Compost	58 °C	N/A	90	230	[37]
$PLLA_mP(PS80NS20)_n$ triblock copolymers	Co-polymerization	Compost	23 °C (RT)	N/A	46-52	52	[38]
QAS-SBO-PLA	Co-polymerization	Enzymolysis/PBS	N/A	N/A	35-44	30	[39]
PLA/Chitosan composites	Blending	Compost	58 ± 5 °C	ASTM D5338–15	90	37	[40]
PLA/TPS/ESO compositions	Blending	Compost	58 °C	PN-EN 14806:2010	100	64	[41]
PLA/PCL/MCC blends	Blending	Compost	58 °C	ASTM D5338-15	90	37	[42]
PBAT	-	Compost	58 °C	ISO 14855	35	230	[43]
PLA/PBAT blends	Blending	Compost	28±2 °C	ASTM D5988-12	17	126	[44]
PBAT/PPC films	Blending	Compost	N/A	ASTM D5988-96	24–29	120	[45]
PBAT/TPS	Blending	Compost	58 °C	ISO 14855-1: 2012	100	18	[46]
PBAT/TPS/PBAT-*g*-MA	Blending	Compost	58 °C	ISO 14855-2:2018	72–74	90	[47]
PBAT/lignin composites	Blending	N/A	N/A	GB/T 20197-2006	77–95	90	[48]

2. Modification of PLA

2.1. Chemical Modification of PLA

The chemical modification of PLA can be carried out by stereo controlling ring-opening polymerization (ROP) of lactide, by copolymerization reaction such as block copolymerization or graft copolymerization, or by crosslinking or chain extension. As shown in Figure 3, the PLA-block copolymer can be prepared *via* ROP of the lactide with other monomers or polymers. Here are three grafting methods: “grafting-from”, “grafting-onto” and “grafting-through”. The first two methods are widely used in the graft copolymerization of PLA: grafting-from ROP of the lactide as side chains; grafting onto PLA with high molecular weight as the backbone. Crosslinking technologies include physical crosslinking and chemical crosslinking. This article mainly discusses the chemical crosslinking of PLA by the chemical reaction of complementary groups. PLA can be directly crosslinking or post-crosslinking of PLA oligomers by ROP of lactide.

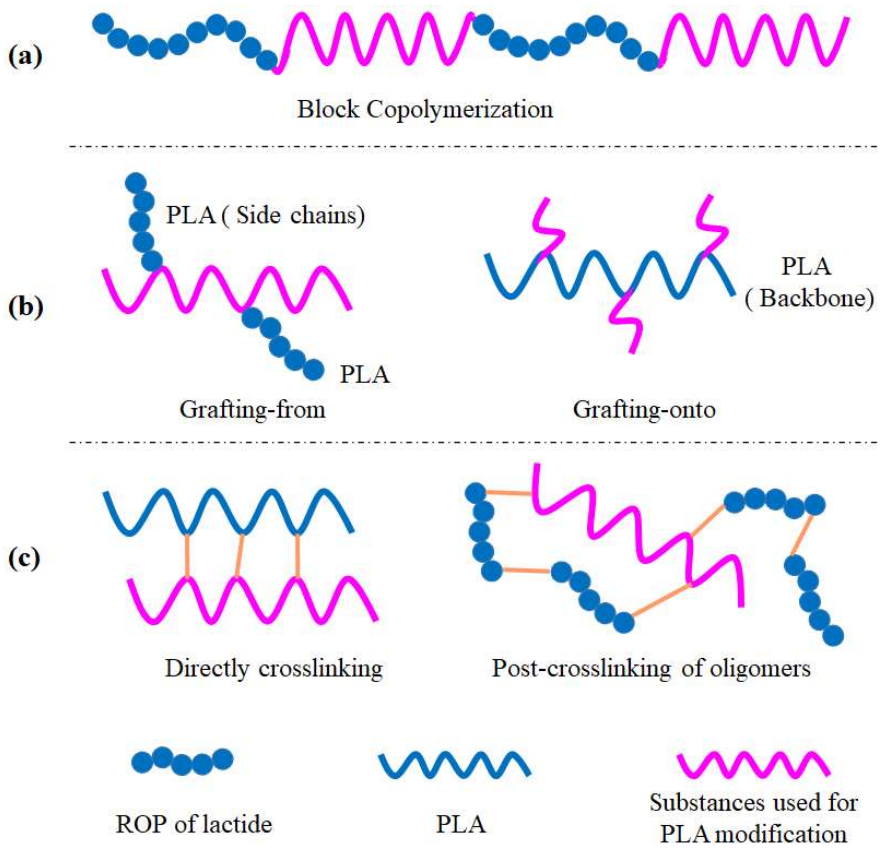

Figure 3. Block copolymerization, grafting and crosslinking of PLA.

2.1.1. Stereocontrolled

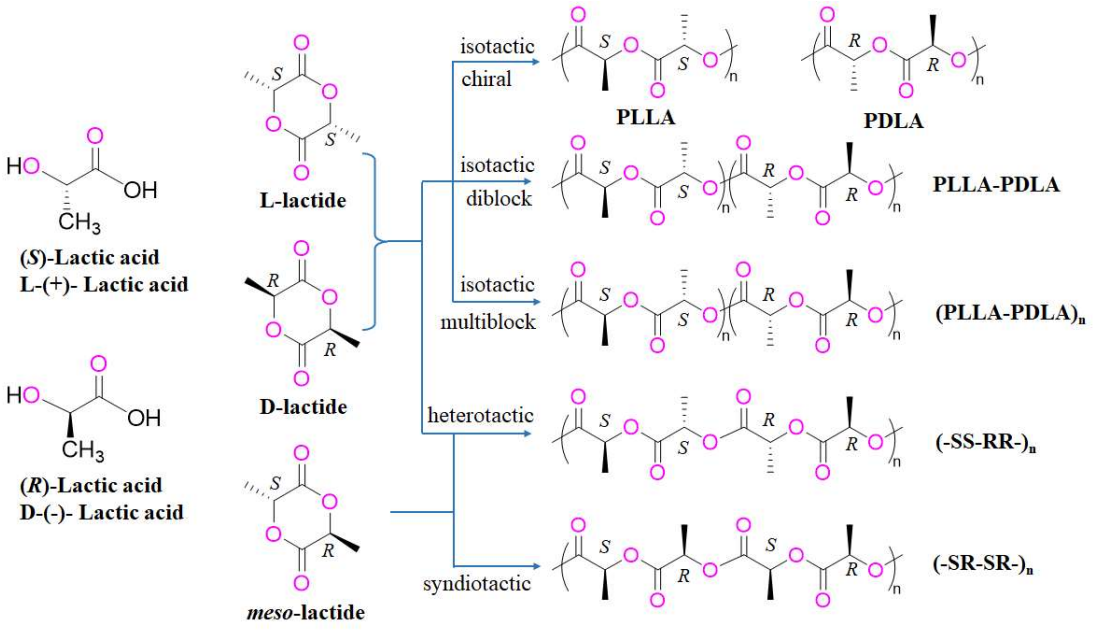

Figure 4. Forms of Lactic acid, lactide and PLA microstructures. Reproduced with permission [49] (Copyright 2016, Elsevier Science).

PLA can be produced from the polycondensation of lactic acid or ring-opening polymerization of lactide [50]. Lactic acid was first isolated by Carl Wilhelm Schele in 1780 and synthesized from petrochemical compounds for a long time until 1980s. Since then, it has been mass-produced from agricultural plants such as corn, wheat, rice, potato, tapioca and saccharose through fermentation. Recently, biomass, such as glycerol, cellulose substrates, and fructose derivatives, has been hydrothermally converted to lactic acid and lactate alkyl esters [36,51]. Lactide is a six-membered dimeric cyclic ester of lactic acid, produced from the depolymerization of lactic acid oligomer. Industrially, PLA with a molecular weight (M_w) greater than 10^5 g·mol^{-1} is made from the lactide by ring opening polymerization technique [52–54]. Lactic acid has two enantiomeric forms: (S)- and (R)- 2-

hydroxypropionic acid. After lactic acid dehydrates to make lactide, three stereoisomers namely D,D-lactide (D-lactide), L,L-lactide (L-lactide) and D,L-lactide (or *meso*-lactide) can be formed. Ring-opening Polymerization (ROP) of lactide can lead to isotactic, syndiotactic and heterotactic/atactic PLA microstructures (Figure 4) [49]. Polymer microstructures of PLA can be stereo controlled by two different mechanisms, chain end control and enantiomorphic site control. The chirality of the propagating chain end determines the chirality of the next monomer is chain end control mechanism, whereas the chirality of the catalyst dictates the chirality of the next insertion is enantiomorphic site control mechanism [55].

Stereocontrolled ROP of lactide enantiopure monomer can result in the isotactic polymer with the stereocenters aligned along the same side of the polymer chain. Stereocontrolled ROP of *meso*-lactide can lead to either syndiotactic PLA or heterotactic PLA. However, the ROP of racemic mixture (*rac*-lactide) can also lead to heterotactic PLA by alternating insertion of D- lactide (D-LA) and L-lactide (L-LA). Controlling the degree of selectivity, chain exchange and insertion errors of polymer microstructure can synthesise not only enantiopure poly(D-lactide) (PDLA) and poly(L-lactide) (PLLA) chains but also stereoblock copolymers, tapered stereoblock copolymers and multiblock (stereoblock) copolymer. The stereoregularity of PLA materials significantly affects the physical properties and thermomechanical properties. Tacticity can alter polymer melting (T_m) and glass transition (T_g) temperatures [35]. The atactic PLA is amorphous, and both the isotactic PLLA and PDLA are highly crystalline giving the polymer higher tensile strength and higher modulus [56].

The ligand chirality, polymer chain end and solvent play important roles in the stereocontrolled. A number of researches about catalyst systems have been studied for the stereocontrolled ROP of lactide, such as anionic, coordination–insertion and organic catalysts [54,55,57,58]. Z. Peng et al. employed chiral tridentate bis(oxazolinylphenyl)amido ligand base zinc complexes catalyst for the asymmetric kinetic resolution polymerization of *rac*-lactide, producing the isotactic polylactide with stereogradient microstructure and narrow dispersity. The combination of enantiomorphic site control and chain-end control is responsible for the stereocontrolled mechanism during the polymerization process [55]. Metal-free organic catalysts for the stereocontrolled ROP of lactide can result in very high levels of controling over the polymerization [57]. Liu, S. et al. have shown that cyclic trimeric phosphazene base (CTPB) due to steric hindrance can catalyze stereoselective ROP of *rac*-lactide (*rac*-LA) to produce isotactic stereoblock PLA (Pi up to 0.93) with high T_m and high crystallinity at low temperature. The chain end control mechanism was proposed to explain the polymerization of isotactic stereoblock PLA from *rac*-LA by an achiral catalyst [59].

2.1.2. Block Copolymerization

- Stereo Block Copolymer

Stereocomplex formation between PLLA and PDLA can improve thermal stability and mechanical properties by copolymerization or blending. Stereocontrolled ROP of *rac*-lactide and *meso*-lactide monomers can be used to synthesize stereo block poly(lactide)s with the blocky stereosequences of L- and D-lactides. Stereo block PLA copolymers include stereo diblock PLA copolymers, stereo triblock PLA copolymers, stereo multiblock PLA copolymers and stereo block PLA copolymers with other types of blocks [60].

Stereo diblock PLA(PLLA-*b*-PDLA) copolymers are commonly synthesized by the two-step ROP method to have head-to-head linkage or head-to-tail linkage (Figure 5) [61]. N. Othman et al. compared thermal properties, rheological behavior and tensile strength of PLLA-*b*-PDLA polymers, PLLA/PDLA blends and neat PLLA, PDLA. They found that diblock copolymers PLLA-*b*-PDLA with an overall molecular weight of about 170 kg/mol synthesized by a chiral dinuclear indium catalyst formed stereocomplex crystallites of high melting point (~200 °C). The PLLA-*b*-PDLA diblock copolymers had a viscosity enhancement and higher tensile strength than the neat PLLA, PDLA and their blends [62]. H. Tsuji et al. synthesized PLLA-*b*-PDLLA and PDLA-*b*-PDLLA enantiomeric stereo diblock poly (lactide) polymers from crystalline poly (L-lactide) or poly (D-lactide) and amorphous poly (DL-lactide) with similar overall molecular weights in the presence of tin(II) 2-ethylhexanoate as the initiator and 1-propanol as the co-initiator. PLLA-*b*-PDLLA was crystallizable for the PLLA fractions down to 25.4% with PDLLA chains restrained in the amorphous regions between the crystalline regions [63,64].

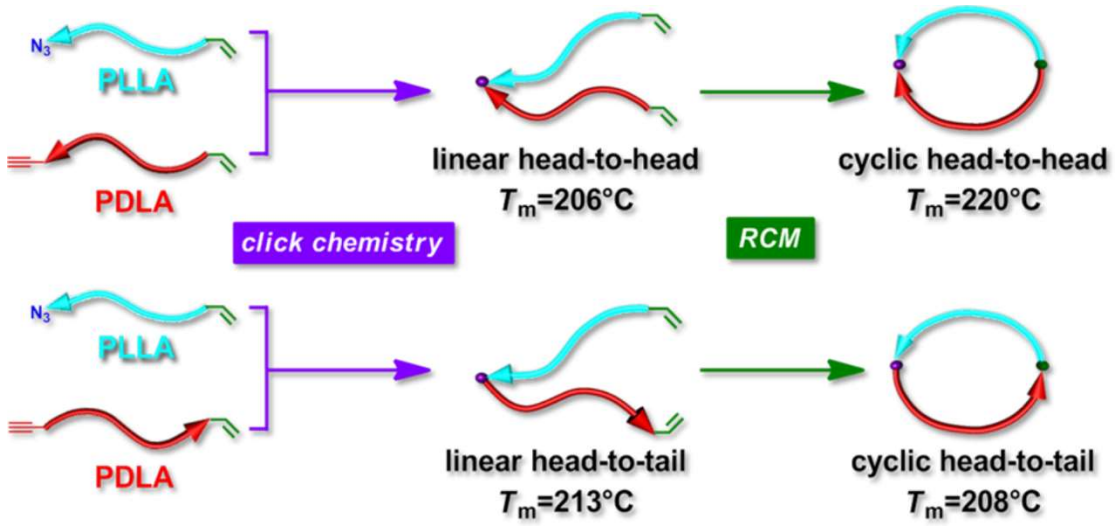

Figure 5. Structures and T_m values of liner and cyclic stereo diblock PLA polymers with head-to-head and head-to-tail linkages. Reproduced with permission [61] (Copyright 2012, AMER CHEMICAL SOC).

Stereo triblock PLA can refer to copolymer synthesized by the three-step polymerization of L- and D-lactides or 2-armed stereo diblock PLA copolymers by two-stage ROP of L- or D-lactide. The terminal Diels-Alder coupling method can be used to prepare the stereo diblock PLA and Stereo triblock PLA copolymers with different PLLA and PDLA block lengths and compositions. The stereo triblock PLA copolymers can be easily fabricated into transparent polymer films by hot-pressing. Due to the high stereocomplex crystallinity, these films have excellent thermal stability and mechanical properties [65]. SA-based linear 2-armed stereo diblock copolymer (LD-SA) is synthesized from ethylene glycol (EG) and succinic anhydride (SA)-based 2-armed PLLA and PDLA. Due to hydroxyl terminal groups (hydrogen bonding) or chain direction, 2-armed PLLA and PDLA have the tail-to-tail (EG-based) or head-to-head (SA-based) architectures [66]. Mono alcohol and di-alcohol are used as initiators to produce mono hydroxy and di-hydroxy terminated poly(lactide)s at the beginning of the first polymerization of L- or D-lactide, and then poly(lactide)s can be further used as monofunctional and di-functional macro-initiators for the subsequent polymerization of the enantiomeric lactide [49].

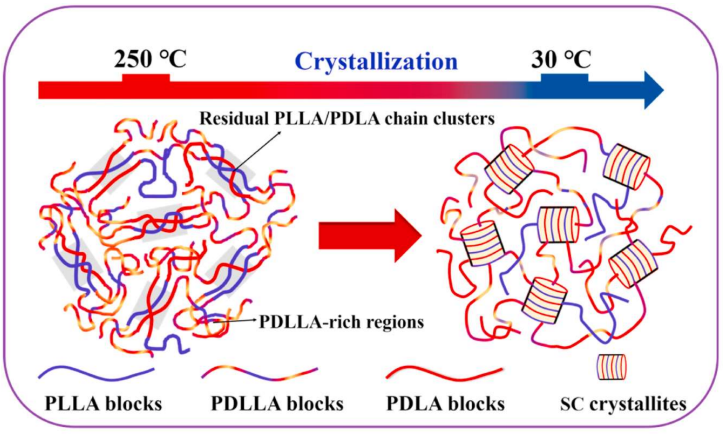

Figure 6. Schematic diagram showing the probable molecular mechanism for the outstanding melt stability and SC crystallizability of the multiblock-like PLLA-*b*-PDLLA-*b*-PDLA copolymers. Reproduced with permission [67] (Copyright 2020, Elsevier Science).

Stereo multiblock PLA copolymers can be synthesized by many methods, such as the enantioselective polymerization of L- or D-lactide [68], dual terminal couplings of poly-L-lactide and poly-D-lactide [69] and solid-state or melt polycondensation of PLLA/PDLA mixture [67,70,71]. Y.W. Widhianto et al. synthesized stereo multiblock PLA copolymers with various block lengths after two-step ROP of L-lactide with 1,12-dodecanediol as the initiator and furthered the chain extension reaction with hexamethylene diisocyanate as the chain extender. The structure of stereo multiblock PLA copolymers is di-block copolymers with block lengths ranging from 1250 to 10,000 connected with flexible methylene chains C6 and C12. T_g and T_m increase with the increase in the block lengths [72]. Stereo multiblock PLA, like PLLA-*b*-PDLLA-*b*-PDLA copolymers, can be designed in a simple and effective solid-state transesterification strategy by one pot reactive melt blending at a low temperature of 180 °C of linear high molecular weight PLLA and PDLA with $SnCl_2$/TSA catalysts. PLLA-*b*-PDLLA-*b*-PDLA copolymers with an excellent melt

stability and unexpectedly strong crystallinity is formed *in situ* in the racemic blend due to selective hetero-chain transesterification in the mobile amorphous (Figure 6) [67].

- PLA-Polyether Block Copolymers

The PLA–polyether block copolymers can be synthesized from commercially available polyether or ROP of cyclic ethers with the ROP of lactide in the presence of multiple metal-based initiators or organo-catalysts [73]. Copolymerization of PLA with a wide range of hydrophilic components is a promising method which can improve the inherent hydrophobicity of PLA and its high hydrolytic stability in tissues [49]. Polyethylene glycol (PEG) is a synthesized hydrophilic polyether composed of repeated units of ethylene oxide. PEG is characterized by the low toxicity, biocompatibility, and inert nature, so it is widely used in foods, cosmetics and pharmaceutical formulations [74]. ROP of lactide in the presence of monomethoxy PEG (mPEG) and stannous octoate could be well-tuned from the stereostructure and PLA blocks sequence. PLLA-*b*-PEG and PDLA-*b*-PEG diblock copolymers with well-defined composition, low polydisperse ability and more importantly high optical purity can be synthesized by this method. PLLA-PEG-PLLA, PDLA-PEG-PDLA and PEG-PLLA-PDLA triblock copolymers with unique material features and properties can be produced through sequential ROP of L- and D-lactide onto a preformed PEG-diol in the presence of metal-catalysts such as stannous octoate, SnO_2, Sb_2O_3, GeO_2 and zinc [49,75,76]. PDLA–PLLA–PEG–PLLA–PDLA stereo pentablock copolymers also can be prepared with the PLLA and PDLA block lengths controlled by changing the PLA/PEG feed ratio in the first and second-step ROP, respectively. PDLA–PLLA–PEG–PLLA–PDLA stereo pentablock copolymers undergo physical gel at high concentration in an aqueous solution and this gel becomes sol with the increase of temperature. The microstructure and physical properties of hydrogels formed by amphiphilic block copolymers can be adjusted according to the stereo structure, crystallization and stereo complexation of hydrophobic blocks (Figure 7) [77]. PEG-*b*-PLA copolymers are the well-known example of the micellar block copolymer, which does not interfere with whole blood or its components and meets the standards required for intravenous injection. Various micelles and NPs prepared *via* the self-assembly of PLA-*b*-PEG copolymers compose hydrophobic PLA and hydrophilic PEG [78–80]. PLA-*b*-PEG copolymers also can be examined as surface modifiers for tissue engineering, bone curing, and drug delivery [81].

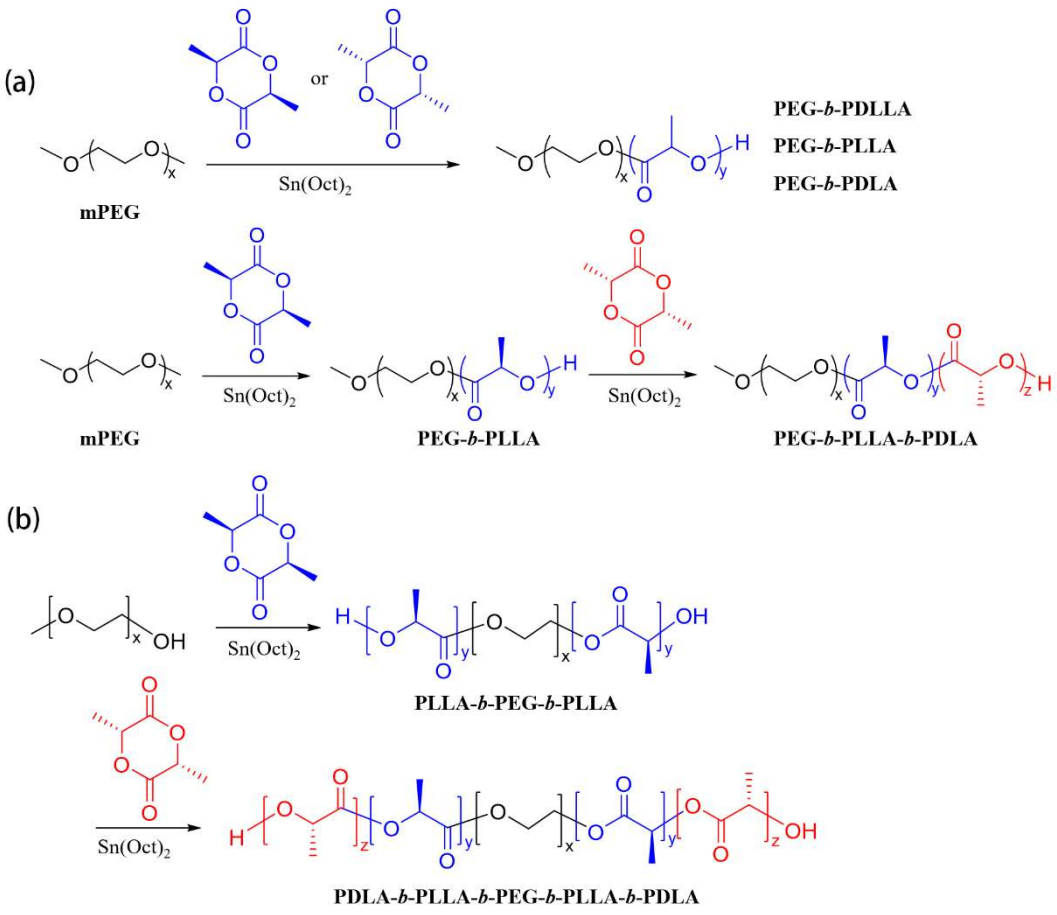

Figure 7. Synthesis of PLA/PEG di-block, stereo-block copolymers (**a**), reproduced with permission [75] (Copyright 2015, AMER CHEMICAL SOC), and PLA/PEG stereo penta-block copolymers (**b**), reproduced with permission [77] (Copyright 2016, Royal Society of Chemistry).

One method to synthesize PLA–polyether block copolymers by ROP of epoxide and lactide requires multiple steps involving different catalytic systems such as bimetallic salen aluminum complex, Lewis acidic titanium and zirconium isopropoxide

complexes [73]. The "activated monomer strategy" can be developed to synthesize functional epoxides to generate aliphatic polyether [82]. A nascent catalytic process called switchable polymerization catalysis can synthesize sequence-controlled block polymers from mixtures of monomers [83,84]. Representative structure of epoxides is shown in Figure 8a. Y. Liu et al. designed the anionic to H-bonding switchable catalysis to prepare PLA–polyether block copolymers. Poly(GPE-*b*-LA) with precise molecular weights and narrow dispersion were prepared by the addition of thiourea to initiate ROP of lactide at room temperature in a solution composed of ROP of glycidyl phenyl ether (GPE) [84]. H. Kudo et al. synthesized poly(GPE-co-LA) gradient copolymer in high yield by ring-opening copolymerization of GPE and lactide proceeded in the presence of DBU as a catalyst at 180 ℃ for 2 h in bulk [85].

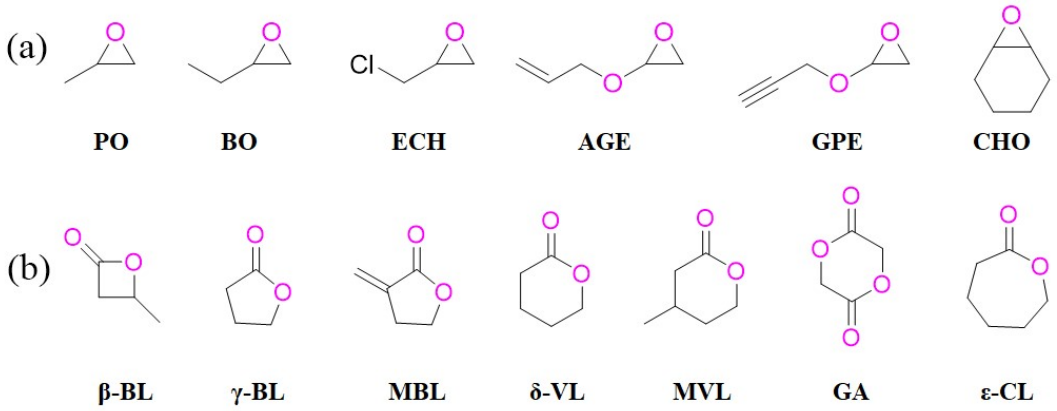

Figure 8. Representative structure of epoxides (**a**) and cyclic esters (**b**).

- PLA-Polycarbonate Copolymers

Aliphatic Polycarbonate is the polymer containing carbonate group in the molecular chain with excellent biodegradability, high toughness and tunable glass transition temperatures. Carbon dioxide (CO_2)-based polycarbonate has been regarded as one of the most promising green bioplastics [86–88]. Synthesis of PLA-polycarbonate copolymers can be performed through ROCOP of lactide and cyclic ether involving CO_2 incorporation. With the attractive chain growth, ROP/ROCOP systems of cyclic monomers are atomic economic and require much milder reaction temperature. The controllable molecular weight and lower dispersity make it possible to customize polymer composition, structure and topology of polymers [88,89].

Poly(propylene carbonate) (PPC) has excellent light transmission and good oxygen barrier properties with potential and wide applications in barrier materials, foaming materials, electrolytes, etc. PLLA-*b*-PPC can be effectively synthesized by one-step and one-pot method with long L-lactide rich sequence by utilizing zinc adipate as the catalyst. The introduction of L-lactide monomer can enhance the catalytic activity and improve the polymer selectivity from 43 to 99% [90]. X. Deng et al. designed a heterogeneous ternary catalyst system containing SalenCoIII, zinc glutarate and PPNCl to prepare PLA-*b*-PPC with the molecular weight-as high as 698.0 $kg \cdot mol^{-1}$ [91]. Metal-free organic catalysts can also be used for the synthesis of PLA-polycarbonate copolymers [83]. PLLA-*b*-PTMC(poly trimethylene carbonate) can be synthesized through ROP of L-lactide (L-LA) and trimethylene carbonate (TMC) by two-component organocatalyst adenine/sac which can effectively reduce the energy barrier of the rate-determining step during the ROP of L-LA and TMC [92]. PLA-*b*-PTMC can be synthesized in solutions at room temperature by hydrogen bond donor (HBD)/organic base cocatalyst, which is a gold standard in organocatalytic ring-opening polymerizations (ROPs). Y. Zhu et al. proposed genuine HBD/LB cocatalyst for ROPs of lactide and TMC by 3-amino-1,2,4-benzothiadiazine-1,1-dioxide (ABTD) and triethylamine (TEA) without proton abstraction [93]. Many other multicomponent systems have been reported for tandem ROCOP/ROP of lactide with other cyclic monomers to prepare PLA-polycarbonate copolymers (Figure 9) [73,82,83,86,94].

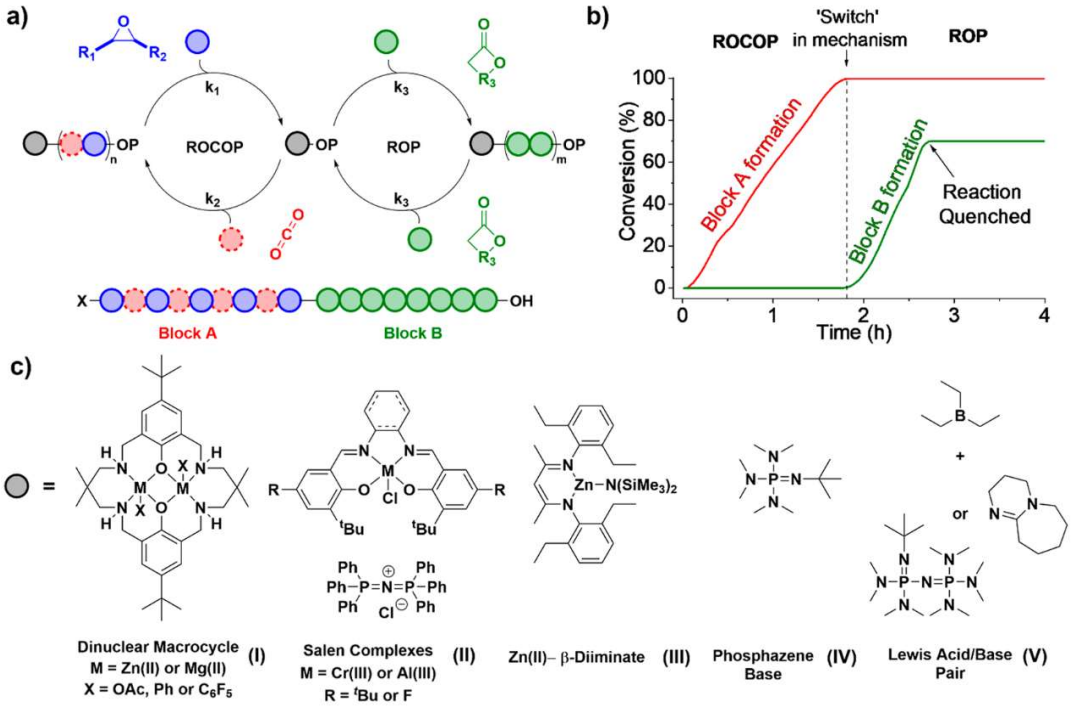

Figure 9. (**a**) Illustration of representative heterocycle ROCOP and ROP pathways. (**b**) Reaction conversion versus time plot showing the growth of each block. (**c**) Examples of switch catalysts. Reproduced with permission [83] (Copyright 2021, AMER CHEMICAL SOC).

- PLA-Polyester Block Copolymers

PLA displays high tensile strength, high Young modulus, high intrinsic brittleness, low impact strength and thermal instability. Toughening and increasing the performance of PLA has been attractive by introducing polyester blocks due to their flexibility as well as tunable biodegradation on the basis of ensuring the degradability of PLA copolymers. Some cyclic esters for the synthesis of PLA copolymer are shown in Figure 8b. Synthesis of PLA-polyester block copolymers can employ the method of sequential feeding that lactide and cyclic ester monomers are added successively in the presence of one or multiple suitable initiators, or simultaneous feeding that the lactide and cyclic ester monomers with very different reactivity are added at the same time in the presence of a particular catalyst. Although the reaction follows the ROP mechanism, the transesterification existing in the system will transform the block microstructure into a random copolymer with wide dispersion [73].

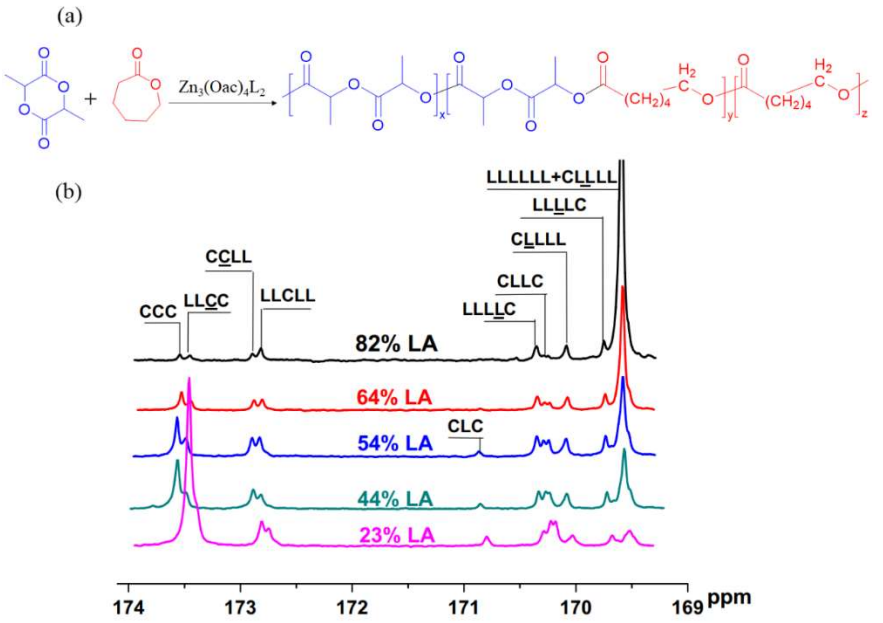

Figure 10. (**a**) Copolymerization of LA and CL; (**b**) Carbonyl signals in ^{13}C NMR spectra of poly(LA-grad-CL). Reproduced with permission [95] (Copyright 2016, Elsevier Science).

ROP of ε-Caprolactone (CL), a lactone with seven membered rings, can be used to prepare polycaprolactone (PCL) [96]. PCL is another FDA-approved aliphatic linear biodegradable semi-crystalline polyester with an excellent performance such as biocompatibility, non-toxicity, appropriate mechanical strength and low cost. Therefore, CL is selected as the representative of cyclic ester to study the copolymerization method and product properties of PLA-polyester block copolymers (Figure 8). Many organometallic catalysts (e.g., zinc [95–97], aluminium [98–101], tin [102], lanthanum [103] and titanium [104]) and organo-catalysts [105] can be used for ROP of ε-caprolactam and lactide to prepare PLA-*b*-PCL copolymers (Figure 10), their synthesis methods, conditions and product performance are shown in Table 3.

Table 3. Summary of PLA-co-PCL copolymer.

Polymer	Feeding	Lactone [a]	Catalyst	T_g (℃)	T_m (℃)	M_n (10^4g/mol)	M_w/M_n	Ref.
PLLA-*b*-PCL	Sequential	ε-CL and L-lactide	β-Pyridylenolate zinc catalysts	37	172	1.77	1.54	[97]
poly(LA-grad-CL)	Simultaneous	L-lactide and ε-CL(82:18)	Schiff base tri-zinc complex	31.4	139.1	2.50	1.69	[95]
PLLA-*b*-PCL	Sequential	L-lactide and ε-CL	Aluminium complexes	50.3	168.9	2.23	1.32	[98]
PLLA-co-PCL	Simultaneous	ε-CL and L-lactide	Stannous octoate ($SnOct_2$) and triphenyl bismuth (Ph_3Bi)	50	165	8.09	1.77	[102]
PLLA-*b*-PCL	Simultaneous	ε-CL and L-lactide	Lanthanum complexes	47.7	N/A	5.92	1.80	[103]
PLA-*b*-CL	Simultaneous	*rac*-lactide and ε-CL(74:26)	Niobium and Tantalum complexes derived from the acids $Ph_2C(X)CO_2H$ (X = OH, NH_2)	N/A	N/A	1.60	1.50	[104]
PLLA-*b*-PCL-*b*-PLLA	Sequential	ε-CL and L-lactide	Benzoic acid-organocatalyzed	−11.6	N/A	0.77	1.14	[105]
PLLA-co-PCL	Simultaneous	ε-CL and L-lactide(1:1)	tetrabutylammonium phthalimide N-oxyl organocatalyst	39.9	56.4	2.21	1.85	[106]

[a] If monomer is sequential feeding, the order of monomer addition.

2.1.3. Grafting

Graft copolymerization provides a significant route to impart a new property or enhance the existing properties depending on the type of monomer, the grafting rate, the grafting method and the distribution of the grafting chain. Graft copolymers can be prepared by grafting-onto multifunctional linear backbone, grafting-from a linear macroinitiator and grafting-through macromonomer [107]. ROP of lactide can be used for grafting-onto or grafting-from method during the grafting process [108]. However, high modulus commercial PLA can be regarded as macromonomer copolymerized with low molecular weight comonomers [109]. PLA-based graft copolymers can be synthesized with monomers like ε-caprolactam [110], glycolic acid, polymers such as PEG [111], inorganic materials like CNTs, graphene oxide and natural macromolecules like dextran starch, chitosan, lignin, cellulose, silk sericin.

- Amphiphilic Graft Copolymers

PLA-based amphiphilic graft copolymers have increased hydrophilicity, higher degradability, and better histocompatibility. We had introduced PLA-*b*-PEG block copolymer in the previous content. However, PEG and PLA also can be used to form PLA-*g*-PEG graft amphiphilic copolymer. Poly((oligoethylene glycol) methacrylate) (POEGMA) has similar biocompatibility with PEG and provides a method to combine a large number of short PEG chains onto the copolymer. POEGMA is composed of a low molecular weight PEG chain along the main chain of methacrylate and the end of PEG side chains can be utilized for further functionalization (Figure 11). P.P. Kalelkar and D.M. Collard have prepared amphiphilic brush graft copolymer PLA-*g*-PEGMA with brominated polylactic acid (Br-PLA) as a multisite macromolecular initiator by atom transfer radical polymerization (ATRP) of methyl methacrylate and oligomeric methacrylate (OEGMA). The brush graft copolymer self-assembled in an aqueous solution forms nanoparticles below 100 nm with the ability to encapsulate and release curcumin [112].

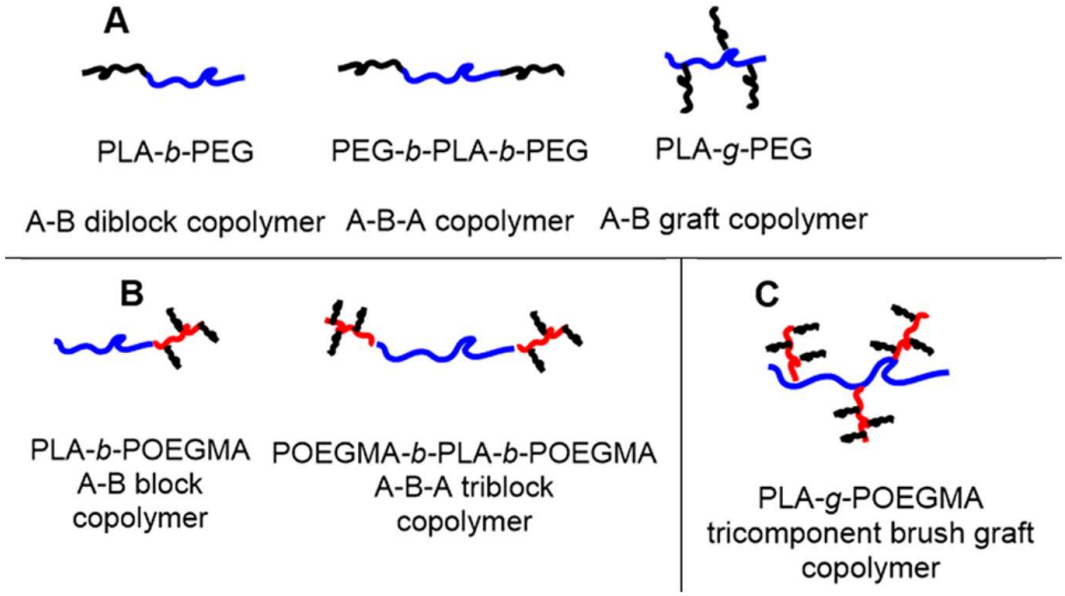

Figure 11. Architectures of amphiphilic PLA-based copolymers. Reproduced with permission [112] (Copyright 2020, AMER CHEMICAL SOC).

Poly(γ-glutamic acid) (γ-PGA) is a naturally occurring water-soluble poly(amino acid) and has unique biodegradability, immunogenicity and immunoreactivity. Y. Zhu et al. prepared the comb-like γ-PGA-*g*-PLLA and γ-PGA-*g*-PDLA amphiphilic graft copolymers, consisting of γ-PGA as the hydrophilic backbone and enantiomeric PLLA or PDLA as the hydrophobic side chains. γ-PGA-*g*-PLA can form stereocomplex NPs through dialysis method to prepare polymer micelles from diblock copolymers (Figure 12) [113]. Poly(acrylic acid) (PAA) is a pH-responsive hydrophilic polymer which is obtained from complete hydrolysis of corresponding polyacrylate. W. Qian et al. synthesized PAA-*g*-PLA amphiphilic graft copolymer with PAA as the fully hydrophilic backbone and PLA as side chains through the grafting-from strategy. PAA-*g*-PLA amphiphilic graft copolymer is formed by reversible addition-fragmentation chain transfer (RAFT) homopolymerization of *tert*-butyl 2-((4-hydroxybutanoyloxy) methyl) acrylate (*t*BHBMA) followed by initiating ROP of lactide to provide PLA side chains and the main chain is subsequently hydrolyzed to PAA (Figure 13). PAA-*g*-PLA amphiphilic graft copolymer shows pH-responsive micellization behavior and it can self-assemble into spheres in aqueous media which can load and gradually release Doxorubicin (DOX) [114].

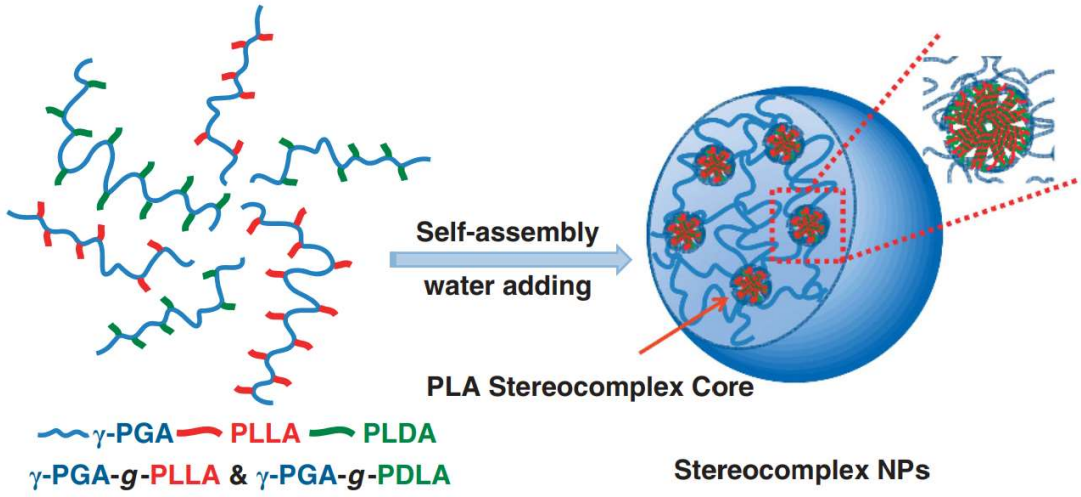

Figure 12. Illustration of nanoparticle formation by stereocomplexation of γ-PGA-*g*-PLLA/PDLA copolymers. Reproduced with permission [113] (Copyright 2012, Springer Nature).

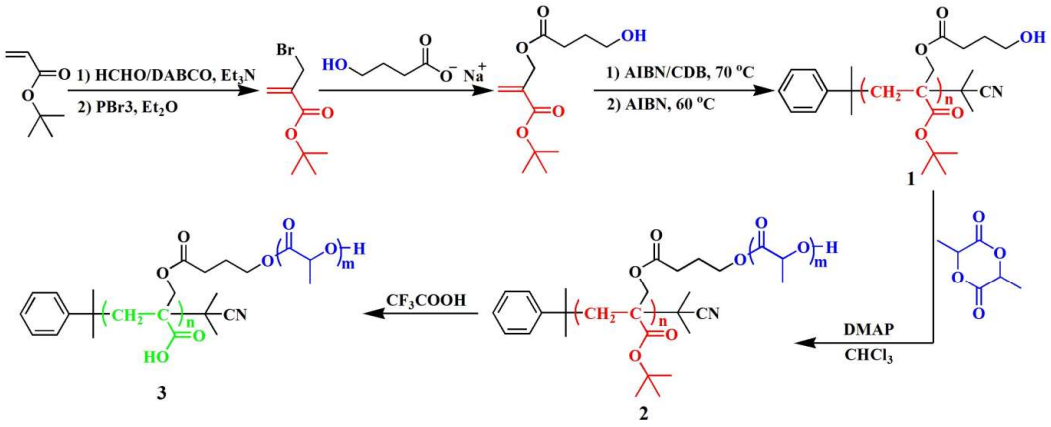

Figure 13. Synthesis of PAA-*g*-PLA Well-Defined Amphiphilic Graft Copolymer. Reproduced with permission [114] (Copyright 2017, Royal Society of Chemistry).

- PLA-Natural Macromolecules Graft Copolymers

Alkaline lignin (LG) is a low-cost, green natural renewable biomass resource. N. Zhang et al. investigated lignin grafted lactide (LG-*g*-LA) as the toughening agent to toughen PLA *via* solution casting to prepare PLA/lignin composite films with high elongation, excellent UV barrier, water resistance and controllable gas permeation. LG-*g*-LA copolymer was synthesized using DBU as the catalysis by ROP of lactide. GLG-*g*-LA copolymer was successfully synthesized by selectively alkylated of the phenolic hydroxyl and partial carboxylic hydroxyl groups on the LG surface and ROP of lactide. PLA/GLG-*g*-LA composite films have a broad application prospect in active food packaging and UV-protecting materials (Figure 14) [108]. Another commonly used biopolymer to remedy PLA's weaknesses is thermoplastic starch (TPS) with inherent biodegradability, high oxygen resistance and low cost. B.M. Trinh et al. prepared a starch-graft-poly(lactic acid) (St-*g*-PLA) copolymer through ROP reaction of lactide to deposit PLA oligomer on the starch skeleton and used it as compatibilizer thermoplastic starch (TPS)/PLA blends. Using the St-PLA compatibilizer tremendously improved the elastic modulus, similar to the tensile strength and flexibility of TPS/PLA films, to supplement the limitations of PLA in packaging and other commercial applications (Figure 15) [115]. Silk sericin (SS) is a natural biological macromolecule. Sericin is a water-soluble protein produced from silkworm cocoons regarded as waste by the degumming process. K. Boonpavanitchakul et al. demonstrated the possibilities of using silk sericin protein as a protein backbone to construct biodegradable SS-*g*-PLA copolymers by combining sericin and polylactide (PLA) *via* ROP with $Sn(Oct)_2$ as a catalyst. Sericin is not only used as a biological initiator but also provides a connection to form the SS-*g*-PLA copolymers (Figure 16) [116].

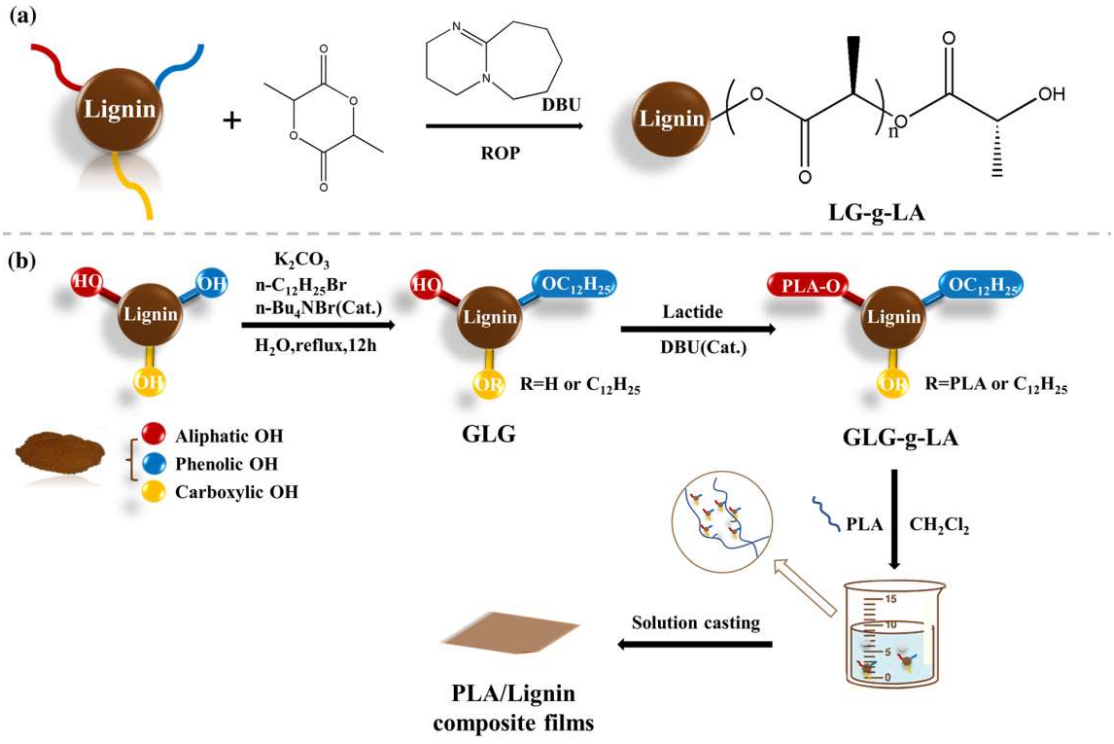

Figure 14. (**a**) Mechanism diagram of LG-*g*-LA by ring-open polymerization; (**b**) Preparation of GLG-*g*-LA for effective toughening of PLA. Reproduced with permission [108] (Copyright 2022, Springer Nature).

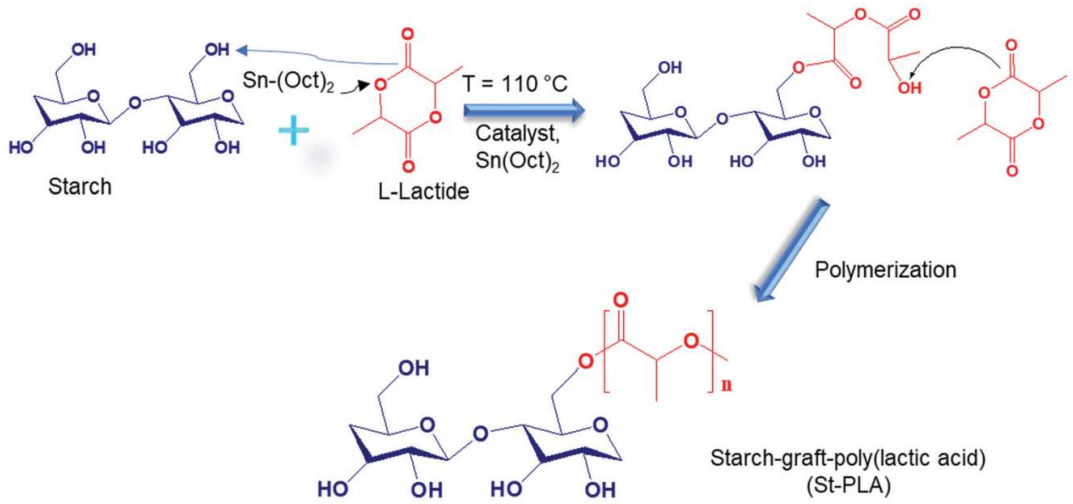

Figure 15. Ring open polymerization reaction to synthesize Starch-graft-PLA (St-PLA) copolymer. Reproduced with permission [115] (Copyright 2022, Royal Society of Chemistry).

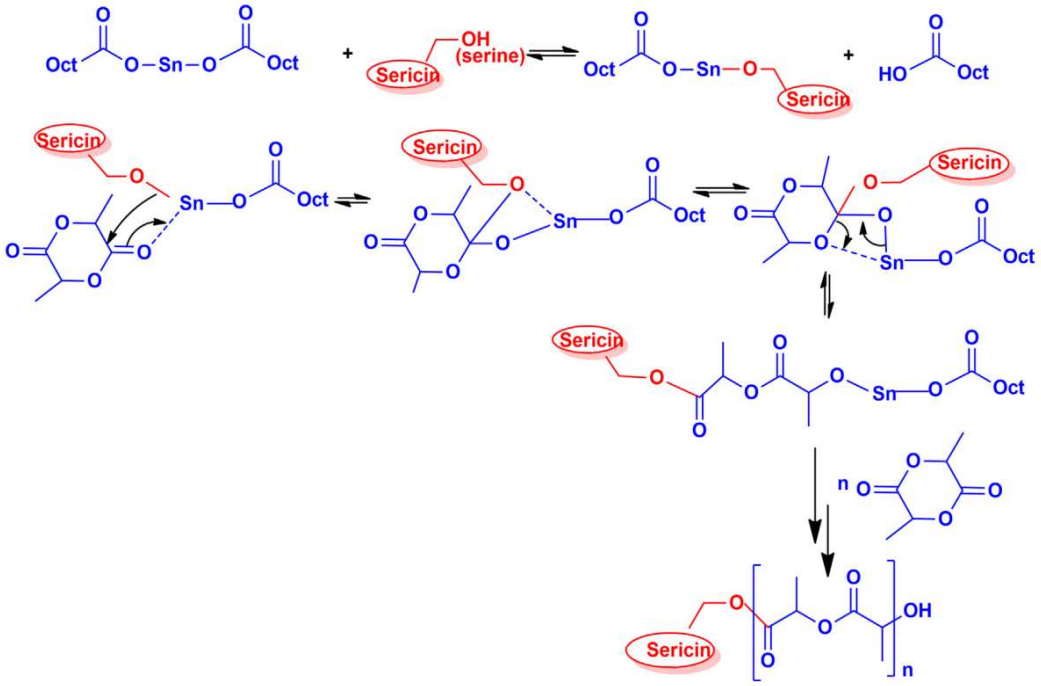

Figure 16. Proposed reaction mechanism of SS-*g*-PLA copolymer. Reproduced with permission [116] (Copyright 2019, Elsevier Science).

- PLA-Inorganic Graft Copolymers

The preparation of inorganic materials such as nanocarbon materials is also a recognized method to improve the properties of PLA. The properties of the prepared PLA-based nanocomposites are closely related to the compatibility between nanoparticles and polymers and the spatial separation of nanoparticles [117]. Carbon nanotube (CNT) has high tensile strength, high Young's modulus and low density due to the perfect arrangement of carbon-carbon covalent bonds along the nanotube axis [118]. M.G. Jang et al. prepared lactic acid-grafted MWCNT (LA-*g*-MWCNT) by mixing L-lactic acid solution with COOH-MWCNT and then used LA-*g*-MWCNT as a compatibilizer to prepare polycarbonate (PC)/poly(lactic acid) (PLA)/LA-*g*-MWCNT composite, increasing values of the electrical conductivity and rheological properties [119]. J.M. Campos et al. prepared the GO-*g*-PLA hybrid by "click" coupling alkynyl-functionalized PLA with azido-functionalized GO (Figure 17). The "click" reaction between Alkynyl-PLA and GO-N_3 was mainly manifested in N1s and O1s regions. The increase in glass transition temperature indicated that the mobility of PLA chain decreased, which may be caused by their fixation on GO surface. The GO-*g*-PLA hybrid obtained contains at least 20% biopolymer, showing a certain exfoliated graphene structure. From the perspective of the potential application of GO-*g*-PLA hybrid as the reinforcement filler in the preparation of PLA nanocomposites, this grafting method is very useful for adjusting the graphene-biopolymer interface, because it can keep the microstructure of biopolymers under complete control [120].

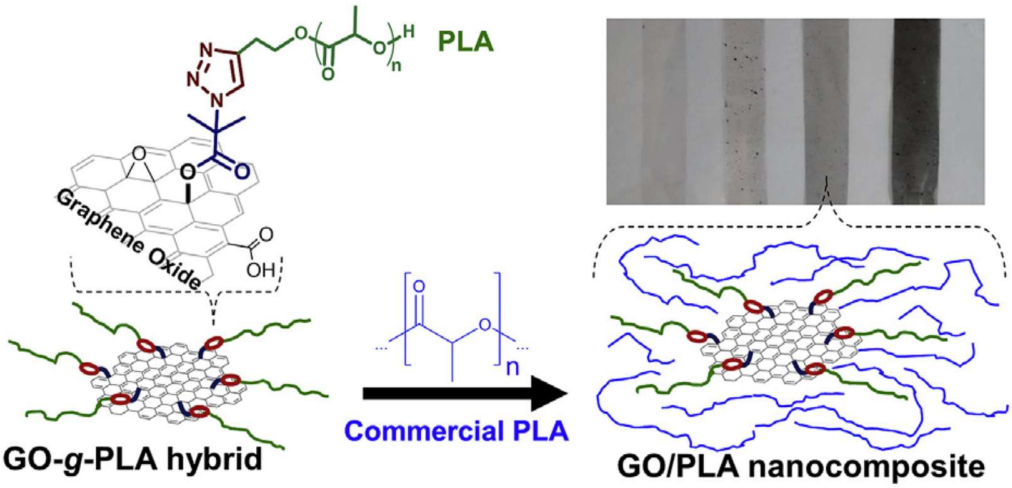

Figure 17. Preparation of GO-*g*-PLA. Reproduced with permission [120] (Copyright 2015, Amsterdam: Elsevier).

Inorganic oxides such as silica [121–125], titanium oxide [126,127] and cuprous oxide [128] can be also used for graft copolymerization of PLA to enhance its properties. SiO_2 is a biocompatible nanofiller with stable and high heat resistance properties. PLA-*g*-SiO_2 can be used to improve the crystallisation rate and the relative crystallinity and enhance the melt strength and impact strength of PLA [121,124]. Zhang Y. et al. prepared PLA/SiO_2 nanocomposites by synthetizing PLA-*g*-SiO_2 *via* ROP of L-Lactide with the stannous octoate as the catalyst and the surface hydroxyl groups of SiO_2 as the initiator first, and then melting extrusion. The degree of relative crystallinity increased from 11.6% of pure PLA to 44.7% of PLA/SiO_2 nanocomposites [121]. PLA-*g*-SiO_2 can be prepared by "grafting to" or "grafting from" method with silane coupling agents such as KH550, KH-560 treated silica nanoparticles [122,123]. The research group of M.B. Yang prepared PLLA-*g*-SiO_2 by grafting from method and grafting to method, respectively, and then prepared PLLA/PLLA-*g*-SiO_2 nanocomposites by melt blending. PLLA-*g*-SiO_2 with high density-low molecular weight can be prepared by ROP of L-lactide (grafting from) with varying content of SiO_2-NH_2, while PLLA-*g*-SiO_2 with high molecular weight-low grafting density can be prepared by nucleophilic addition reaction (grafting to) which the PLLA homopolymer was reacted with SiO_2-NCO from the reaction between SiO_2-NH_2 and 2,4-Diisocyanatotoluene (TDI). [122]. They also prepared 4-Arm PLLA-*g*-SiO_2 by 4A-PLLA-NCO and then introduced 4A-PLLA-*g*-SiO_2 into the PLLA. They found that the crystallization rate and melt strength of PLLA can be enhanced by adding PLLA-*g*-SiO_2 [124]. Wang B. et al. prepared PLA-*g*-SiO_2 *via* functionalized SiO_2 with grafting degraded PLA chains and then used it to strengthen and toughen PLA. The impact strength significantly increased from 3.3 to 4.3 KJ/m^2 when compared to pure PLA (Figure 18) [125].

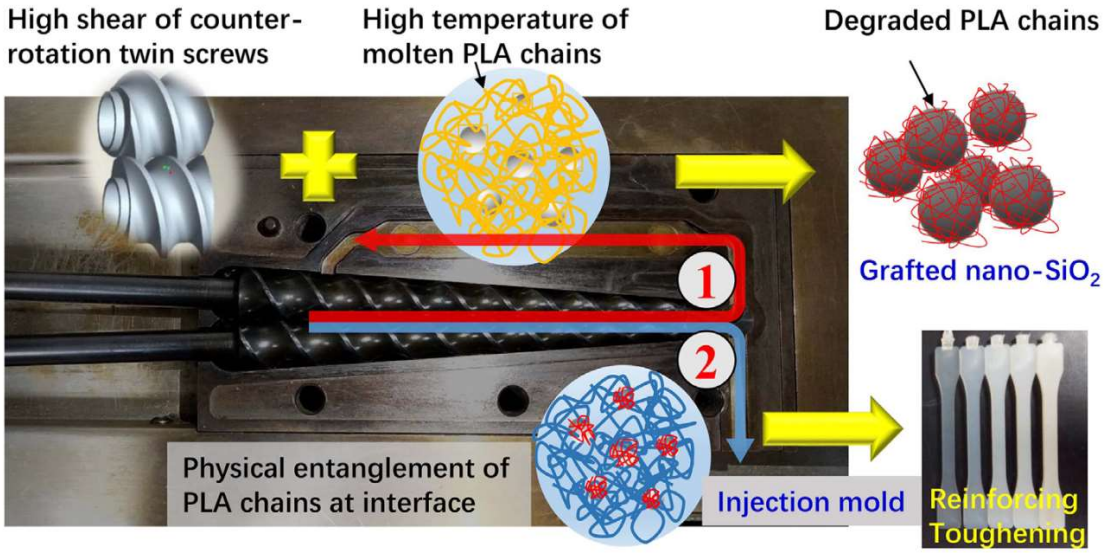

Figure 18. Schematic illustration for the preparation processes of (1) PLA functionalized nano-SiO_2 (f-SiO_2) and (2) f-SiO_2 reinforced PLA composites. Reproduced with permission [125] (Copyright 2020, Wiley).

2.1.3. Crosslinking

Crosslinking, a cost-effective and efficient method, can improve the mechanical, thermal and physicochemical properties of PLA *via* the connected intra- or intermolecularly by covalent or non-covalent links with the polymer chains [129]. Chemical and

physical methods both have been used for PLA crosslinked. We aim to review the developments in the chemical crosslinking of PLA. Chemical crosslinking of PLA can distinguish into two different approaches: (1) directly crosslinking during the synthesis of the polymer by designing the polymer architecture, using multifunctional initiators, or branching agents; (2) post-crosslinking of oligomers with controlled architecture *via* condensation reactions [130–133]. Crosslinking of high molecular weight PLA in the presence of radical initiators to create polymer radicals on the polymer backbone are generally faster but leads to less controlled structures and secondary reactions. An efficient crosslinking method to compatibilize different polyesters is to mix the polymer and the radical initiator in the solid state without solvent during high molecular weight polymer extrusion [134]. Among the different initiators, organic peroxides and multifunctional co-agent are widely applied. Peroxide-induced crosslinking begins with the formation of primary radicals generated by the thermal decomposition of peroxides, and then hydrogen abstraction from polymer chains to generate polymer radicals, recombining to form carbon-carbon cross-linking [133]. The peroxide efficiency depends on the amount of peroxide required for the crosslinking reactions and whether or not the free radicals can cause more chain scissions than crosslinking reactions. Using organic peroxides in the melt state during polymer extrusion can cause severe chain scissions leading to the loss of mechanical properties. To solve this negative effect and prepare better performance polymer, a multifunctional co-agent is added during polymer extrusion [130].

Cross-linked PLA can be prepared simply by solution casting of PLA with dicumyl peroxide (DCP). The quantitative analysis of chain scission and cross-linking reaction showed that the increase in reaction temperature weakened the occurrence of cross-linking and reduced the gel fraction [135]. C. Yamoum et al. introduced crosslinking structures into PLA by the initiation of DCP and ethoxylated bisphenol A dimethacrylates (Bis-EMAs) as a crosslinking co-agent. The Bis-EMA-crosslinked PLAs have better processability and shape stability than DCP/PLA and the glass transition of the crosslinked PLAs moves to higher temperature region (before melting) [136]. Bis(tert-butyl dioxy isopropyl) benzene (BIBP) belonging to peroxide is a radical crosslinking agent similar to DCP. Y. Hao et al. obtained the crosslinked poly(lactic acid) (PLA) with different gel fractions by adding small amounts of BIBP and triallyl isocyanurate (TAIC). The crosslinked structure introduced to PLA can enhance the modulus and complex viscosity in the melting state, increase the thermal stability and enhance the crystallization of PLA [134].

Post-crosslinking of PLA oligomers requires the preparation of PLA macromonomers by ROP of lactide and then the functionalization proceeded by a condensation reaction [130]. The crosslinking length is directly linked to the molar masses of the PLA oligomers used. Crosslinking by coupling of functionalized PLA oligomers with unsaturated groups, -OH or other end groups can offer the possibility to tailor the properties *via* the chemical structure, crosslinking density and the length of macromonomers. The chemical crosslinking method involving PLA oligomer terminated with functional end group is shown in Figure 19 [133]. Post-crosslinking of PLA oligomers is also used for PLA-based networks and PLA-based gel [130,132,137,138].

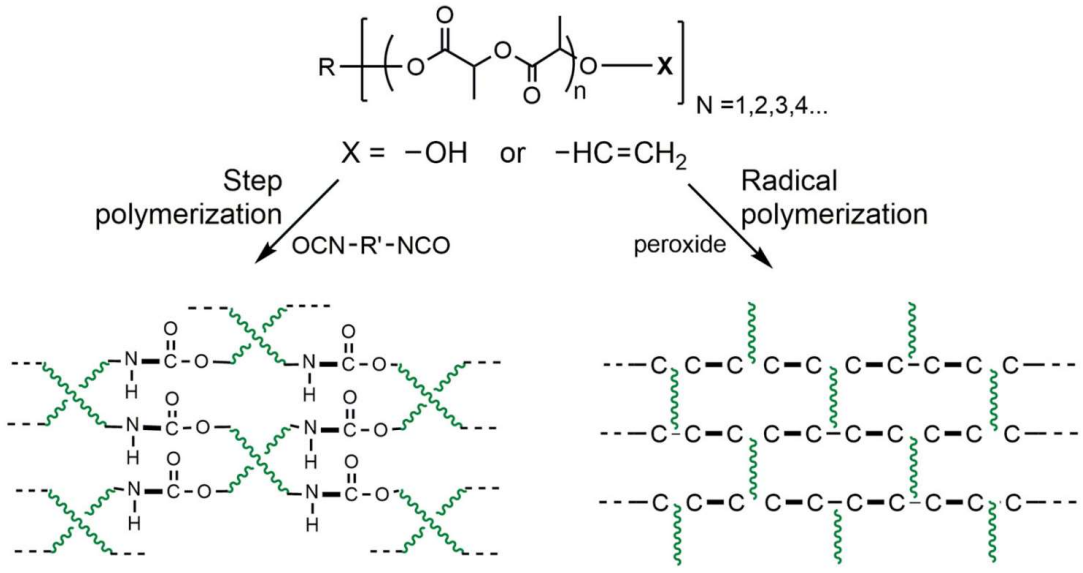

Figure 19. Methods of chemical crosslinking with the participation of PLA oligomers terminated with functional end groups. Reproduced with permission [133] (Copyright 2020, TAYLOR & FRANCIS INC).

Di, tri or tetra functional initiators with hydroxyl groups can initiate the ROP of lactide to obtain bifunctional, 3-arm and 4-arm oligomers. K. Borska et al. synthesized 4-arm PLA oligomers with two different molecular weights, i.e., 3500 and 7000 g/mol, by ROP of D,L-lactide with Di(trimethylolpropane) (diTMP) as initiator and dichloromethane (DCM) /triflic acid as the catalyst. And then, PLA-based networks containing urethane and disulfide linkages were synthesized by coupling hydroxyl-terminated PLA stars with a diol-containing disulfide group using aliphatic diisocyanate. They found that when heated to above 100 ℃, the PLA-based network was rearranged through disulfide exchange, and the hydrogen bond was broken. The ability of disulfide linkages to

rearrange may be influenced by hydrogen bonds leading to lower storage modulus and faster stress relaxation [139]. An interpenetrating polymer network (IPN) is a combination of two independent crosslinked polymers. Because of its special interlocking framework, IPN can form a co-continuous form of microphase separation. G. Rohman et al. synthesized (meso) porous networks using PLA/poly-(methyl methacrylate) (PMMA)-based IPNs, which composed of PLA single network by ROP of D,L-lactide and PMMA single networks with an MMA/DUDMA molar composition of 90/10 mol%. The cross-linked PLA sub-chains can be used as a pore-forming agent template for designing such nanoporous polymer. Two special interlocking frames that make up the sub-networks are related to the extremely favorable dipole-dipole interactions between the ester groups of the main chain from PLA and the ester groups of the side chain of PMMA [140].

2.2. Physical Modification of PLA

2.2.1. Stereocomplex

PLA stereocomplex (PLA-SC) can be formed upon blending enantiomeric PLLA and PDLA or upon the synthesis of stereo block PLA we had viewed in the part of chemical modification of PLA. Due to the higher heat resistance, mechanical performance, and hydrolysis resistance of PLA-SC than the neat PLLA and PDLA, extensive studies have been conducted on PLA-SC in biomedical, pharmaceutical, industrial and environmental applications. Polymers crosslinked by non-covalent interaction have attracted a great deal of attention due to their good mechanical properties and processability [56,60,67]. T.M. Quynh et al. crosslinked PLLA/PDLA stereocomplexes with TAIC by gamma irradiation. Radiation-induced crosslinking improves the thermal stability and mechanical properties of stereo complexes [141]. Y. Zhang et al. applied the Pickering emulsion approach with regenerated cellulose as the reticular structure to prepare the all-biobased, melt-stable, exclusive PLA-SC microspheres in which PLLA and PDLA molecular chains can fully mix and fully combine with the volatilization of solvent. RC can form H-bond with the carbonyl group of PLAs, providing hydrogen bonding sites for the formation of racemic pairs in the PLA-SC matrix. Moreover, regenerated cellulose provided nucleation sites and improved the crystallization property of PLA-SC microspheres after hot pressing (Figure 20) [142]. V. Izraylit et al. prepared PLLA- PCL/PDLA blends by introducing a network of physical cross-links by PLA-SC in blends with PDLA oligomer shown in Figure 21. They tried to study the PLA-SC interacting with the second crystalline component and the influence of its content on the deformation behavior of the whole system *via* PLA-SC as physical net-points at 70 ℃ in PLLA-PCL multiblock copolymer. The mechanical stability of the physical cross-links by PLA-SC in blends with PDLA oligomer is sufficient to provide PLLA-PCL/PDLA blends with an elastic network-like behavior [143].

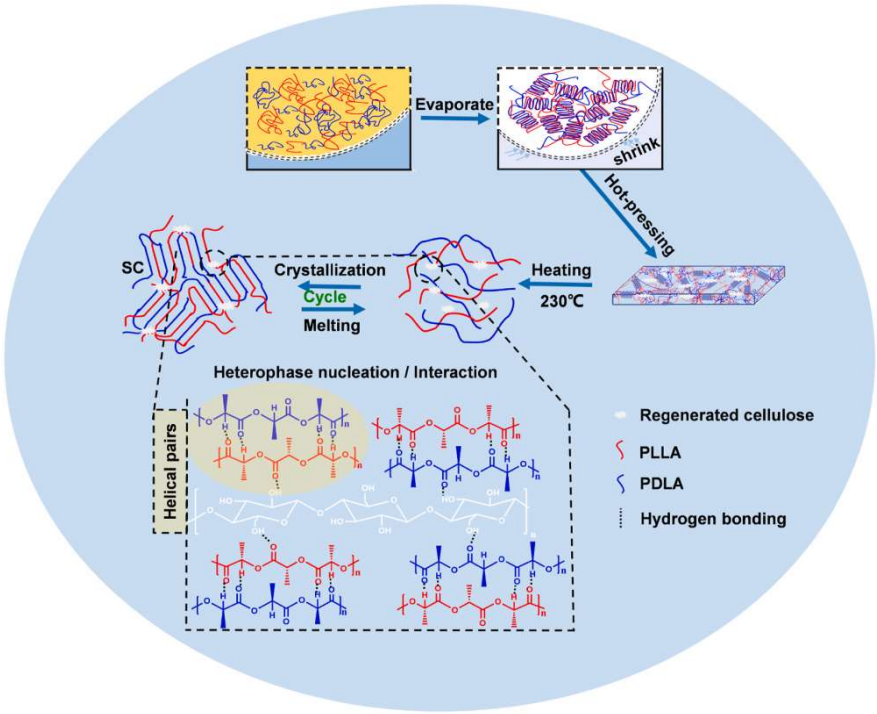

Figure 20. Schematic diagram illustrating the formation of exclusive stereocomplex crystallization and impressive melt stability of stereocomplex-type polylactide *via* Pickering emulsion approach. Reproduced with permission [142] (Copyright 2022, Elsevier Science).

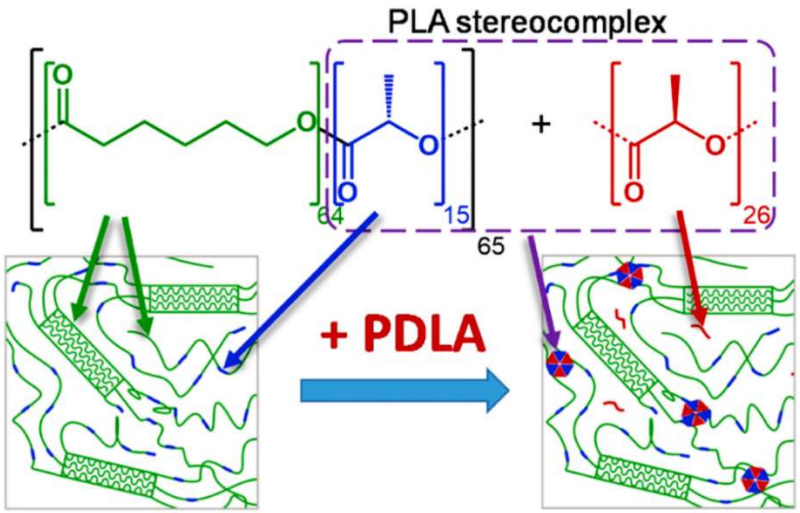

Figure 21. Schematic illustrating PLLA- PCL/PDLA blend structural change upon addition of PDLA homopolymer component. Reproduced with permission [143] (Copyright 2020, Elsevier Science).

2.2.2. Blending

Blending can develop new properties or improve the existing properties of polymer with little or no loss of original performance. Blending PLA with other polymers is an economical and effective approach to tailor the final properties of PLA-based products. According to the compatibility between polymers, polymer blends can be divided into miscible polymer blends, compatible polymer blends and immiscible polymer blends. Compatible polymer blends show good phase morphology, resulting in good physical properties and getting synergistic properties more easily [144]. Incompatible blends are completely immiscible with poor mechanical properties. Interactions between polymer components play an important role in the structure and properties of blends. If the two polymers are incompatible, their interfacial tension will be high. The interfacial tension will be relatively reduced by enhancing the compatibility of two immiscible polymers [145]. One of the important ways to reduce the interfacial tension is to add an interfacial agent called compatibilizer with the molecules arranged along the interface between two polymer phases. Block, graft, or random copolymers containing both similar structure units as the blended two polymer phases can commonly be used as compatibilizers [146–148]. Reactive compatibilization of polymer blends like reactive extrusion can also be used to improve the compatibility of two immiscible polymers by coupling agents or interchange catalysts [149]. Silane coupling agents [150,151], carbodiimide coupling agents [152], isocyanate coupling agents [152–154], biscaprolactam coupling agents [154], epoxide coupling agents [154], anhydride coupling agents [155] and phosphite coupling agents [156] used for modification of PLA-based blends were summarized in Table 4. KH-570 and MDI have better effects on the reactive compatibilization of PLA. Interchange reactions in PLA-based blends are mainly due to the ester exchange reaction between ester and ester, ester and carbonate during melt processing [149]. So interchange catalysts such as tin(II) octoate ($Sn(Oct)_2$), aluminum(III) tri-sec-butoxide ($Al(OsBu)_3$) and titanium(IV) n-butoxide ($Ti(OnBu)_4$) [157], tetrabutyl titanate (TBT) [158] are often used for PLA/polyester blends and PLA/polycarbonate blends.

Table 4. Summary of reactive compatibilization of PLA-based blends.

Polymers/ Composites	PLA	Coupling Agents	T_g (°C)	Tensile Strength (MPa)	Ref.
Wheat straw/PLA composites	4032D	3-aminopropyltrimethoxysilane (APS); γ-glycidoxypropyltrimethoxysilane (KH-560); γ-methacryloxypropyltrimethoxysilane (KH-570); γ-mercaptopropyltrimethoxysilane (KH-590)	N/A	40–50	[150]
PLA/Thermally expanded vermiculite composites	3100HP	bis(2,6-diisopropylphenyl)carbodiimide (KI); 4,4′-methylenebis(phenyl isocyanate) (MDI)	63–66	58–63	[152]
PLA/PEBA Blends	2003D	Poly(ethyleneco-methyl acrylate-co-glycidyl methacrylate) (PEAGM); poly(maleic anhydride-alt-1-octadecene) (PMAOD); 1,1′-carbonyl biscaprolactam (CBC); 4,4-methylene diphenyl diisocyanate (MDI)	53–60	35–40	[154]
PLA-reinforced natural fiber composites	3001D 3251D	Maleic anhydride (MA), dicumyl peroxide (DCP)	61.2	50–62	[155]

From the industrial point of view, semi-crystalline polymers like PLA blends are extremely important [144]. Blending of semi-crystalline polymers can be carried out by blending of two semi-crystalline polymers such as PLA/PCL blends [159], or blending of semicrystalline polymer with an amorphous polymer such as PLA/PPC blends [160]. Blending PLA with flexible or elastic polymers is the simplest and most effective strategy for toughening, improving the ductility and heat deflection temperature of PLA [36,161–163]. As PLA is a kind of bio-based/biodegradable biopolymer with excellent degradation performance, we hope that PLA based blends still maintain good biodegradability. Therefore, we mainly focus on blending PLA with other biodegradable polymers such as polycarbonates, polyester and polyether.

- PLA/Polycarbonate Blends

Y. Yuryev et al. modified polycarbonate (PC Hylex P1025L1HB)/PLA blends by using poly(ethylene n-butylene acrylate glycydyl methacrylate) (EBA-GMA) pellets as the compatibilizer and the multifunctional styrene-acrylic-epoxy random oligomer (Joncryl ADR) as chain extender, studied the hydrolytic degradation of PC/PLA blends and discussed mechanisms of degradation and water transport in polymer blends. The degradation of the blends began with the formation of pits on the polymer surface, which became the entry point for water to enter the polymer quickly, and then areas of accelerated degradation occurred along these pathways. The schematic of degradation inhibition *via* water diffusion limiting in PC/PLA/EBA-GMA blends is shown in Figure 22 [164]. They also prepared biobased PC/PLA glass fiber composites using linear PC/PLA blends and branched PC/PLA blends according to this method. PC/PLA glass fiber composites have excellent heat resistance due to co-continuous morphology, in which all the impact modifier phases are concentrated in the PLA phase [165]. V. Gigante et al. prepared the recycled PLA/PC co-continuous blends by reactive extrusion with triacetin and tetrabutylammonium tetraphenylborate as catalysts for the interchange reactions. After upcycling, the ductility of recycled-PLA/recycled-PC blends was improved compared with the pure recycled PLA [166].

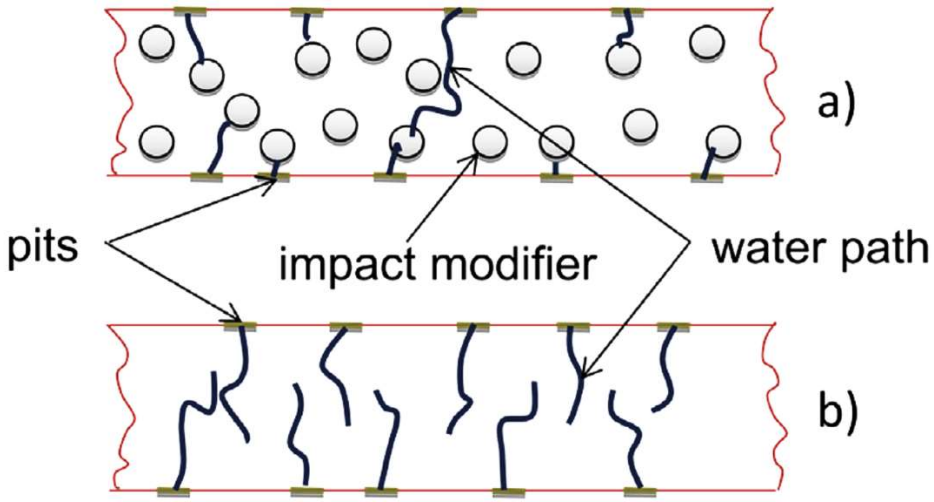

Figure 22. Schematic of degradation inhibition *via* water diffusion limiting in PC/PLA/EBA-GMA blends: (**a**) an impact modified PC/PLA/EBA-GMA blend; (**b**) non-modified PC/PLA blend. Reproduced with permission [164] (Copyright 2016, Elsevier Science).

Polypropylene carbonate (PPC) is an amorphous thermoplastic polymer. PPC could be used to prepare not only PLA-*b*-PPC copolymers introduced in chemical modification of PLA, but also PLA/PPC blends due to its high compatibility and impact resistance. PLA/PPC blends can be directly prepared by the melt-mixing method. With the amount of PPC increasing, the elongation at break of PLA/PPC blends increased, whereas the tensile strength decreased [89,160,167]. Therefore, it is necessary to further improve the compatibility between PLA and PPC, such as adding compatibilizers or a third component that can react with PLA or PPC to prepare blends with ideal properties by reactive extrusion. Z. Wang et al. introduced SiO_2-*g*-PLA/PPC into PLA/PPC blends to enhance the performance of PLA material. The SiO_2-*g*-PLA/PPC was synthesized *via* the "grafting to" method, and then PLA/PPC blends with SiO_2-*g*-PLA/PPC as processing modifier were prepared by melt blending at 165 °C [168]. L. Zhou et al. prepared PLA/PPC-MA blends by the melt-processing with maleic acid anhydride (MA) end-capped PPC-MA and PLA using Tetrabutyl titanate (TBT) as the catalyst [158]. Low molecular weight reagents can also be used to improve the properties of PLA/PPC blends, such as 2,4-toluene diisocyanate (TDI) [169], diphenylmethane 4,4 diisocyanate (MDI) [170].

- PLA/Polyester Blends

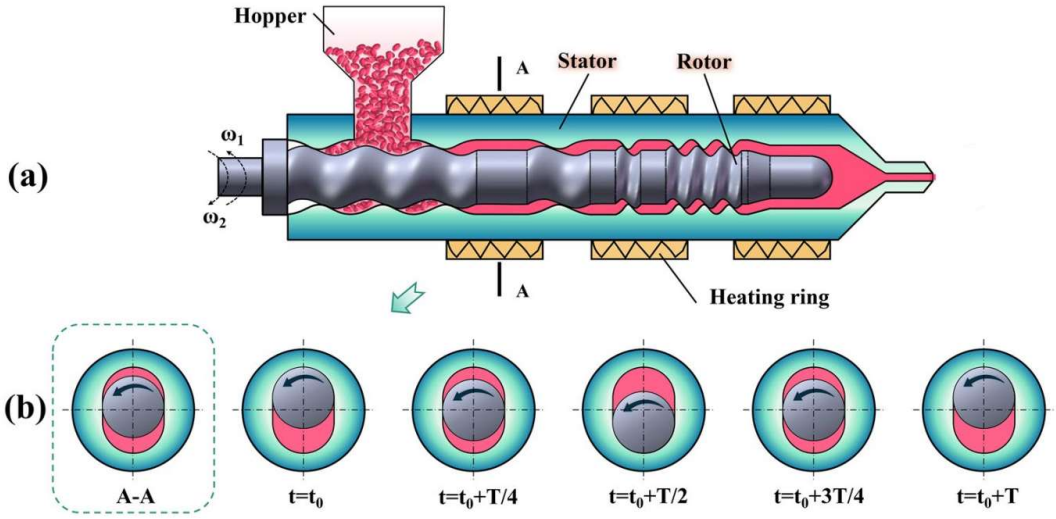

Figure 23. Schematic configuration of eccentric rotor extruder (**a**) and A-A cross-section evolution (**b**) during rotator rotating. Reproduced with permission [171] (Copyright 2022, Springer Nature).

Polycaprolactone (PCL) is a semi-crystalline biodegradable polyester. PLA/PCL blends can enhance the toughness of PLA with good biocompatibility and biodegradability. Solution blending and melt blending are widely used to prepare PLA/PCL blends and composites. T. Patrício and P. Bártolo prepared PCL/PLA blends with different percentages by solvent casting method [172]. A.K. Matta et al. extruded PLA/PCL blends by melt blending at 170 °C. The addition of PCL could accelerate the crystallization rate of PLA, but had little effect on its final crystallinity [159]. The polymer melt usually bears complex stress in an instant when being extruded. PLA/PCL blends show lower cold crystallization temperature and higher crystallinity when extruded by an eccentric rotor extruder (ERE) than by a twin screw extruder (TSE). This shows that ERE can improve the crystallization rate of PLA and can be used to expand the commercial application of PLA. Schematic configuration of eccentric rotor extruder and A-A cross-section evolution during rotator rotating is shown in Figure 23 [171]. K.M.V. Voorde et al. prepared PLA/PCL fibers using multilayer coextrusion and explored morphological effects on the mechanics of the fibers. They found that the addition of PCL increased the ductility and toughness, especially for the blends with co-continuous morphology [173].

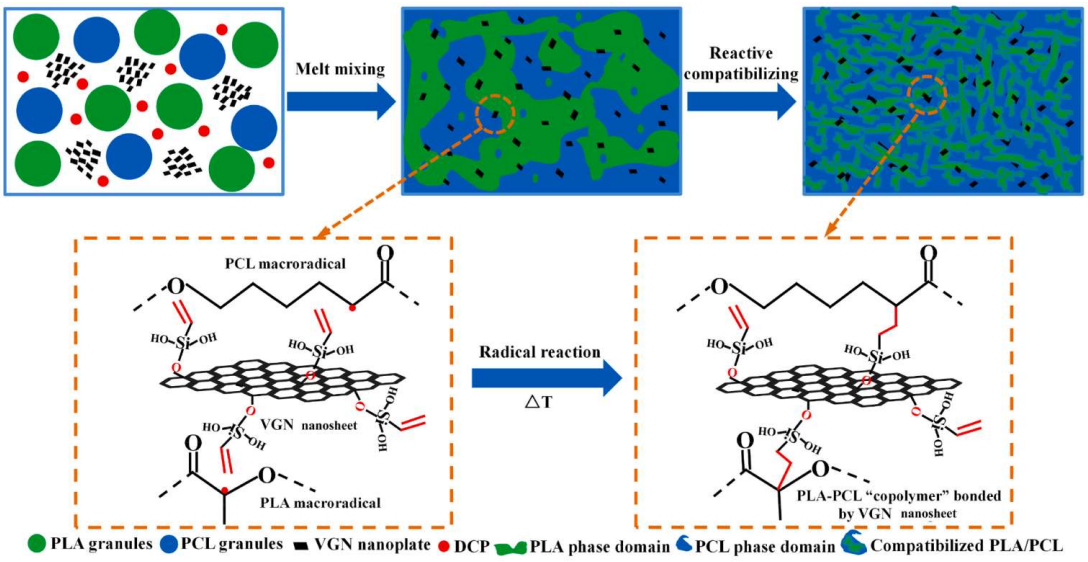

Figure 24. Schematics of compatibilizing PLA/PCL blend using reactive graphene (VGN) with the aid of DCP during melt mixing. Reproduced with permission [174] (Copyright 2022, Elsevier Science).

As PLA and PCL are immiscible, many approaches to improve the compatibility and interfacial adhesion between PLA and PCL, such as block copolymer used as compatibilizers. P.P. Dias and M.A. Chinelatto added low molecular weight ε-caprolactone-tetrahydrofuran-ε-caprolactone triblock copolymer to promote better interaction between PLA and PCL phases [175]. Because of the amphiphilic structure and self-assembly characteristics of ionic liquids (IL), organic/inorganic molten salts can be used to adjust

the aggregation structure of polymers and enhance the macro properties of materials during the melting process. There are more and more studies on the use of block copolymers containing ionic elements as interfacial compatibilizers and regulators for PLA/PCL blends. P. Wang et al. introduced PCL-*b*-PEG and its derivative containing ionic elements (Ils) into PLA/PCL blends by solution blending. The introduction of Ils into PLA/PCL blends can improve the crystallinity, tensile strength and elongation at break [176]. PLA/PCL blends could also be compatibilized by adding nanoparticles as compatibilizers and reinforcers simultaneously during melt mixing. B. Wang et al. prepared PLA/PCL blends using vinyl functionalized graphene (VGN) as a highly efficient compatibilizer with the aid of DCP. The strong interfacial interactions due to molecular chains reacting with the vinyl groups of VGN with the aid of DCP improved the storage modulus of PLA/PCL/VGN nanocomposites (Figure 24) [174].

The blending research of other commercially available biodegradable polyesters and PLA is very extensive, such as polyhydroxyalkanoates (PHAs), poly(butylene succinate) (PBS), polyglycolic acid (PGA) and PBAT. PHAs are water-insoluble polyesters produced by the fermentation of natural resources (especially sugars or lipids), mainly made of saturated and unsaturated hydroxyalkanoic acid [177]. M.A.V. Fuentes et al. improved the 3D printability and enhanced the mechanical properties of poly(ε-hydroxybutyrate-co-ε-hydroxyvalerate) (PHBV)/PLA blends *via* a functionalized styrene-acrylate copolymer with oxirane moieties as a chain extender using fused filament fabrication [178]. PBS and PLA blends were mixed in chloroform modified by benzoyl peroxide (BPO) as a cross-linking agent. The addition of BPO improved the compatibility and hydrophilicity of PBS/PLA blends [179]. PGA is a biodegradable polyester with a similar chemical structure but different characteristics to PLA. Due to high stereo regularity, PGA has high thermal deformation temperature and good mechanical properties [180]. PGA/PLA blends can be blended by extracting the required amount of polymer from PGA and PLA dissolved in 1,1,1,3,3,3,-hexafluoro-2-propanol HFP [181]. The introduction of PLA/PBAT blends is highlighted in the subsequent modification of PBAT.

- PLA-Polyether Blends

M. Sheth et al. prepared PLA/PEG blends by melting using a counterrotating twin-screw extruder and studied the effect of PEG dosage on mechanical properties. When the PEG content is lower than 50%, PEG makes PLA plasticized, resulting in higher elongation and lower modulus. When the PEG content exceeds 50%, the morphology of the blend is driven by the increase of the crystallinity of PEG, resulting in an increase in modulus and a corresponding decrease in elongation at break [182]. T. Nazari and H. Garmabi prepared PLA/PEG blends fibers *via* melt electrospinning with the PEG concentration varying from 0 to 30wt%. At the spinning temperature of 200 ℃ and PEG content of 30%, PLA/PEG blends microfibers with 5.9 ± 1.7 μm can be obtained [183]. PEG is known as poly(ethylene oxide) (PEO) when the molecular weight is up to 2 million [184]. W. Kong et al. prepared PLA/PEO blends by melt blending *via* a flexible polymer PEO **(**average molecular weight of 2.0×10^6 $g \cdot mol^{-1}$) nucleated by N,N′,N″-tricyclohexyl-1,3,5-benzenetricarboxylamide (BTCA) as self-assembly nucleating agent with PLA. Blending with PEO can increase the elongation at break and promote crystallization of PLA [185].

3. Modification of PBAT

3.1. Chemical Modification of PBAT

3.1.1. Improvement on the Synthesis

PBAT is a fossil-based biodegradable aliphatic-aromatic co-polyester obtained from 1,4-butanediol (BDO), terephthalic acid (TPA) and adipic acid (AA), which has highly complex micro-structure with well-differentiated soft segment and hard segments domains [186–188]. Due to the good degradability and excellent mechanical properties of PBAT, many PBAT-based products have been used in the fields of shopping bags, garbage bags, tableware, mulching film and so on. There have been many studies on the synthesis, modification and degradation of PBAT in the past two decades [32]. W. Neng et al. prepared high molecular weight PBAT (Mn 40~50kDa) thermoplastic elastomer with methyl branch introduced into the main chains from the monomers of 3-methyl adipic acid (AA_m), BDO, and TPA using tetrabutyl titanate (TBT) as a catalyst *via* a process of esterification and polycondensation. They constructed PBA_mT copolymers by soft segment PBA_m and rigid segment PBT. With the increase of rigid segment, the crystallinity of PBA_mT was improved significantly, leading to excellent strength. However, the increase of soft segment makes PBA_mT more elastic [189].

I.E. Nifant'ev et al. synthesized long-chain branched PBAT by using branching agents *via* a direct polycondensation of BDO, AA and dimethyl terephthalate (DMT) in the presence of titanium (IV) butoxide ($Ti(Obu)_4$). Introducing long-chain branch to the polymer backbone is an efficient method to reduce film thickness and enhance film strength. They studied branching agents (Bas) **1–7** in the two-stage polycondensation and found that **2** and **5** represented an excellent branching agent for the synthesis of PBAT due to their higher thermal stability [187]. They also studied Aryloxy 'biometal' complexes as efficient catalysts for PBAT synthesis. They use low-MW PBAT as the starting material for further experiments to synthesize high-MW PBAT in the presence of aryloxy complexes and $Ti(Obu)_4$. Mg phenolates complexes **8** and Zn phenolates complexes **9** showed low catalytic activity in PBAT formation, while Al complexes with 2,6-di-tert-butyl-4-methylphenate **10a–c** which 'generally recognized as safe' by US FDA represented excellent catalysts for the synthesis of PBAT [190]. Branching agents **1–7** and aryloxy 'bio-metal' complexes in the synthesis of PBAT are shown in Figure 25.

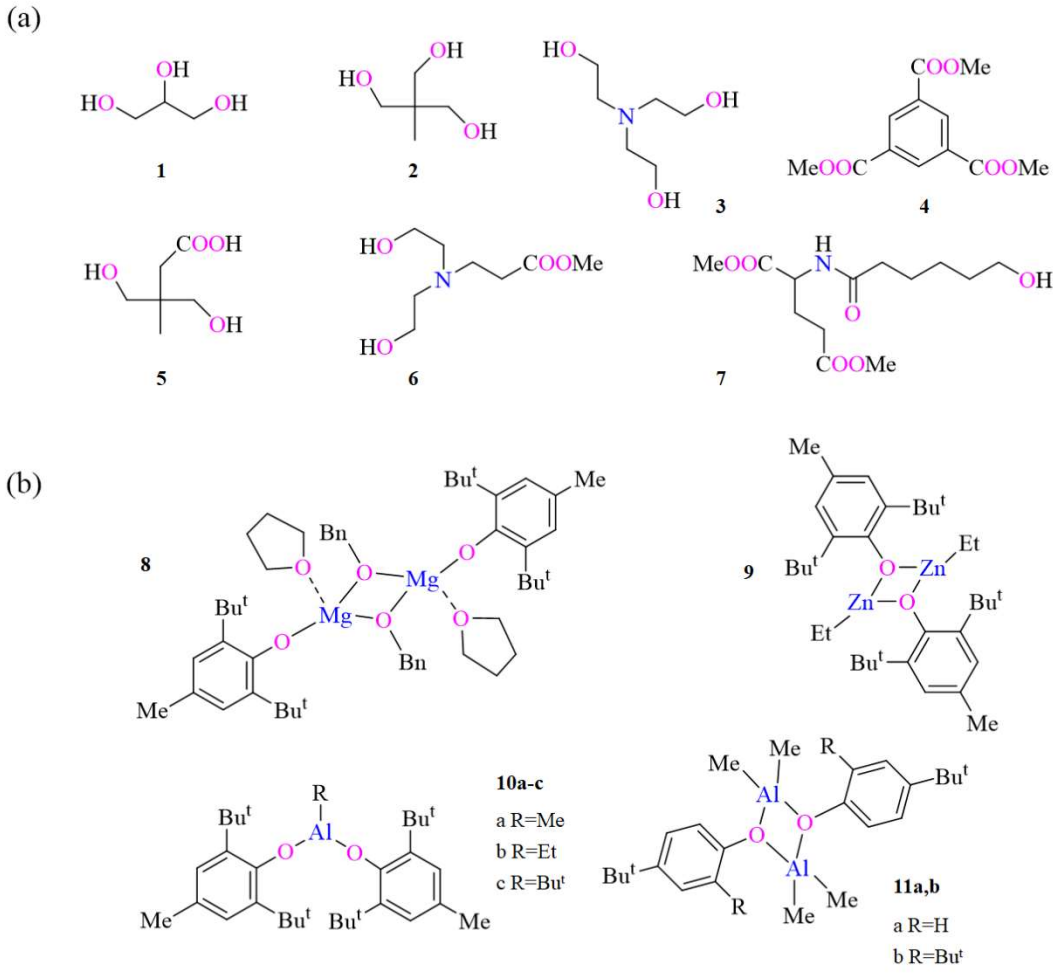

Figure 25. (**a**) Branching agents **1–7** Reproduced with permission [187] (Copyright 2022, MDPI) and (**b**) aryloxy 'biometal' complexes Reproduced with permission [190] (Copyright 2022, Elsevier Science) in the synthesis of PBAT.

3.1.2. Copolymerization

Since PBAT is a synthetic linear aliphatic-aromatic co-polyester, the copolymerization modification of PBAT mainly involves the addition of monomers or polymers during the synthesis process [191]. PEO-*b*-PPO-*b*-PEO tri-block copolymers (Pluronic F127) are commonly used as macromolecular additives and widely used in many fields, such as surfactants, microfluidic devices and 3D printing. D. Mahata et al. synthetized Pluronic-functionalized PBAT (PPBAT) copolymer with Pluronic F127 as a secondary diol monomer *via* a two-step melt polycondensation reaction using the esterification pathway. The oligomers were prepared by BDO, AA, TPA and Pluronic at 200 °C in the first step and then it was used to synthetized PBAT random co-polyester at 230 °C for a polycondensation reaction. With the increase of Pluronic, the thermo-responsive properties and the plasticization effect of PPBAT copolymer are improved [192]. R. Li et al. synthesized PEG-*mb*-PBAT multiblock copolymers via chain extension/coupling of PEG and PBAT diols using HDI as an extension/coupling agent and then applied the copolymers as modifiers to prepare PLLA/PEG-*mb*-PBAT blends. PLLA/PEG-*mb*-PBAT blends have highly improved toughness and excellent ductility due to the immiscible PBAT segments forming compatibilized microphases and acting as effective toughening (Figure 26) [188].

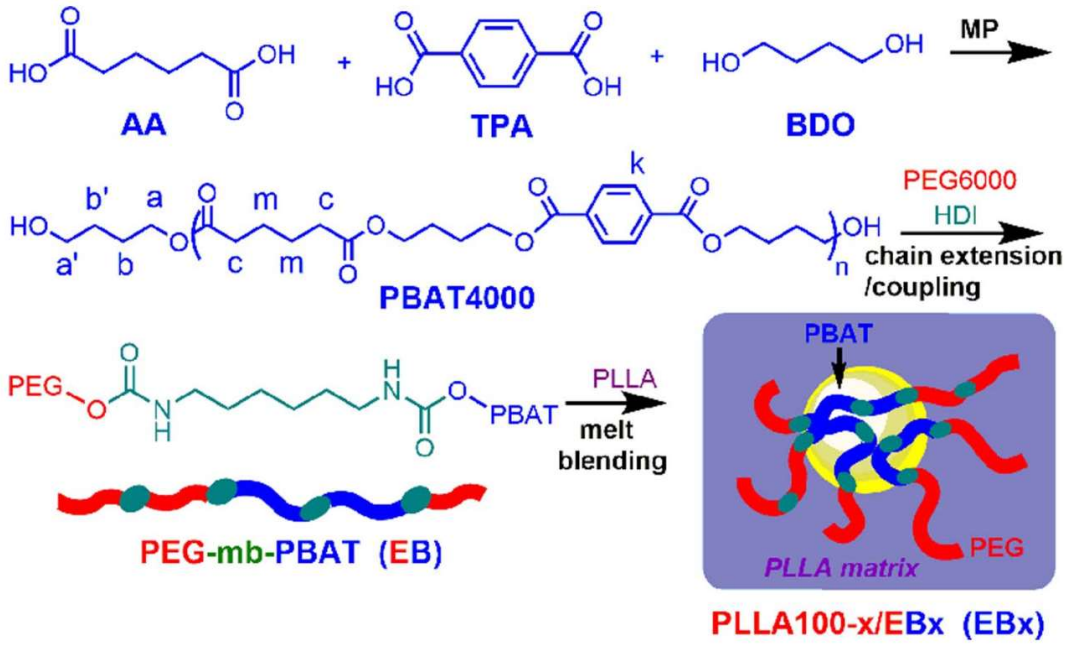

Figure 26. Schematic diagram of preparation of PLLA/PEG-mb-PBAT blends. Reproduced with permission [188] (Copyright 2018, Elsevier Science).

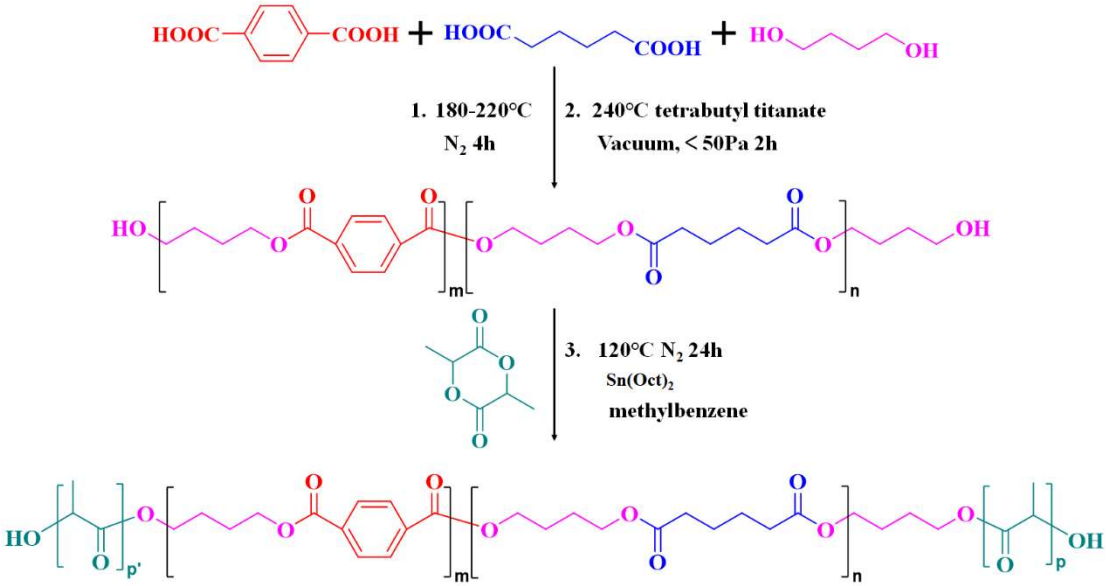

Figure 27. Reaction route for PLA-PBAT-PLA tri-block copolymers. Reproduced with permission [193] (Copyright 2018, Elsevier Science).

Z. Sun et al. prepared HO–PBAT–OH macro-initiators by polycondensation of DMT, AA, and BDO using $Sn(Oct)_2$ as a catalyst with BDO overdosed to ensure that PBAT was terminated by –OH on both ends. The HO–PBAT–OH was used to initiate the ROP of L-lactide to obtain PLLA–PBAT–PLLA tri-block copolymers, which were applied as compatibilizers for PLA/PBAT blends [194]. Y. Ding et al. also synthesized PLA–PBAT–PLA tri-block copolymers with different chain lengths to improve the compatibilization of PLA/PBAT blends. They found that due to the long chains interpenetrating better with the relevant homopolymers and increasing the entanglement density, the PLA–PBAT–PLA triblock copolymer with long chain PLA had more effective compatibility for PLA/PBAT blends. The reaction route for PLA-PBAT-PLA tri-block copolymers is shown in Figure 27 [193].

3.1.3. Grafting

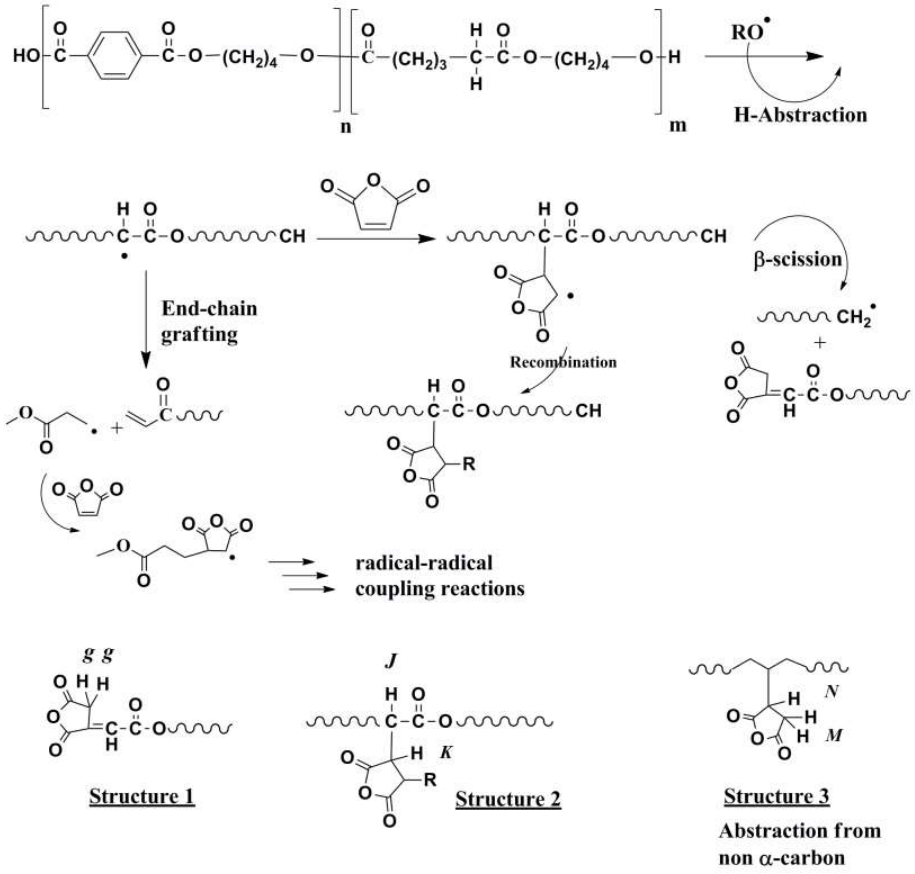

Figure 28. Reaction scheme showing the mechanism of MA grafting onto PBAT chains followed by subsequent termination routes. Reproduced with permission [195] (Copyright 2017, AMER CHEMICAL SOC).

Acrylic acid (AA), maleic anhydride (MA), Glycidyl methacrylate (GMA) and (ethylene-methyl acrylate-glycidyl methacrylate) (EMAG) can be used to graft PBAT, and then the grafting PBAT is used for blending reactions. Chin-San Wu introduced AA into molten PBAT using benzoyl peroxide (BPO) as the initiator, and then formed the PBAT-*g*-AA/MWCNT-OH hybrid material by polycondensation reaction between the carboxylic acid group of PBAT-*g*-AA and hydroxyl group of MWCNT-OH [196], and PBAT-*g*-AA/ polyaniline (PANI) material by an amide bond between PBAT-*g*-AA and PANI [197]. The grafting of maleic anhydride (MA) for functionalizing polyesters using a free-radical initiator is a well-known reaction. Maleic anhydride (MA) grafted PBAT (PBAT-*g*-MA) can be used to improve interfacial compatibility to prepare PBAT-based blends or composites such as PBAT-*g*-MA/SiO_2 composites [198], PBAT-*g*-MA/peanut husks composite [199], PBAT-*g*-MA/cellulose acetate composite films [200], PBAT/Sunflower head residue composites [201], PBAT-*g*-MA/modified layered zinc phenyl phosphonate (m-PPZn) [202,203] and PBAT-*g*-MA/cellulose nanocrystal [195,204]. S.K. Rahimi et al. obtained cellulose nanocrystal (CNC)-reinforced MA-*g*-PBAT bio-nanocomposites *via* reactive extrusion process and analyzed the mechanism of MA grafting onto PBAT chain and the subsequent termination path (Figure 28) [195].

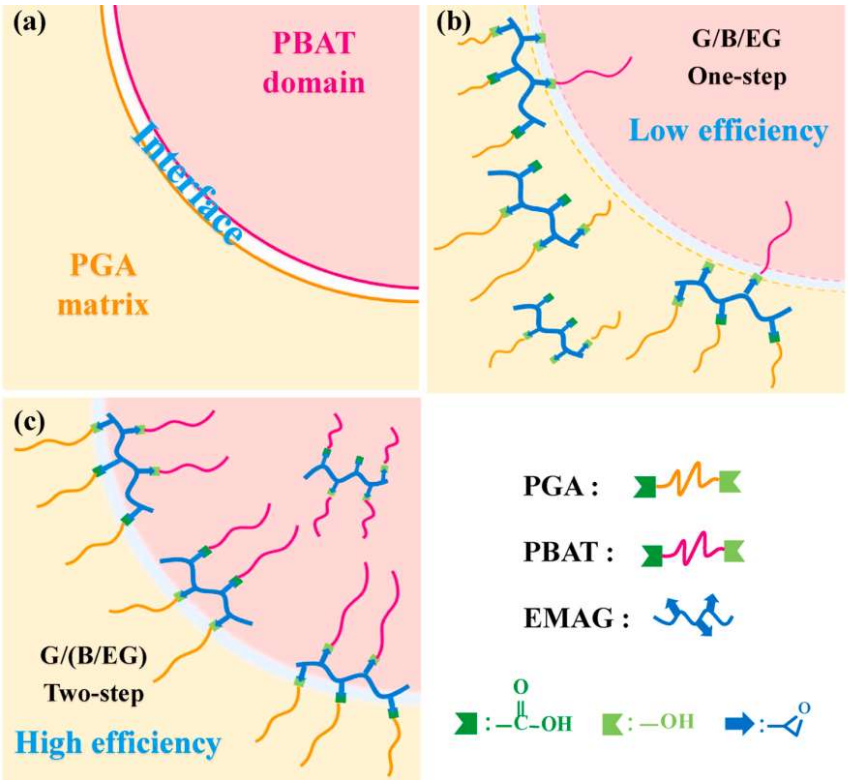

Figure 29. Schematic illustration of the morphology and the compatibilization mechanisms of (**a**) PGA/PBAT, (**b**) PGA/PBAT/EMAG, (**c**) PGA/PGA-*g*-EMAG-*g*-PBAT/PBAT blends. Reproduced with permission [205] (Copyright 2021, Elsevier Science).

J.M. Raquez et al. prepared maleated thermoplastic starch (MTPS) *via* reactive extrusion processing of starch in the presence of glycerol as plasticizer and MA as esterification agent, and then prepared PBAT/MTPS blends through reactive extrusion processing. They selectively obtained PBAT-*g*-MTPS graft copolymers through transesterification reactions for 60 and 70 wt% polyester fractions. The Tensile properties of the MTPS-*g*-PBAT graft copolymers with 70wt% polyester were much higher than TPS-*g*-PBAT copolymers in the presence of MA [206]. GMA could be expected to be an alternative to MA and used to graft onto hydrophobic polymer backbones *via* reactive extrusion. M. Xiao et al. prepared PBAT-*g*-GMA copolymer by melt grafting GMA using BPO as the initiator. PBAT-*g*-GMA copolymers were used as a compatibilizer for PBAT/thermoplastic starch (TPS) blends by melt mixing [207]. D. Niu et al. prepared PGA/PBAT/EMAG blends in two ways. One of them is preparing PBAT/EMAG mixtures first and subsequently compounding the PBAT/EMAG mixtures with PGA. According to this method, they *in-situ* formed PGA-*g*-EMAG-*g*-PBAT copolymers by the reaction between epoxy groups of EMAG and hydroxyl/carboxyl groups of PGA and PBAT. PGA-*g*-EMAG-*g*-PBAT copolymers as a bridge to transfer more effective energy from PGA matrix to PBAT domain enhanced the interfacial adhesion and compatibility of PGA/PBAT blends (Figure 29) [205].

3.1.4. Crosslinking

The crosslinking of PBAT can be realized by electron beam induced crosslinking, chemical micro-crosslinking or adding crosslinking agent to improve its thermal and mechanical properties. Electron beam induced crosslinking is a promising physical modification technology for biodegradable polymers and can also be used for the crosslinking modification of PBAT [208–210]. Chemical micro-crosslinking or adding crosslinking agents are mainly used for PLA/PBAT blend. B. Wang et al. used epoxy-terminated branched polymer (ETBP) as an interface compatibilizer to modify the PLA/PBAT (70/30) blends. They found that both physical and chemical micro-crosslinking were formed through the strong physical hydrogen bonding and chemical micro-crosslinking reaction between the epoxy groups of ETBP and the terminal groups with PLA and/or PBAT. The physical and chemical micro-crosslinking can improve the elongation at break and impact strength and change the structure of PLA/PBAT blends from a linear structure to 3D micro-crosslinking network structure [211]. Crosslinking agents such as 2,5-Dimethyl 2,5-di(tert-butylperoxy) hexane [212] and bis(tertbutyl dioxy isopropyl) benzene [213] can be used to increase the elongation at break of PLA/PBAT blend.

3.2. Physical Modification of PBAT

3.2.1. Blending with Biodegradable Biopolymer

PBAT is also a biodegradable biopolymer with excellent degradation performance. We hope that PBAT-based blends still have degradation capability. We mainly focus on blending PBAT with other biodegradable polymers such as polycarbonates, polyester and polyether. Many polycarbonates (e.g., PPC, PTMC, PC) and polyester (e.g., PLA, PCL, PHBV, PBS) have been used for preparing PBAT-based biodegradable polymers blends, while few work was reported to blend polyether with PBAT due to the similar flexibility of PBAT and polyether. Polyether may be used as a compatibilizer for PBAT-based blends.

- PBAT/Polyester Blends

PBAT and PLA offer complementary functional properties as discussed in previous paragraphs. PBAT is a flexible material with high elongation at break and low Young modulus, whereas PLA is a rigid material with low elongation at break and high Young modulus. PLA/PBAT blends are highly synergistic biodegradable polymers, so they play an important role in the research of PBAT-based blends. PLA/PBAT blends can be prepared by the melt-mixing extrusion, reactive extrusion or solvent casting. L. Wang et al. prepared PLA/PBAT blends by solvent casting method. They dissolved PLA and PBAT into chloroform respectively, and then formed PLA/PBAT films by pouring PLA/PBAT solutions with different mixing ratios onto Teflon coated glass plate. The properties of PLA/PBAT films can be adjusted by changing the blend ratio of PLA and PBAT [214]. Melt mixing extrusion is the most widely used method for preparing PLA/PBAT blends, and it is also the preferred method for industrial production. H. Xiao et al. prepared PLA/PBAT blends by melt-mixing the neat PLA and PBAT granules at 185 °C and investigated the isothermal crystallization kinetics of PLA/PBAT blends, founding that the crystallization mechanism of PLA/PBAT was similar to the crystallization mechanism of PLA [215]. E.J. Dil et al. studied the morphology and miscibility of PLA/PBAT blends. They found that because the approximate equivalent cohesive energy density between PLA and PBAT leads to negligible energy change and very small mixing enthalpy, the unidirectional partial miscibility of PBAT was found in the PLA/PBAT enriched phase [216]. Unidirectional partial miscibility may be an important factor in determining the success of melt blending of PLA and PBAT. Y. Deng et al. investigated the synergistic effects of PLA/PBAT blends by melt-mixing extrusion method *via* a range of melt-blended compounds at various PLA/PBAT weight ratios and validated that the concentration of PBAT in the co-continuous phase structure in the PLA matrix was about 19%. In the range of PBAT weight from 10% to 20%, the elongation at break of PLA/PBAT blends increased sharply from about 10% to 300%. Schematic diagram and elongation at break of PLA/PBAT blends are shown in Figure 30 [217].

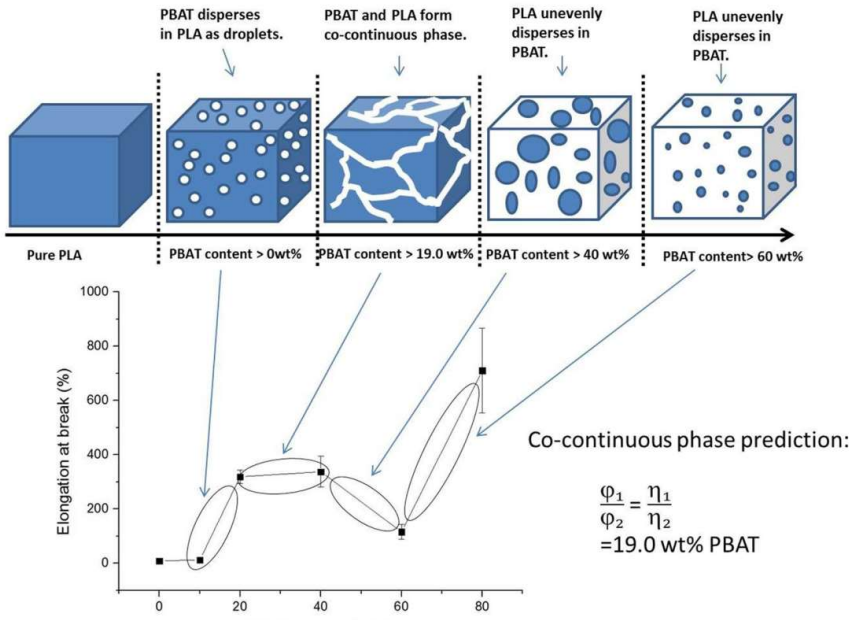

Figure 30. Schematic diagram of phase structure as a function of composition and elongation at break of PLA/PBAT blends. Reproduced with permission [217] (Copyright 2018, Springer Nature).

The unidirectional partial miscibility and co-continuous phase structure of PBAT in PLA matrix could not meet the requirements of melt miscibility of blends, especially for industrial production. It is an important strategy to improve the compatibility of PLA/PBAT blends by using copolymers or compatibilizers to increase the miscibility and obtain better homogeneity. We have introduced some PBAT-based block copolymers and graft copolymers for compatibilization of PLA/PBAT blends in chemical modification of PBAT. In addition to PBAT-based copolymers, some other copolymers can be used for the

compatibilization of PLA/PBAT blends. Y. Ding et al. synthesized PLA-PEG-PLA tri-block copolymers with different chain lengths [218] and MPEG-PLA di-block copolymers [219] as effective compatibilizers to improve the interfacial adhesion of PLA/PBAT blends. X. Sui et al. prepared PLA/PBAT blends with random PMMA-co-GMA copolymer as a compatibilizer. PMMA-co-GMA copolymer is a macromolecular methyl methacrylate-co-glycidyl methacrylate (MG) reactive epoxy copolymer, which formed PBAT-co-MG-co-PLA macromolecules by the compatibilization reaction to promote the homogeneous dispersion and reduction of particle size of PLA phase and induce the higher crystallization temperature of PBAT (Figure 31) [220].

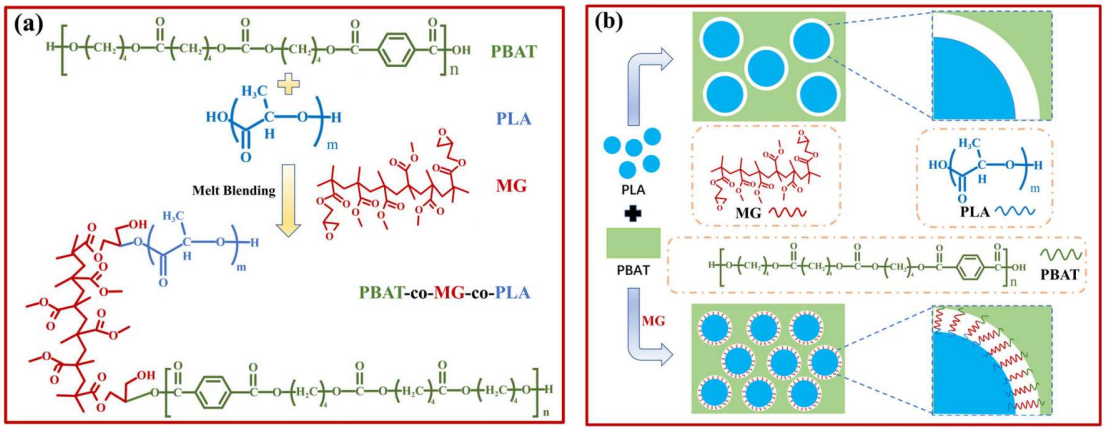

Figure 31. Schematics for compatibilization reaction (**a**) and interface emulsification mechanism (**b**) Reproduced with permission [220] (Copyright 2022, Wiley).

Compatibilizers can form at surfaces or provide an interphase for PLA/PBAT blends. The functional groups such as epoxy groups in the compatibilizer interact with carboxyl and/or hydroxyl groups of PLA and/or PBAT to enhance the interface adhesion and phase dispersion, and improve the compatibility of the system [221]. D.D. Wu et al. studied the effect of ADRs as chain extenders on the properties of PBAT/PLA blends and found the modification effect was in the order of ADR4368>ADR4380> ADR4370. ADR4368 can significantly improve the intermolecular entanglement of the blend, enhance the interfacial adhesion of the blend, and increase the compatibility of the blend. The addition of ADRs enhanced the thermal stability of the blends [222]. P. Wang et al. prepared PLA/PBAT/MWCNTs composites using multifunctional epoxy oligomer (ADR) as a chain extender to enhance the compatibility. They fabricated different types of multi-walled carbon nanotubes (CNTs) such as hydroxyl and carboxyl-functionalized CNTs. ADR can orient CNTs-OH at the interface between PLA and PBAT, but agglomerate CNTs-COOH in the PABT phase (Figure 32) [223]. Y. Han et al. prepared PLA/PBAT blends using epoxidized soybean oil (ESO) as a compatibilizer *via* the chemical reaction of ESO with terminated hydroxyl/carboxyl groups of PLA and PBAT. ESO is an environmentally friendly, renewable and low-cost reactive compatibilizer with high epoxy value which is easy to react with the hydroxyl/carboxyl terminated groups of the PLA and PBAT during the blending process to form branched polymers and microgels (Figure 33) [224].

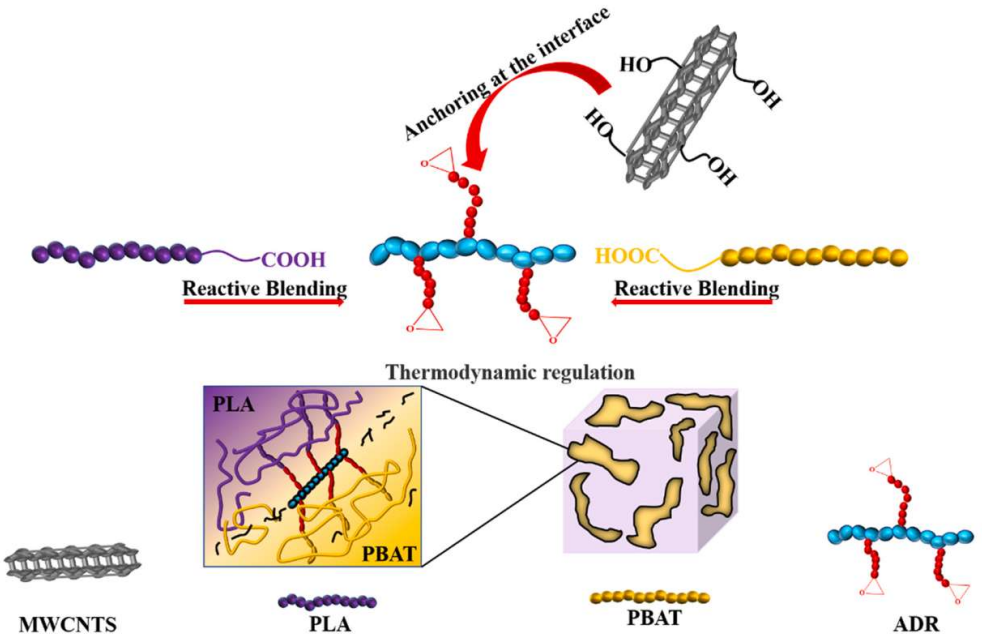

Figure 32. Enhancement mechanism of the PLA/PBAT composites. Reproduced with permission [223] (Copyright 2022, Elsevier Science).

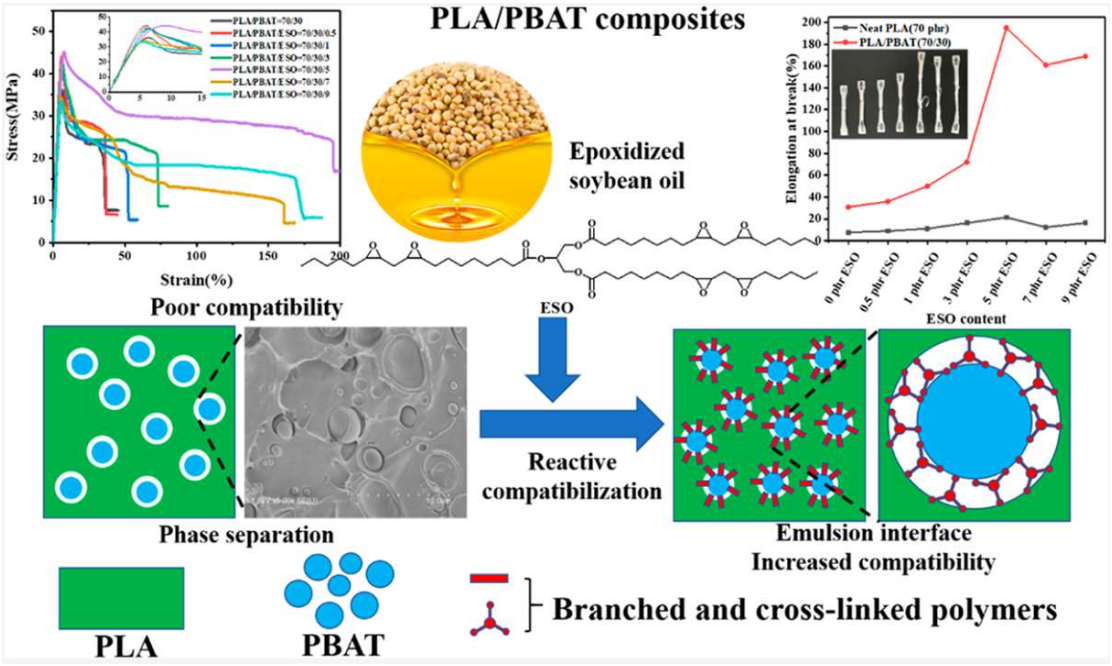

Figure 33. PLA/PBAT Composites with Epoxidized Soybean Oil as Compatibilizer. Reproduced with permission [224] (Copyright 2020, AMER CHEMICAL SOC).

The comprehensive properties of PLA/PBAT can be improved by the synergistic effect of organic reactive compatibilizing and toughening with the inorganic particles in strengthening and promoting crystallization. Y. Lyu et al. prepared PLLA/PBAT biodegradable nanocomposites with SiO_2-PDLA as fillers and PLLA-*g*-GMA as the compatibilizer and achieved controllable "strength-toughness transition''. They found that SiO_2-PDLA reacted with PLLA-*g*-GMA to form initial stereocomplex crystallites (SC), then excessed SiO2-PDLA and PLLA continued to combine to form new SC leading to the content of SC reaching 69.2% when the nanocomposite contained 5 wt% SiO_2-PDLA. The temperature of the 3D printing nozzle can induce the "strength-toughness transition". At 180 °C, tensile strength was improved due to the homogeneous distribution of SC and SiO_2-PDLA, while at 210 °C, the toughness was improved because SC melted and the PDLA coated-SiO_2 acted as a low molecular weight plasticizer (Figure 34) [33].

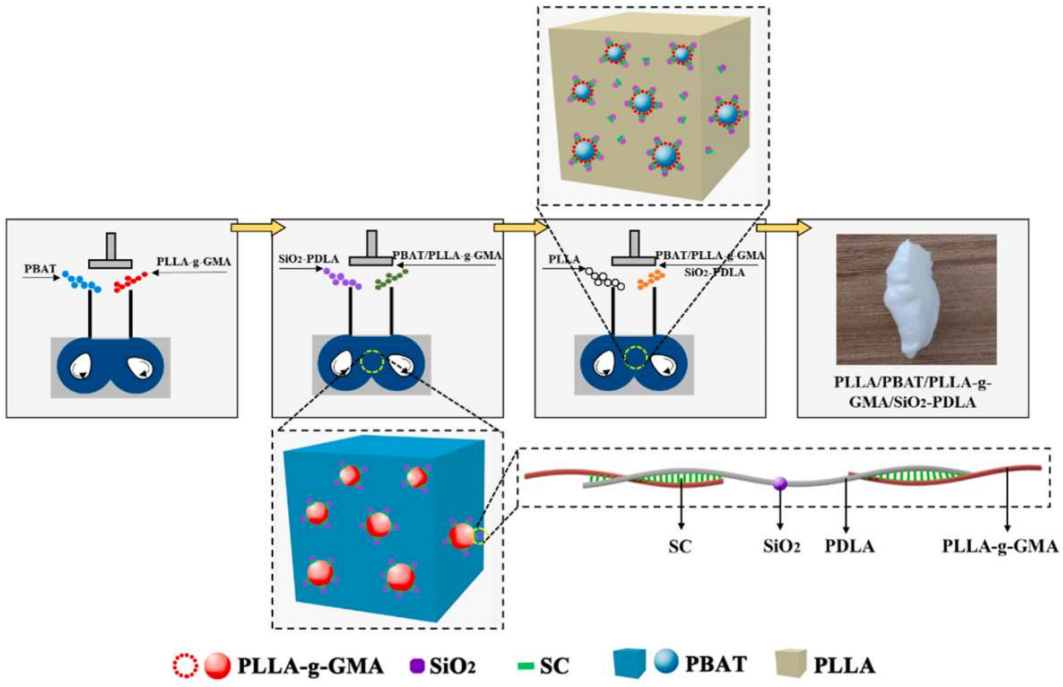

Figure 34. Schematic diagram for the preparation of nanocomposites and phase structure. Reproduced with permission [33] (Copyright 2022, Elsevier Science).

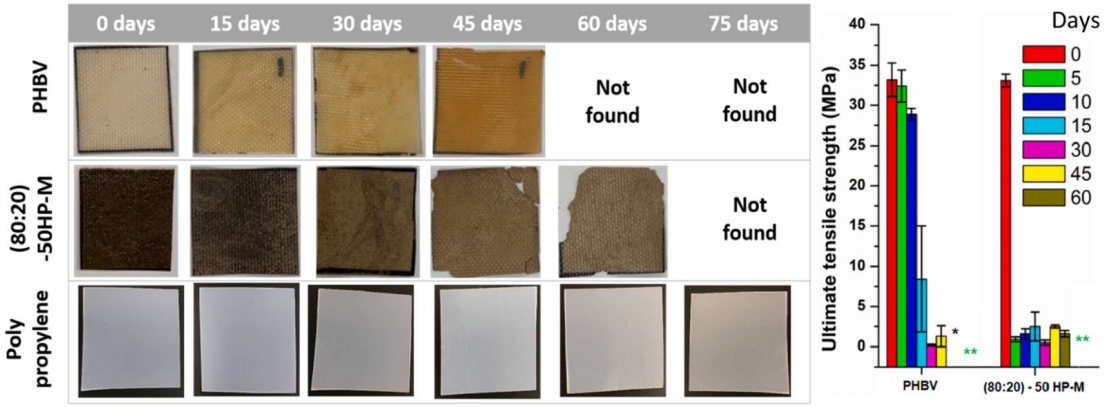

Figure 35. Representative images of samples from compost disintegration test and its corresponding tensile strength. Reproduced with permission [225] (Copyright 2022, Elsevier Science).

Due to the biodegradability, biocompatibility and competitive mechanical properties of PHBV, PBS and PCL， PBAT/PHBV blends, PBAT/PBS blends and PBAT/PCL blends also have good degradation ability as well as improved mechanical properties. A. Gupta et al. developed sustainable PHBV-PBAT-based bio-composites containing 60% hemp residue (HP) with MA-grafted PBAT as compatibilizer *via* a reactive melt extrusion process. HP is a lignocellulosic material and has high moisture absorption. Using MA-grafted PBAT as a compatibilizer formed a coating on HP to prevent water molecules from directly contacting HP and improved the interfacial interaction between the HP and PHBV-PBAT matrix (Figure 35) [225]. PCL/PBAT blends can be prepared by mixing in the melt or solution. F.M. Sousa et al. prepared PCL/PBAT blends by melting with different compositions at 150 °C and found that although PCL/PBAT blends are immiscible, strong interaction exists between the components as pseudoplastic fluids in the molten state [226]. V. Pagno et al. prepared PBAT/PCL blends by solvating PBAT and PCL in chloroform and N,N-dimethylformamide and then prepared PBAT/PCL/carbon from Brazil nutshell biomass (CA-BCB) composites by electrospinning for drug retention [227]. R. Muthuraj et al. prepared PBS/PBAT blends by melting them in a twin screw extruder at 140°C. By blending PBAT into PBS, the tensile strength and elongation at break are significantly improved, indicating that good compatibility between polymers is achieved due to the transesterification between pure polymers to form copolyesters. The phase morphology of PBS/PBAT blends shows a two-phase structure in which PBAT is the minor phase interfering with the growth of matrix spherulites [228]. X.Y. Wei et al. prepared the fully biodegradable PBS-*g*-GMA/TPS/PBAT composites with good comprehensive properties by melt blending at 145 °C. The addition of PBAT significantly increased the toughness of the composites while had little effect on the crystallinity [229].

- PBAT/Polycarbonate Blends

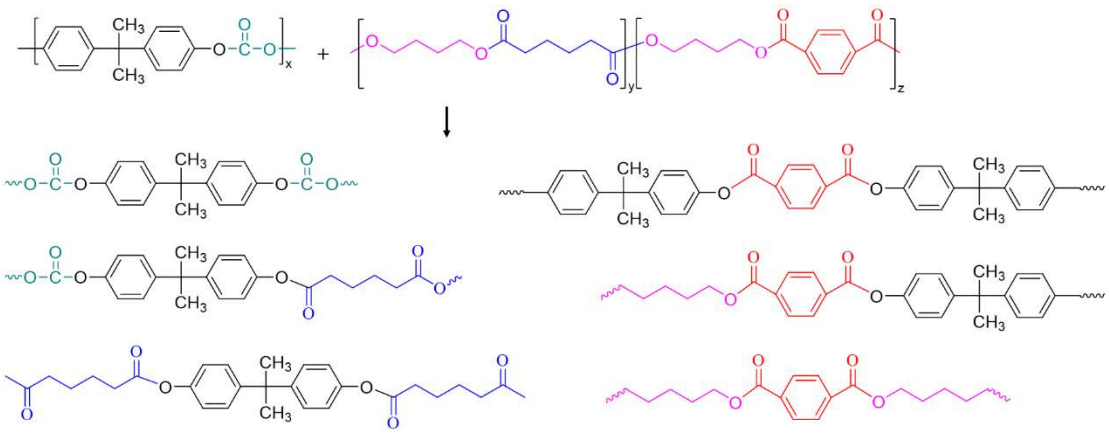

Figure 36. Expected chemical structures of transesterification products of PC and PBAT. Reproduced with permission [230] (Copyright 2011, Springer Nature).

PBAT/Polycarbonate blends can combine the high toughness and thermal stability of polycarbonates with the biodegradability and processability of PBAT. M. Jang et al. prepared PC/PBAT blends by melting them in a twin-screw extruder and subsequently annealing at 260 ℃ for 5 h. They found that the transesterification reaction between PC and PBAT through annealing played an important role in improving their miscibility and thermal properties by forming random copolymers as compatibilizers after annealing (Figure 36) [230]. Z. Liu et al. prepared PPC/PBAT blends by mixing PPC, PBAT and ADR-4368 in varying weight ratios at 150 ℃. The PPC/PBAT blends were used for preparing resilient biodegradable foams with high foaming ratio under high

CO_2 pressure foaming [231]. G. Jiang et al. investigated the melting reactive of PPC/PBAT blends with ethylene-methyl acrylate-glycidyl methacrylate (EMA-GMA) as a compatibilizer and prepared PBAT/PPC films by blowing film extrusion. The addition of EMA-GMA increased the crystallization temperature and melting temperature, improved the tensile strength and elongation, made the film surface smoother and more uniform, enhanced the film gas passing resistance, and improved the oxygen barrier performance [232].

3.2.2. Blending with Natural Macromolecules

- PBAT/TPS Blends

Starch-based biodegradable polymers have low cost and broad possibilities to meet significant requirements. Thermoplastic starch (TPS) is a homogeneous melt with thermoplastic characteristics obtained by disrupting the starch granule structure. TPS is a renewable and flexible material with excellent biodegradability used in different thermos-plasticization processes, including injection molding, extrusion blow molding, injection compression molding, and extrusion. Using TPS in the modification of PBAT can not only greatly reduce the cost, but also accelerate the degradation rate of PBAT [233]. X. Zhai et al. prepared PBAT/TPS blends at various weight proportions by extrusion blowing and identified phase morphologies and continuous structures of PBAT/TPS composite films using iodine dyeing-assisted light microscopy. The blue dyed TPS phase and the white PBAT phase without iodine staining are clearly shown in Figure 37. They found that when PBAT content was 30–70%, PBAT-TPS co-continuous phases were interconnected throughout the membrane matrix and mechanical properties of PBAT/TPS composite films improved with the increase in PBAT content. PBAT-TPS has two-phase transition points- one is that when the PBAT content is 30 wt%, the PBAT phase starts to coalesce into a continuous structure, and the other is that when the PBAT content is 70wt%, the continuous structure of the TPS phase decreases and almost disappears [234].

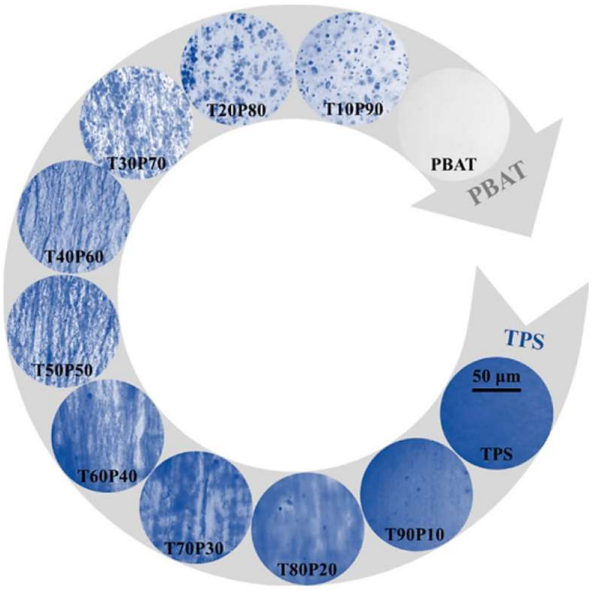

Figure 37. Optical images of TPS/PBAT composite films dyed with iodine. Vertical direction is parallel to the traction during film-blowing. Reproduced with permission [234] (Copyright 2020, Elsevier Science).

There are three main methods to increase the compatibility of PBAT/TPS blends, (1) adding compatibilizer or plasticizer, (2) treating PBAT before blending and (3) using modified TPS for blending. K. Yimnak et al. prepared PBAT/TPS blends with 3wt% zeolite 5A (Z5A) and glycerol as compatibilizer and plasticizer by two compounding sequences. Mixing TPS with Z5A first and then blending with PBAT with a glycerol content of 40 phs (parts per hundred parts of starch) effectively improved the compatibility and mechanical properties of PBAT/TPS blends. During the melt blending process, the uniform distribution of Z5A particles in PBAT/TPS blends and the migration of Z5A particles from the TPS/Z5A phase to the PBAT matrix made the PBAT/TPS blends exhibit excellent tensile and oxygen barrier properties [235]. In the chemical modification of PBAT, we had introduced the using of PBAT-based graft copolymer such as PBAT-*g*-MA and PBAT-*g*-GMA to improve the compatibility of PBAT/TPS blends, so we would not repeat it here. In addition to the grafting of PBAT, other methods can also be used to modify PBAT to enhance the compatibility of blends. J. Bai et al. used reactive epoxy compatibilizer (REC) to improve the compatibility of PBAT/TPS blends by two-step extrusion in which TPS pellets were obtained by extruding and granulating starch/glycerol blends using a twin-screw extruder first, and then TPS pellets, PBAT and REC were mixed using the high-speed mixer as shown in Figure 38. The PBAT/TPS blends obtained by two-step extrusion had higher tensile strength, impact strength and elongation at break than those obtained by one-step extrusion, forming a bicontinuous phase structure without any phase separation or starch particles [236].

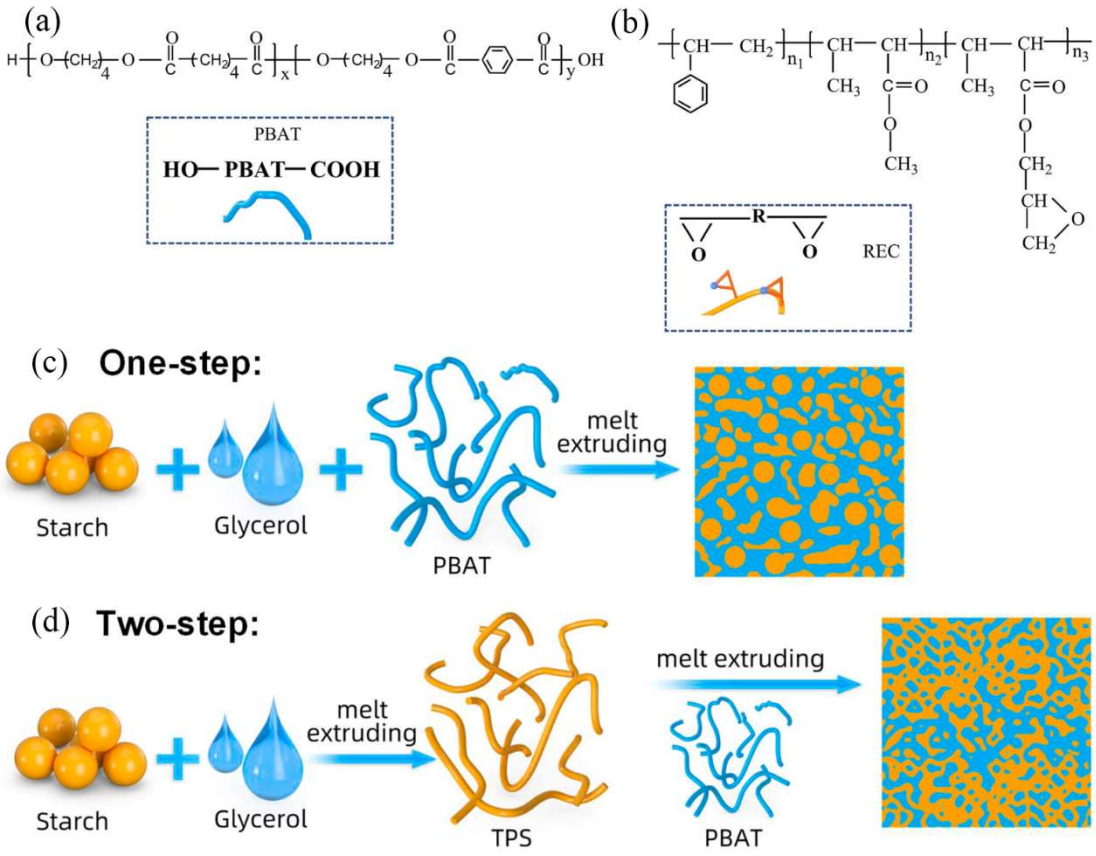

Figure 38. Chemical structures of PBAT (**a**) and REC (**b**); Compatibility mechanism of different preparation methods: (**c**) one-step; (**d**) two-step. Reproduced with permission [236] (Copyright 2021, Elsevier Science).

The research group of N. Harnkarnsujarit enhanced the compatibility of PBAT/TPS blends by compounding nisin (3, 6 and 9%) and nisin-ethylenediaminetetraacetic acid (EDTA) (3 and 6%) mixtures [237] and Native (NS), acetylated (AS), octenyl-succinated (OS) and hydroxypropylated (HS) starch [46]. The combination of nisin and EDTA involving C–O stretching of ester bonds effectively improved the compatibility and adhesion between TPS and PBAT polymer networks, providing a more uniform membrane microstructure. Nisin-EDTA increased the crystallinity and hydrophilicity of the PBAT/TPS blends, and inhibited microbial growth, preserving the quality of packaged pork [237]. They prepared PBAT/TPS (40/60 and 50/50 ratios) blend films with NS, AS, OS and HS starch by blown-film extrusion and found that controlling the hydrophobicity of the interface between incompatible polymers had a great influence on the dispersion and morphology of starch particles (Figure 39). NS starch as hydrophilic modified TPS formed larger clumps of granule aggregates and gave a more homogeneous surface topography in PBAT/NS, increasing affinity at the interface of starch aggregates. OS starch as hydrophobically modified TPS formed smaller clump sizes with more individually dispersed granules and gave the least number of voids on particle surfaces, improving compatibility and interaction with PBAT [46].

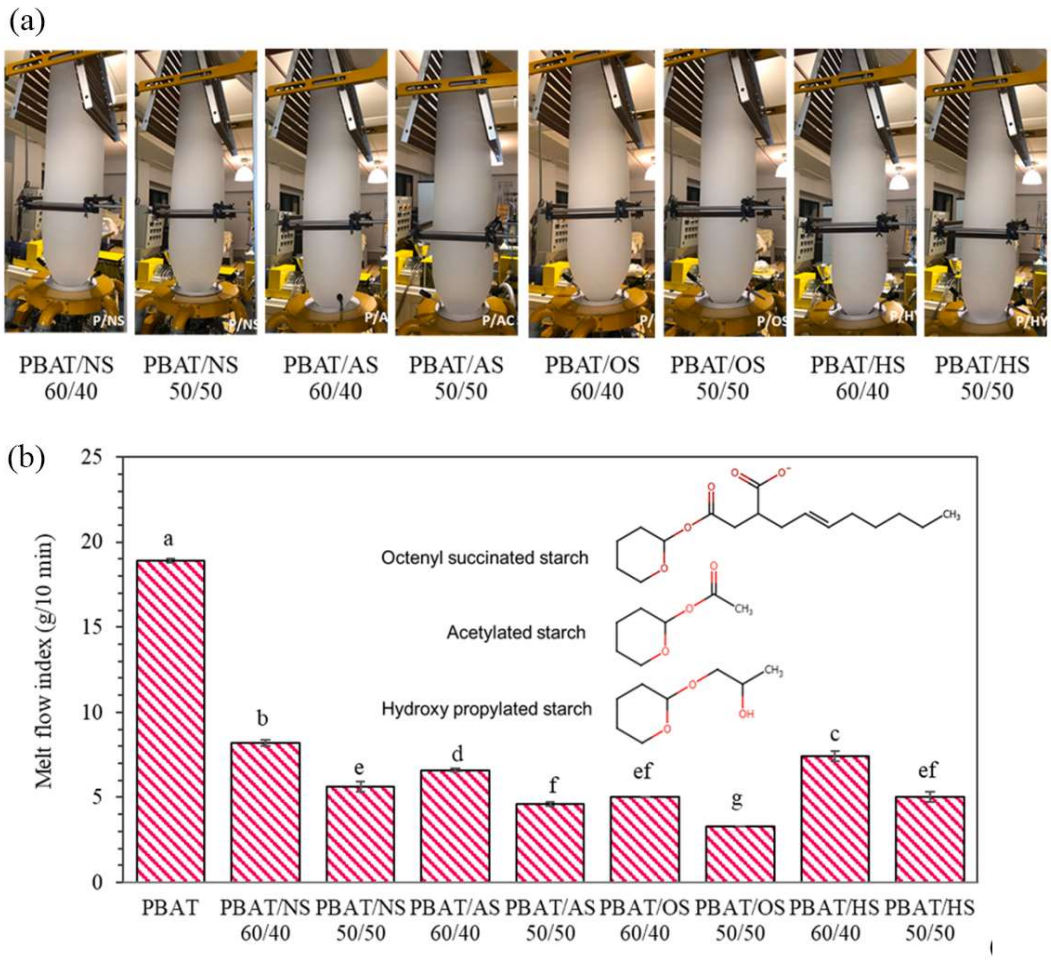

Figure 39. Appearance of the blown film, (**a**) and melt flow indices of pellets of PBAT and TPS from modified starch as native starch (NS), acetylated starch (AS), octenyl-succinated starch (OS) and hydroxypropylated starch (HS) blend films at PBAT/TPS ratios of 60/40 and 50/50 (**b**). Reproduced with permission [46] (Copyright 2022, Elsevier).

- PBAT/ Lignin Blends

Lignin is a natural biodegradable, nontoxic polyphenolic compound obtained from biomass like plant fibers with high impact strength and good heat resistance. Lignin also can be used to blend with PBAT to reduce costs. However, the hydrogen bond in lignin leads to the incompatibility between lignin and PBAT, so many treated lignin is used for PBAT blending. H. Kargarzadeh et al. prepared PBAT/Kraft lignin particles (KLPs) composites by twin-screw extruder at 180 ℃ and found that introducing KLPs into PBAT can improve the tensile properties of PBAT and strongly nucleate the crystallization of PBAT. With the increasing KLPs (0.5, 2, 4, and 6 wt%) contents, the storage modulus of PBAT/ KLPs composites increased and T_g decreased slightly [238]. Y. Liu et al. prepared vinyltrimethoxysilane (VTMS)-grafted lignin (VL) by mixing VTMS ethanol/aqueous solution and lignin /DMF solution and introduced VL into PBAT, which significantly improved the tensile strength, Young's modulus and biodegradation efficiency of PBAT/VL-30% composites [48]. L. Xiao et al. prepared the lignin-zinc oxide (LZn) hybrids by hydrothermal method and blended LZn with PBAT-*g*-GMA *via* solvent casting (Figure 40). They found that the tensile modulus and yield strength of PBAT/LZn composite films were improved, and PBAT/LZn composite films also had obvious UV shielding, anti-oxidation and antibacterial activities [239].

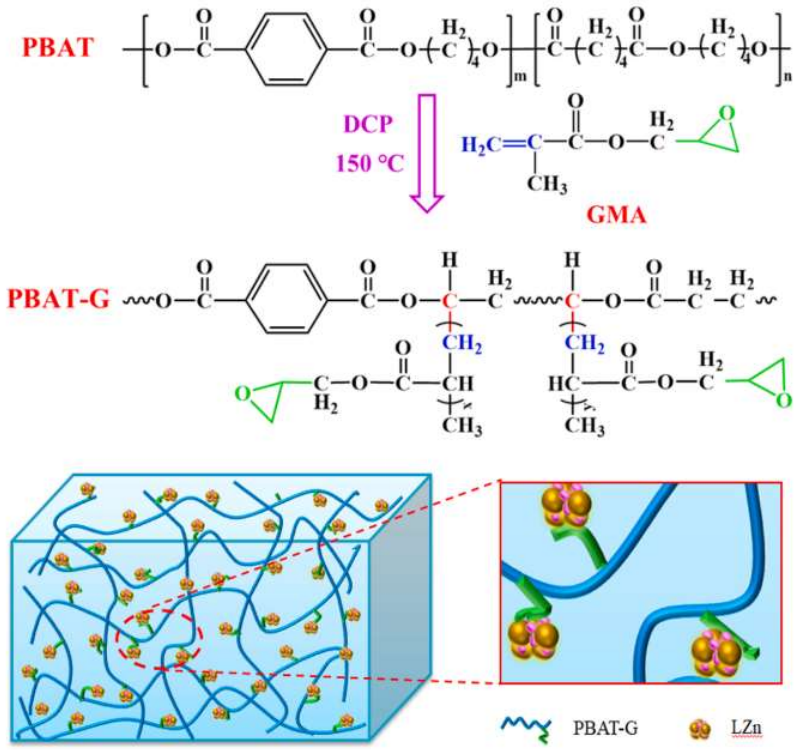

Figure 40. Preparation process of PBAT/LZn composite films and their possible interaction. Reproduced with permission [239] (Copyright 2020, Elsevier Science).

3.2.3. Blending with Inorganic Materials

Calcium carbonate ($CaCO_3$) is a low-cost inorganic filler for biodegradable polyester to enhance its mechanical properties. E. Nunes et al. prepared PBAT/$CaCO_3$ composites using ADR as a chain extender to enhance the compatibility. This interaction of the hydroxyl and carboxyl end groups of PBAT with the epoxy group of ADR increased the size of the polymer chains and the crosslinks and improved the dispersion of the $CaCO_3$ particles [240]. T. Zhang et al. prepared PBAT/$CaCO_3$ composite films by extrusion-blown and compared the impact of $CaCO_3$ content (0–40 wt%), particle size (5–12 μm), and surface modification with silane coupling agents on the properties of the films. The viscosity, tensile strength and elongation at break of PBAT/$CaCO_3$ composites increased when particle content increased and particle size decreased. PBAT/$CaCO_3$ composites with 5 μm (3000 mesh) and 30 wt% of $CaCO_3$ particles coated with 2 wt% nonpolar aliphatic silane coupling agent had better mechanical properties [241]. This research group also prepared PBAT/$CaCO_3$ composites with polyethylene glycol 600 (PEG-600) as a coating agent of $CaCO_3$ to improve the compatibility due to the high affinity between hydroxyl end groups of PEG and the polar surface of $CaCO_3$. In addition, the hydrophilicity of PEG-600 increased the diffusion rate of water molecules, thus promoting the degradation of PBAT [242]. K. Helanto et al. compared the performance of PLA, PBAT, PHBV melt-compounded with inorganic fillers such as talc, kaolin and $CaCO_3$, respectively. They found that talc and kaolin had good polymer–filler adhesion, they were well surrounded by the polymer, and they were more effective as nucleating agents for PLA and PHBV composites, while $CaCO_3$ had poor polymer–filler adhesion with cavities around $CaCO_3$ particles. The elongation of PLA can be enhanced by $CaCO_3$ in the injection molded specimens and films. The addition of fillers leading to the crystallinity of PBAT composites decreased, which may be due to the reduction of crystal growth space [243].

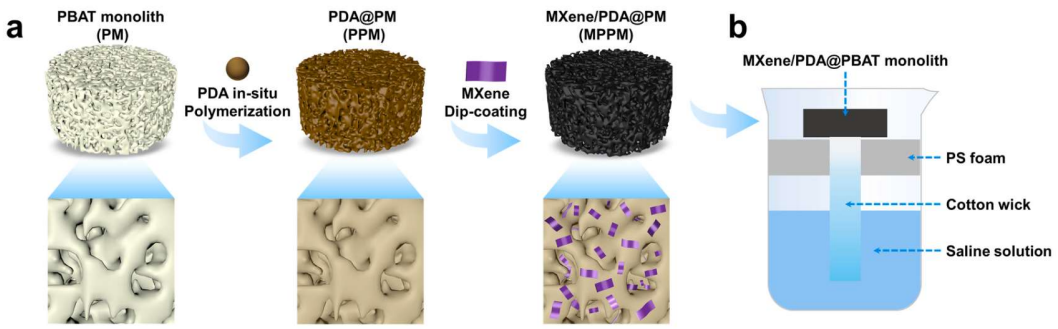

Figure 41. (**a**) Schematic illustration of the preparation process of the MPPM. (**b**) Schematic illustration of the home-made evaporation device. Reproduced with permission [244] (Copyright 2022, Elsevier Science).

The blends of PBAT and inorganic materials can be modified for other purposes such as biomedical applications and solar-driven seawater desalination, besides food packaging. G. Bheemaneni et al. prepared PBAT/wollastonite composites by melt blending process and evaluated cytotoxicity through in vitro cytotoxicity test (MTT Assay). PBAT/wollastonite composites may be used as new biomaterials due to better cell viability with 3 wt% filler content [245]. G.S. Balbinot et al. synthesized niobium-containing bioactive glasses (BAGNb) and prepared PBAT/BAGNb composites *via* hot-melt extrusion as casting films to develop bioactive guided bone regeneration membranes [246]. R. Zhang et al. fabricated a degradable interfacial solar vapor generator (DISVG) using PBAT monoliths with hierarchical porous morphology to provide sites for MXene loading and reduce solar reflection loss. PBAT monoliths were prepared by nonsolvent thermally induced phase separation method and the porous morphology was obtained by freeze-drying. MXene/PDA@PBAT monoliths were prepared by *in-situ* polymerization of polydopamine (PDA) and dip-coating of MXene and can be used for seawater evaporation and sewage purification (Figure 41) [244].

4. Conclusions and Remarks

Polylactide (PLA) and poly(butylene adipate-co-terephthalate) (PBAT) are the most promising biodegradable polymers. This review introduced the modification and preparation strategies and technologies of PLA and PBAT, and provided ideas for the chemical and physical modification and preparation of degradable polymers.

The stereoregularity of PLA materials significantly affects the physical properties and thermomechanical properties. Stereocomplex formation between PLLA and PDLA can improve thermal stability and mechanical properties by copolymerization or blending. Stereocontrolled ROP of *rac*-lactide and *meso*-lactide monomers can result in isotactic polymer with the stereocenters aligned along the same side of the polymer chain *via* controlling the degree of selectivity, chain exchange and insertion errors of polymer microstructure. Stereocontrolled ROP can synthesize enantiopure PDLA, PLLA, stereo diblock PLA copolymers, stereo triblock PLA copolymers, stereo multiblock PLA copolymers and stereo block PLA copolymers with other types of blocks. PLLA/PDLA stereocomplexes can be prepared by crosslinking with TAIC in gamma irradiation, blending with PLA oligomer, or emulsion approach with regenerated cellulose (RC) as a reticular structure.

PLA–polyether, PLA–polycarbonate, and PLA–polyester block copolymers can be synthesized by ROP of lactide with commercially available polymers or monomers in the presence of multiple metal-based initiators or organo-catalysts to improve the inherent hydrophobicity or increase toughness, mechanical and thermal properties of PLA. PLA-based graft copolymers can be synthesized by grafting-onto multifunctional linear backbone or grafting-from a linear macroinitiator during the grafting process. Various PLA-based graft copolymers were synthesized with monomers like ε-caprolactone, glycolic acid, polymers such as PEG, inorganic materials like CNTs, graphene oxide and natural macromolecules like dextran starch, chitosan, lignin, cellulose, silk sericin. Crosslinking can improve the mechanical, thermal and physicochemical properties of PLA *via* intra- or intermolecular connecting by covalent or non-covalent links. PLA-based crosslinked polymers can be prepared directly during polymer synthesis by designing the polymer architectures, or post-crosslinking of oligomers with controlled architecture *via* condensation reactions. PLA-based blends can improve the PLA processability by omitting the polymerization step. One of the important ways to enhance the compatibility of two immiscible polymers is to add compatibilizers such as block, graft, or random copolymers with the molecules arranged along the interface between two polymer phases. PLA-based blends can be carried out by blending two semicrystalline polymers or PLA with an amorphous polymer. Blending PLA with flexible or elastic polymers is the simplest and most effective strategy for toughening, improving the ductility and heat deflection temperature PLA.

Due to the good degradability and excellent mechanical properties of PBAT, many PBAT-based products have been used in the fields of shopping bags, garbage bags, tableware, mulching film. The copolymerization modification of PBAT mainly involves the addition of monomers or polymers during the synthesis process. Acrylic acid, maleic anhydride, glycidyl methacrylate and (ethylene-methyl acrylate-glycidyl methacrylate) can be used to graft PBAT. PBAT-based block copolymers and graft copolymers are used for blending reactions. The crosslinking of PBAT can be realized by electron beam induced crosslinking, chemical micro-crosslinking or adding crosslinking agent to improve its thermal and mechanical properties. Many polycarbonates (e. g. PPC, PTMC, PC) and polyester (e. g. PLA, PCL, PHBV, PBS) are used for preparing PBAT-based biodegradable polymers blends. PBAT can also be blended with degradable natural macromolecules (e. g. TPS, lignin) and inorganic materials such as $CaCO_3$ to obtain better performance and more applications.

The summary of modification methods of PLA and PBAT provides strong support for the modification of degradable polymers, especially in the modification and preparation of both biomass-based and fossil-based degradable polymers. The modification of PLA and PBAT makes the performance more excellent and improves their commercial value. We hope that more breakthroughs in modification for degradable polymers will be made to increase their comprehensive performances, so as to obtain wider applications and better prospects, effectively solve the problem of environmental pollution of plastics.

Acknowledgments

The authors would like to thank the National Natural Science Foundation of China (Grant No. 51673131) and the Fundamental Research Funds for the Central Universities (171gjc37) for financial support of this work. We also appreciate the financial supports from industrials: Shandong Lecron Industrial Development Group, Co., Ltd, China, Guangdong Tianxin New Material Technology Co., Ltd, China, Hebei CNC Risun Energy Co., Ltd, China, Huanghua Xinnuolixing Fine Chemicalstock Co., Ltd. China.

Ethics Statement

Not applicable.

Informed Consent Statement

Not applicable.

Funding

This research was funded by [National Natural Science Foundation of China] grant number [51673131] and the Fundamental Research Funds for the Central Universities grant number [171gjc37].

Declaration of Competing Interest

The authors declare that they have no known competing financial interests or personal relationships that could have appeared to influence the work reported in this paper.

References

1. Jiang J, Shi K, Zhang XN, Yu K, Zhang H, He J, et al. From plastic waste to wealth using chemical recycling: A review. *J. Environ. Chem. Eng.* **2022**, *10*, 106867.
2. Singh N, Ogunseitan OA, Wong MH, Tang YY. Sustainable materials alternative to petrochemical plastics pollution: A review analysis. *Sustain. Horiz.* **2022**, *2*, 100016.
3. Li H, Aguirre-Villegas HA, Allen RD, Bai X, Benson CH, Beckham GT, et al. Expanding plastics recycling technologies: Chemical aspects, technology status and challenges. *Green Chem.* **2022**, *24*, 8899–9002.
4. Thiounn T, Smith, RC. Advances and approaches for chemical recycling of plastic waste. *J. Polym. Sci.* **2020**, *58*, 1347–1364.
5. Monteiro R, Andrades R, Noleto-Filho E, Pegado T, Morais L, Goncalves, M, et al. GLOVE: The Global Plastic Ingestion Initiative for a cleaner world. *Mar. Pollut. Bull.* **2022**, *185*, 114244.
6. Haward M. Plastic pollution of the world's seas and oceans as a contemporary challenge in ocean governance. *Nat. Commun.* **2018**, *9*, 667.
7. MacLeod M, Arp HPH, Tekman MB, Jahnke A. The global threat from plastic pollution. *Science* **2021**, *373*, 61–65.
8. Knepper TP, Martin W, Scott L. Freshwater microplastics: emerging environmental contaminants? *Anal. Bioanal. Chem.* **2018**, *410*, 6337–6338.
9. Surendran U, Jayakumar M, Raja P, Gopinath G, Chellam PV. Microplastics in terrestrial ecosystem: Sources and migration in soil environment. *Chemosphere* **2023**, *318*, 137946.
10. Mahbub MS, Shams M. Acrylic fabrics as a source of microplastics from portable washer and dryer: Impact of washing and drying parameters. *Sci. Total Environ.* **2022**, *834*, 155429.
11. Dalla Fontana G, Mossotti R, Montarsolo A. Assessment of microplastics release from polyester fabrics: The impact of different washing conditions. *Environ. Pollut.* **2020**, 264, 113960.
12. Narancic T, O'Connor KE. Plastic waste as a global challenge: Are biodegradable plastics the answer to the plastic waste problem? *Microbiology* **2019**, *165*, 129–137.
13. Chen GQ, Patel MK. Plastics derived from biological sources: present and future: a technical and environmental review. *Chem. Rev.* **2012**, *112*, 2082–2099.
14. Emadian SM, Onay TT, Demirel B. Biodegradation of bioplastics in natural environments. *Waste Manag.* **2017**, *59*, 526–536.
15. Schnurr REJ, Alboiu V, Chaudhary M, Corbett RA, Quanz ME, Sankar K, et al. Reducing marine pollution from single-use plastics (SUPs): A review. *Mar. Pollut. Bull.* **2018**, *137*, 157–171.
16. Chu JW, Zhou Y, Cai YP, Wang X, Li CH, Liu Q. Flows and waste reduction strategies of PE, PP, and PET plastics under plastic limit order in China. *Resour. Conserv. Recycl.* **2023**, *188*, 106668–106679.
17. Nwafor N, Walker TR. Plastic Bags Prohibition Bill: A developing story of crass legalism aiming to reduce plastic marine pollution in Nigeria. *Marine Policy* **2020**, *120*, 104160.
18. Arriagada R, Lagos F, Jaime M, Salazar C. Exploring consistency between stated and revealed preferences for the plastic bag ban policy in Chile. *Waste Manag.* **2022**, 139, 381–392.
19. UNEP. Nations Sign up to End Global Scourge of Plastic Pollution. UN News 2022. Available online: https://news.un.org/en/story/2022/03/1113142 (accessed on 26 October 2022).
20. Álvarez Chávez CR, Edwards S, Moure Eraso R, Geiser K. Sustainability of bio-based plastics: general comparative analysis and recommendations for improvement. *J. Clean. Prod.* **2012**, *23*, 47–56.
21. Rosenboom JG, Langer R, Traverso G. Bioplastics for a circular economy. *Nat. Rev. Mater.* **2022**, *7*, 117–137.

22. Reddy MM, Vivekanandhan S, Misra M, Bhatia SK, Mohanty AK. Biobased plastics and bionanocomposites: Current status and future opportunities. *Prog. Polym. Sci.* **2013**, *38*, 1653–1689.
23. Rahman MH, Bhoi PR. An overview of non-biodegradable bioplastics. *J. Clean. Prod.* **2021**, *294*, 126218.
24. Hahladakis JN, Iacovidou E, Gerassimidou S. Plastic waste in a circular economy. In *Plastic Waste and Recycling*; Elsevier: Oxford, UK, 2020; pp. 481–512.
25. Samantaray PK, Little A, Wemyss AM, Iacovidou E, Wan C. Design and Control of Compostability in Synthetic Biopolyesters. *ACS Sustain. Chem. Eng.* **2021**, *9*, 9151–9164.
26. Aversa C, Barletta M, Cappiello G, Gisario A. Compatibilization strategies and analysis of morphological features of poly(butylene adipate-co-terephthalate) (PBAT)/poly(lactic acid) PLA blends: A state-of-art review. *Eur. Polym. J.* **2022**, *173*, 111304–111331.
27. Accelerated Growth: Global Production Capacities of Bioplastics 2021–2026. European Bioplastics 2021. Available online: https://www.european-bioplastics.org/global-bioplastics-production-will-more-than-triple-within-the-next-five-years/ (accessed on 28 October 2022).
28. Zhang X, Fevre M, Jones GO, Waymouth RM. Catalysis as an Enabling Science for Sustainable Polymers. *Chem. Rev.* **2018**, *118*, 839–885.
29. Ainali NM, Kalaronis D, Evgenidou E, Kyzas GZ, Bobori DC, Kaloyianni M, et al. Do poly(lactic acid) microplastics instigate a threat? A perception for their dynamic towards environmental pollution and toxicity. *Sci. Total Environ.* **2022**, *832*, 155014–155030.
30. Maadani AM, Salahinejad E. Performance comparison of PLA- and PLGA-coated porous bioceramic scaffolds: Mechanical, biodegradability, bioactivity, delivery and biocompatibility assessments. *J. Control Release* **2022**, *351*, 1–7.
31. Mehmood A, Raina N, Phakeenuya V, Wonganu B, Cheenkachorn K. The current status and market trend of polylactic acid as biopolymer: Awareness and needs for sustainable development. *Mater. Today Proc.* **2022**, *72*, 3049–3055.
32. Jiao J, Zeng XB, Huang XB. An overview on synthesis, properties and applications of poly(butylene-adipate-co-terephthalate)–PBAT. *Adv. Ind. Eng. Polym. Res.* **2020**, *3*, 19–26.
33. Lyu Y, Wen XL, Wang GL, Zhang QH, Lin LY, Schlarb AK, et al. 3D printing nanocomposites with controllable "strength-toughness" transition: Modification of SiO_2 and construction of Stereocomplex Crystallites. *Compos. Sci. Technol.* **2022**, *218*, 109167.
34. Souza PMS, Sommaggio LRD, Marin-Morales MA, Morales AR. PBAT biodegradable mulch films: Study of ecotoxicological impacts using Allium cepa, Lactuca sativa and HepG2/C3A cell culture. *Chemosphere* **2020**, *256*, 126985.
35. Farah S, Anderson DG, Langer R. Physical and mechanical properties of PLA, and their functions in widespread applications—A comprehensive review. *Adv. Drug Deliv. Rev.* **2016**, *107*, 367–392.
36. Tábi T, Ageyeva T, Kovács JG. Improving the ductility and heat deflection temperature of injection molded Poly(lactic acid) products: A comprehensive review. *Polym. Testing* **2021**, *101*, 107282.
37. Saadi Z, Rasmont A, Cesar G, Bewa H, Benguigui L. Fungal Degradation of Poly(L-lactide) in Soil and in Compost. *J. Polym. Environ.* **2011**, *20*, 273–282.
38. Genovese L, Soccio M, Lotti N, Gazzano M, Siracusa V, Salatelli E, et al. Design of biobased PLLA triblock copolymers for sustainable food packaging: Thermo-mechanical properties, gas barrier ability and compostability. *Eur. Polym. J.* **2017**, *95*, 289–303.
39. Acik G. Preparation of antimicrobial and biodegradable hybrid soybean oil and poly (L-lactide) based polymer with quaternized ammonium salt. *Polym. Degrad. Stab.* **2020**, *181*, 109317.
40. Kalita NK, Sarmah A, Bhasney SM, Kalamdhad A, Katiyar V. Demonstrating an ideal compostable plastic using biodegradability kinetics of poly(lactic acid) (PLA) based green biocomposite films under aerobic composting conditions. *Environ. Challenges* **2021**, *3*, 100030.
41. Przybytek A, Sienkiewicz M, Kucińska-Lipka J, Janik H. Preparation and characterization of biodegradable and compostable PLA/TPS/ESO compositions. *Ind. Crops Prod.* **2018**, *122*, 375–383.
42. Kalita NK, Bhasney SM, Mudenur C, Kalamdhad A, Katiyar V. End-of-life evaluation and biodegradation of Poly(lactic acid) (PLA)/Polycaprolactone (PCL)/Microcrystalline cellulose (MCC) polyblends under composting conditions. *Chemosphere* **2020**, *247*, 125875.
43. Saadi Z, Cesar G, Bewa H, Benguigui L. Fungal Degradation of Poly(Butylene Adipate-Co-Terephthalate) in Soil and in Compost. *J. Polym. Environ.* **2013**, *21*, 893–901.
44. Freitas ALPdL, Tonini Filho LR, Calvão PS, Souza AMCd. Effect of montmorillonite and chain extender on rheological, morphological and biodegradation behavior of PLA/PBAT blends. *Polym. Test.* **2017**, *62*, 189–195.
45. Pan HW, Hao YP, Zhao Y, Lang XZ, Zhang Y, Wang Z, Zhang HL, Dong LS. Improved mechanical properties, barrier properties and degradation behavior of poly(butylenes adipate-co-terephthalate)/poly(propylene carbonate) films. *Korean J. Chem. Eng.* **2017**, *34*, 1294–1304.
46. Wongphan P, Panrong T, Harnkarnsujarit N. Effect of different modified starches on physical, morphological, thermomechanical, barrier and biodegradation properties of cassava starch and polybutylene adipate terephthalate blend film. *Food Pack. Shelf Life* **2022**, *32*, 100844.
47. Dammak M, Fourati Y, Tarrés Q, Delgado-Aguilar M, Mutjé P, Boufi S. Blends of PBAT with plasticized starch for packaging applications: Mechanical properties, rheological behaviour and biodegradability. *Ind. Crops Prod.* **2020**, *144*, 112061.
48. Liu YF, Liu S, Liu ZT, Lei Y, Jiang SY, Zhang K, et al. Enhanced mechanical and biodegradable properties of PBAT/lignin composites via silane grafting and reactive extrusion. *Compos. Part B Eng.* **2021**, *220*, 108980.
49. de Albuquerque TL, Marques Junior JE, de Queiroz LP, Ricardo ADS, Rocha MVP. Polylactic acid production from biotechnological routes: A review. *Int. J. Biol. Macromol.* **2021**, *186*, 933–951.
50. Fang TQ, Liu MY, Li ZZ, Xiong L, Zhang DP, Meng KX, et al. Hydrothermal Conversion of Fructose to Lactic Acid and Derivatives: Synergies of Metal and Acid/Base Catalysts. *Chin. J. Chem. Eng.* **2022**, *53*, 381–401.

51. Upare PP, Yoon JW, Hwang DW, Lee UH, Hwang YK, Hong DY, et al. Design of a heterogeneous catalytic process for the continuous and direct synthesis of lactide from lactic acid. *Green Chem.* **2016**, *18*, 5978–5983.
52. Dusselier M, Van Wouwe P, Dewaele A, Makshina E, Sels BF. Lactic acid as a platform chemical in the biobased economy: The role of chemocatalysis. *Energy Environ. Sci.* **2013**, *6*, 1415–1442.
53. Stanford MJ, Dove AP. Stereocontrolled ring-opening polymerisation of lactide. *Chem. Soc. Rev.* **2010**, *39*, 486–494.
54. Li Z, Tan BH, Lin T, He C. Recent advances in stereocomplexation of enantiomeric PLA-based copolymers and applications. *Prog. Polym. Sci.* **2016**, *62*, 22–72.
55. Peng ZP, Xu GQ, Yang RL, Guo XH, Sun HG, Wang QG. Isoselective mechanism for asymmetric kinetic resolution polymerization of *rac*-lactide catalyzed by chiral tridentate bis(oxazolinylphenyl)amido ligand supported zinc complexes. *Eur. Polym. J.* **2022**, *180*, 111571.
56. Chen Q, Auras R, Uysal-Unalan I. Role of stereocomplex in advancing mass transport and thermomechanical properties of polylactide. *Green Chem.* **2022**, *24*, 3416–3432.
57. Bhattacharjee J, Sarkar A, Panda TK. Recent development of alkali metal complex promoted iso-selective ring-opening polymerization of *rac*-Lactide. *Curr. Opin. Green Sustain. Chem.* **2021**, *31*, 100545–100553.
58. Xu JX, Wang X, Liu JJ, Feng XS, Gnanou Y, Hadjichristidis N. Ionic H-bonding organocatalysts for the ring-opening polymerization of cyclic esters and cyclic carbonates. *Prog. Polym. Sci.* **2022**, *125*, 101484.
59. Liu S, Li H, Zhao N, Li Z. Stereoselective Ring-Opening Polymerization of *rac*-Lactide Using Organocatalytic Cyclic Trimeric Phosphazene Base. *ACS Macro Lett.* **2018**, *7*, 624–628.
60. Tsuji H. Poly(lactic acid) stereocomplexes: A decade of progress. *Adv. Drug Deliv. Rev.* **2016**, *107*, 97–135.
61. Sugai N, Yamamoto T, Tezuka Y. Synthesis of Orientationally Isomeric Cyclic Stereoblock Polylactides with Head-to-Head and Head-to-Tail Linkages of the Enantiomeric Segments. *ACS Macro Lett.* **2012**, *1*, 902–906.
62. Othman N, Xu C, Mehrkhodavandi P, Hatzikiriakos SG. Thermorheological and mechanical behavior of polylactide and its enantiomeric diblock copolymers and blends. *Polymer* **2012**, *53*, 2443–2452.
63. Tsuji H, Iguchi K, Tashiro K, Arakawa Y. Crystallization behavior, structure, morphology, and thermal properties of crystalline and amorphous stereo diblock copolymers, poly(L-lactide)-*b*-poly(DL-lactide). *Polym. Chem.* **2020**, *11*, 5711–5724.
64. Tsuji H, Iguchi K, Arakawa Y. Stereocomplex- and homo-crystallization behavior, structure, morphology, and thermal properties of crystalline and amorphous stereo diblock copolymers, enantiomeric Poly(L-lactide)-*b*-Poly(DL-lactide) and Poly(D-lactide)-*b*-Poly(DL-lactide). *Polymer* **2021**, *213*, 123226.
65. Masutani K, Lee CW, Kimura Y. Synthesis and properties of stereo di- and tri-block polylactides of different block compositions by terminal Diels-Alder coupling of poly-L-lactide and poly-D-lactide prepolymers. *Polym. J.* **2012**, *45*, 427–435.
66. Tsuji H, Tamai K, Kimura T, Kubota A, Tahahashi A, Kuzuya A, et al. Stereocomplex- and homo-crystallization of blends from 2-armed poly(L-lactide) and poly(D-lactide) with identical and opposite chain directional architectures and of 2-armed stereo diblock poly(lactide). *Polymer* **2016**, *96*, 167–181.
67. Li XL, Yang DS, Zhao YB, Diao XY, Bai HW, Zhang Q, et al. Toward all stereocomplex-type polylactide with outstanding melt stability and crystallizability via solid-state transesterification between enantiomeric poly(L-lactide) and poly(D-lactide). *Polymer* **2020**, *205*, 122850.
68. Tang Z, Chen X, Yang Y, Pang X, Sun J, Zhang X, et al. Stereoselective polymerization of *rac*-lactide with a bulky aluminum/Schiff base complex. *J. Polym. Sci. Part A Polym. Chem.* **2004**, *42*, 5974–5982.
69. Masutani K, Lee CW, Kimura Y. Synthesis of stereo multiblock polylactides by dual terminal couplings of poly-L-lactide and poly-D-lactide prepolymers: A new route to high-performance polylactides. *Polymer* **2012**, *53*, 6053–6062.
70. Maharana T, Mohanty B, Negi YS. Melt–solid polycondensation of lactic acid and its biodegradability. *Prog. Polym. Sci.* **2009**, *34*, 99–124.
71. Takenaka M, Kimura Y, Ohara H. Molecular weight increase driven by evolution of crystal structure in the process of solid-state polycondensation of poly(l-lactic acid). *Polymer* **2017**, *126*, 133–140.
72. Widhianto YW, Yamamoto M, Masutani K, Kimura Y, Yamane H. Thermal properties of the multi-stereo block poly(lactic acid)s with various block lengths. *Polym. Degrad. Stab.* **2017**, 142, 188–197.
73. Diaz C, Mehrkhodavandi P. Strategies for the synthesis of block copolymers with biodegradable polyester segments. *Polym. Chem.* **2021**, *12*, 783–806.
74. Ibrahim M, Ramadan E, Elsadek NE, Emam SE, Shimizu T, Ando H, et al. Polyethylene glycol (PEG): The nature, immunogenicity, and role in the hypersensitivity of PEGylated products. *J. Control Release* **2022**, *351*, 215–230.
75. Ma C, Pan P, Shan G, Bao Y, Fujita M, Maeda M. Core-shell structure, biodegradation, and drug release behavior of poly(lactic acid)/poly(ethylene glycol) block copolymer micelles tuned by macromolecular stereostructure. *Langmuir* **2015**, *31*, 1527–1536.
76. Sun L, Pitto-Barry A, Kirby N, Schiller TL, Sanchez AM, Dyson MA, et al. Structural reorganization of cylindrical nanoparticles triggered by polylactide stereocomplexation. *Nat. Commun.* **2014**, *5*, 5746.
77. Mao H, Shan G, Bao Y, Wu ZL, Pan P. Thermoresponsive physical hydrogels of poly(lactic acid)/poly(ethylene glycol) stereoblock copolymers tuned by stereostructure and hydrophobic block sequence. *Soft Matter* **2016**, *12*, 4628–4637.
78. Cho H, Gao J, Kwon GS. PEG-*b*-PLA micelles and PLGA-*b*-PEG-*b*-PLGA sol-gels for drug delivery. *J. Control. Release* **2016**, *240*, 191–201.

79. Sadowski LP, Singh A, Luo DH, Majcher MJ, Urosev I, Rothenbroker M, et al. Functionalized poly(oligo(lactic acid) methacrylate)-block-poly(oligo(ethylene glycol) methacrylate) block copolymers: A synthetically tunable analogue to PLA-PEG for fabricating drug-loaded nanoparticles. *Eur. Polym. J.* **2022**, *177*, 111443.
80. Ye WB, Zhu FT, Cai Y, Wang LY, Zhang GL, Zhao GK, et al. Improved paclitaxel delivery with PEG-*b*-PLA/zein nanoparticles prepared via flash nanoprecipitation. *Int. J. Biol. Macromol.* **2022**, *221*, 486–495.
81. Nakajima M, Nakajima H, Fujiwara T, Kimura Y, Sasaki S. Nano-ordered surface morphologies by stereocomplexation of the enantiomeric polylactide chains: specific interactions of surface-immobilized poly(D-lactide) and poly(ethylene glycol)-poly(L-lactide) block copolymers. *Langmuir* **2014**, *30*, 14030–14038.
82. Dau H, Jones GR, Tsogtgerel E, Nguyen D, Keyes A, Liu YS, et al. Linear Block Copolymer Synthesis. *Chem. Rev.* **2022**, *122*, 14471–14553.
83. Deacy AC, Gregory GL, Sulley GS, Chen TTD, Williams CK. Sequence Control from Mixtures: Switchable Polymerization Catalysis and Future Materials Applications. *J. Am. Chem. Soc.* **2021**, *143*, 10021–10040.
84. Liu YY, Wang X, Li ZJ, Wei FL, Zhu H, Dong H, et al. A switch from anionic to bifunctional H-bonding catalyzed ring-opening polymerizations towards polyether–polyester diblock copolymers. *Polym. Chem.* **2018**, *9*, 154–159.
85. Kudo H, Nishioka S, Jin H, Maekawa H, Nakamura S, Masuda T. Thermosetting epoxy resin system: Ring-opening by copolymerization of epoxide with D,L-Lactide. *Polymer* **2022**, *240*, 124489.
86. Ye SX, Wang SJ, Lin LM, Xiao M, Meng YZ. CO_2 derived biodegradable polycarbonates: Synthesis, modification and applications. *Adv. Ind. Eng. Polym. Res.* **2019**, *2*, 143–160.
87. Ye SX, Wang WJ, Liang JX, Wang SJ, Xiao M, Meng YZ. Metal-Free Approach for a One-Pot Construction of Biodegradable Block Copolymers from Epoxides, Phthalic Anhydride, and CO_2. *ACS Sustain. Chem. Eng.* **2020**, *8*, 17860–17867.
88. Zhang M, Xu YH, Williams BL, Xiao M, Wang SJ, Han DM, et al. Catalytic materials for direct synthesis of dimethyl carbonate (DMC) from CO_2. *J. Clean. Prod.* **2021**, *279*, 123344.
89. Xu Y, Lin L, Xiao M, Wang S, Smith AT, Sun L, et al. Synthesis and properties of CO_2-based plastics: Environmentally-friendly, energy-saving and biomedical polymeric materials. *Prog. Polym. Sci.* **2018**, *80*, 163–182.
90. Tang L, Luo W, Xiao M, Wang S, Meng Y. One-pot synthesis of terpolymers with long L-lactide rich sequence derived from propylene oxide, CO_2, and L-lactide catalyzed by zinc adipate. *J. Polym. Sci. Part A Polym. Chem.* **2015**, *53*, 1734–1741.
91. Li X, Duan RL, Hu CY, Pang X, Deng MX. Copolymerization of lactide, epoxides and carbon dioxide: A highly efficient heterogeneous ternary catalyst system. *Polym. Chem.* **2021**, *12*, 1700–1706.
92. Li S, Lu H, Zhu L, Yan MX, Kang XH, Luo Y. Ring-opening polymerization of L-lactide catalyzed by food sweetener saccharin with organic base mediated: A computational study. *Polymer* **2022**, *246*, 124747.
93. Zhu YJ, Hu YZ, Li ZJ, Liu B, Qu YY, Zhang ZH, et al. A genuine H-bond donor and Lewis base amine cocatalyst in ring-opening polymerizations. *Eur. Polym. J.* **2021**, *143*, 110184.
94. Hu CY, Pang X, Chen XS. Self-Switchable Polymerization: A Smart Approach to Sequence-Controlled Degradable Copolymers. *Macromolecules* **2022**, *55*, 1879–1893.
95. Lin L, Xu Y, Wang S, Xiao M, Meng Y. Ring-opening polymerization of L-lactide and ε-caprolactone catalyzed by versatile tri-zinc complex: Synthesis of biodegradable polyester with gradient sequence structure. *Eur. Polym. J.* **2016**, *74*, 109–119.
96. Luo W, Xiao M, Wang S, Han D, Meng Y. Gradient terpolymers with long ε-caprolactone rich sequence derived from propylene oxide, CO_2, and ε-caprolactone catalyzed by zinc glutarate. *Eur. Polym. J.* **2016**, *84*, 245–255.
97. Bai J, Xiao X, Zhang Y, Chao J, Chen X. beta-Pyridylenolate zinc catalysts for the ring-opening homo- and copolymerization of epsilon-caprolactone and lactides. *Dalton Trans.* **2017**, *46*, 9846–9858.
98. Liu Y, Dong WS, Liu JY, Li YS. Living ring-opening homo- and copolymerisation of epsilon-caprolactone and L-lactide by cyclic beta-ketiminato aluminium complexes. *Dalton Trans.* **2014**, *43*, 2244–2251.
99. Huang HC, Wang B, Zhang YP, Li YS. Bimetallic aluminum complexes with cyclic β-ketiminato ligands: the cooperative effect improves their capability in polymerization of lactide and ε-caprolactone. *Polym. Chem.* **2016**, *7*, 5819–5827.
100. Santulli F, D'Auria I, Boggioni L, Losio S, Proverbio M, Costabile C, et al. Bimetallic Aluminum Complexes Bearing Binaphthyl-Based Iminophenolate Ligands as Catalysts for the Synthesis of Polyesters. *Organometallics* **2020**, *39*, 1213–1220.
101. Jiang YS, Zhang WJ, Han MY, Wang X, Solan GA, Wang R, et al. Phenoxy-imine/-amide aluminum complexes with pendant or coordinated pyridine moieties: Solvent effects on structural type and catalytic capability for the ROP of cyclic esters. *Polymer* **2022**, *242*, 124602–124623.
102. Sangroniz A, Sangroniz L, Hamzehlou S, Río, J.d.;Santamaria A, Sarasua JR, et al. Lactide-caprolactone copolymers with tuneable barrier properties for packaging applications. *Polymer* **2020**, *202*, 122681.
103. Shao JJ, Zhou HR, Wang YR, Luo YJ, Yao YM. Lanthanum complexes stabilized by a pentadentate Schiff-base ligand: synthesis, characterization, and reactivity in statistical copolymerization of epsilon-caprolactone and L-lactide. *Dalton Trans.* **2020**, *49*, 5842–5850.
104. Zhang X, Prior TJ, Redshaw C. Niobium and Tantalum complexes derived from the acids $Ph_2C(X)CO_2H$ (X = OH, NH_2): Synthesis, structure and ROP capability. *New J. Chem.* **2022**, *46*, 14146–14154.
105. Mezzasalma L, De Winter J, Taton D, Coulembier O. Benzoic acid-organocatalyzed ring-opening (co)polymerization (ORO(c)P) of L-lactide and ε-caprolactone under solvent-free conditions: from simplicity to recyclability. *Green Chem.* **2018**, *20*, 5385–5396.

106. Feng ZH, Wu L, Dong H, Liu BP, Cheng RH. Copolyesters of epsilon-caprolactone and l-lactide catalyzed by a tetrabutylammonium phthalimide-N-oxyl organocatalyst. *RSC Adv.* **2021**, *11*, 19021–19028.
107. Maharana T, Pattanaik S, Routaray A, Nath N, Sutar AK. Synthesis and characterization of poly(lactic acid) based graft copolymers. *React. Funct. Polym.* **2015**, *93*, 47–67.
108. Zhang N, Zhao M, Liu GF, Wang JY, Chen YZ, Zhang ZJ. Alkylated lignin with graft copolymerization for enhancing toughness of PLA. *J. Mater. Sci.* **2022**, 57, 8687–8700.
109. Han XX, Huang LJ, Wei ZH, Wang YN, Chen HB, Huang CX, et al. Technology and mechanism of enhanced compatibilization of polylactic acid-grafted glycidyl methacrylate. *Ind. Crops Prod.* **2021**, *172*, 114065.
110. Coudane J, Nottelet B, Mouton J, Garric X, Van Den Berghe H. Poly(ε-caprolactone)-Based Graft Copolymers: Synthesis Methods and Applications in the Biomedical Field: A Review. *Molecules* **2022**, *27*, 7339–7368.
111. Hassouna F, Raquez JM, Addiego F, Dubois P, Toniazzo V, Ruch D. New approach on the development of plasticized polylactide (PLA): Grafting of poly(ethylene glycol) (PEG) via reactive extrusion. *Eur. Polym. J.* **2011**, *47*, 2134–2144.
112. Kalelkar PP, Collard DM. Tricomponent Amphiphilic Poly(oligo(ethylene glycol) methacrylate) Brush-Grafted Poly(lactic acid): Synthesis, Nanoparticle Formation, and In Vitro Uptake and Release of Hydrophobic Dyes. *Macromolecules* **2020**, *53*, 4274–4283.
113. Zhu Y, Akagi T, Akashi M. Preparation and characterization of nanoparticles formed through stereocomplexation between enantiomeric poly(γ-glutamic acid)-graft-poly(lactide) copolymers. *Polym. J.* **2012**, *45*, 560–566.
114. Qian WH, Song T, Ye M, Xu PC, Lu GL, Huang XY. PAA-*g*-PLA amphiphilic graft copolymer: synthesis, self-assembly, and drug loading ability. *Polym. Chem.* **2017**, *8*, 4098–4107.
115. Trinh BM, Tadele DT, Mekonnen TH. Robust and high barrier thermoplastic starch – PLA blend films using starch-graft-poly(lactic acid) as a compatibilizer. *Mater. Adv.* **2022**, *3*, 6208–6221.
116. Boonpavanitchakul K, Jarussophon S, Pimpha N, Kangwansupamonkon W, Magaraphan R. Silk sericin as a bio-initiator for grafting from synthesis of polylactide via ring-opening polymerization. *Eur. Polym. J.* **2019**, *121*, 109265.
117. Kang Y, Wang CL, Shi XT, Zhang GC, Chen P, Wang J. Crystallization, rheology behavior, and antibacterial application of graphene oxide-graft -poly (L -lactide)/poly (L -lactide) nanocomposites. *Appl. Surface Sci.* **2018**, *451*, 315–324.
118. Basheer BV, George JJ, Siengchin S, Parameswaranpillai J. Polymer grafted carbon nanotubes—Synthesis, properties, and applications: A review. *Nano-Struct. Nano-Objects* **2020**, *22*, 100429.
119. Jang MG, Lee YK, Kim WN. Influence of lactic acid-grafted multi-walled carbon nanotube (LA-*g*-MWCNT) on the electrical and rheological properties of polycarbonate/poly(lactic acid)/ LA-*g*-MWCNT composites. *Macromol. Res.* **2015**, *23*, 916–923.
120. Campos JM, Ferraria AM, Botelho do Rego AM, Ribeiro MR, Barros-Timmons A. Studies on PLA grafting onto graphene oxide and its effect on the ensuing composite films. *Mater. Chem. Phys.* **2015**, *166*, 122–132.
121. Zhang Y, Deng BY, Liu QS. Rheology and crystallisation of PLA containing PLA-grafted nanosilica. *Plast. Rubber Compos.* **2014**, *43*, 309–314.
122. Wu F, Zhang B, Yang W, Liu ZY, Yang MB. Inorganic silica functionalized with PLLA chains via grafting methods to enhance the melt strength of PLLA/silica nanocomposites. *Polymer* **2014**, *55*, 5760–5772.
123. Lv HX, Song SX, Sun SL, Ren L, Zhang HX. Enhanced properties of poly(lactic acid) with silica nanoparticles. *Polym. Adv. Technol.* **2016**, *27*, 1156–1163.
124. Lai XL, Yang W, Wang Z, Shi DW, Liu ZY, Yang MB. Enhancing crystallization rate and melt strength of PLLA with four-arm PLLA grafted silica: The effect of molecular weight of the grafting PLLA chains. *J. Appl. Polym. Sci.* **2018**, *135*, 45675–45687.
125. Wang B, Zhang X, Zhang LT, Feng YZ, Liu CT, Shen CY. Simultaneously reinforcing and toughening poly(lactic acid) by incorporating reactive melt-functionalized silica nanoparticles. *J. Appl. Polym. Sci.* **2020**, *137*, 48834–48855.
126. Shaikh T, Kaur H. Synthesis and characterization of nanosized polylactic acid/TiO_2 particle brushes by azeotropic dehydration polycondensation of lactic acid. *J. Polym. Res.* **2017**, *25*, 22–41.
127. Shaikh T, Rathore A, Kaur H. Poly (Lactic Acid) Grafting of TiO_2 Nanoparticles: A Shift in Dye Degradation Performance of TiO_2 from UV to Solar Light. *ChemistrySelect* **2017**, *2*, 6901–6908.
128. Xu Q, Huang Z, Ji ST, Zhou J, Shi RZ, Shi WY. Cu_2O nanoparticles grafting onto PLA fibers via electron beam irradiation: bifunctional composite fibers with enhanced photocatalytic of organic pollutants in aqueous and soil systems. *J. Radioanal. Nuclear Chem.* **2019**, *323*, 253–261.
129. Zhou L, He H, Li MC, Huang SW, Mei CT, Wu QL. Enhancing mechanical properties of poly(lactic acid) through its in-situ crosslinking with maleic anhydride-modified cellulose nanocrystals from cottonseed hulls. *Ind. Crops Prod.* **2018**, *112*, 449–459.
130. Mangeon C, Renard E, Thevenieau F, Langlois V. Networks based on biodegradable polyesters: An overview of the chemical ways of crosslinking. *Mater. Sci. Eng. C. Mater. Biol. Appl.* **2017**, *80*, 760–770.
131. Garavand F, Rouhi M, Razavi SH, Cacciotti I, Mohammadi R. Improving the integrity of natural biopolymer films used in food packaging by crosslinking approach: A review. *Int. J. Biol. Macromol.* **2017**, *104*, 687–707.
132. Hennink WE, van Nostrum CF. Novel crosslinking methods to design hydrogels. *Adv. Drug Del. Rev.* **2012**, *64*, 223–236.
133. Bednarek M, Borska K, Kubisa P. New Polylactide-Based Materials by Chemical Crosslinking of PLA. *Polym. Rev.* **2020**, *61*, 493–519.
134. Hao YP, Chen J, Wang F, Liu Y, Ai X, Tian HC. Influence of Crosslinking on Rheological Properties, Crystallization Behavior and Thermal Stability of Poly(lactic acid). *Fibers Polym.* **2022**, *23*, 1763–1769.

135. Pourshooshtar R, Ahmadi Z, Taromi FA. Formation of 3D networks in polylactic acid by adjusting the cross-linking agent content with respect to processing variables: a simple approach. *Iranian Polym. J.* **2018**, *27*, 329–337.
136. Yamoum C, Maia J, Magaraphan R. Rheological and thermal behavior of PLA modified by chemical crosslinking in the presence of ethoxylated bisphenol A dimethacrylates. *Polym. Adv. Technol.* **2017**, *28*, 102–112.
137. Basu A, Kunduru KR, Doppalapudi S, Domb AJ, Khan W. Poly(lactic acid) based hydrogels. *Adv. Drug Deliv. Rev.* **2016**, *107*, 192–205.
138. Chan N, An SY, Oh JK. Dual location disulfide degradable interlayer-crosslinked micelles with extended sheddable coronas exhibiting enhanced colloidal stability and rapid release. *Polym. Chem.* **2014**, *5*, 1637–1649.
139. Borska K, Bednarek M, Pawlak A. Reprocessable polylactide-based networks containing urethane and disulfide linkages. *Eur. Polym. J.* **2021**, *156*, 110636.
140. Rohman G, Lauprêtre F, Boileau S, Guérin P, Grande D. Poly(d,l-lactide)/poly(methyl methacrylate) interpenetrating polymer networks: Synthesis, characterization, and use as precursors to porous polymeric materials. *Polymer* **2007**, *48*, 7017–7028.
141. Quynh TM, Mai HH, Lan PN. Stereocomplexation of low molecular weight poly(L-lactic acid) and high molecular weight poly(D-lactic acid), radiation crosslinking PLLA/PDLA stereocomplexes and their characterization. *Radiat. Phys. Chem.* **2013**, *83*, 105–110.
142. Zhang YY, Wang YT, Wang BJ, Feng XL, Ma BM, Sui XF. Exclusive formation of poly(lactide) stereocomplexes with enhanced melt stability via regenerated cellulose assisted Pickering emulsion approach. *Compos. Commun.* **2022**, *32*, 101138.
143. Izraylit V, Heuchel M, Gould OEC, Kratz K, Lendlein A. Strain recovery and stress relaxation behaviour of multiblock copolymer blends physically cross-linked with PLA stereocomplexation. *Polymer* **2020**, *209*, 122984.
144. Sarath CC, Shanks RA, Thomas S. Polymer Blends. In *Nanostructured Polymer Blends*; William Andrew: Norwich, NY, USA, 2014; pp. 1–14.
145. Nofar M, Sacligil D, Carreau PJ, Kamal MR, Heuzey MC. Poly (lactic acid) blends: Processing, properties and applications. *Int. J. Biol. Macromol.* **2019**, *125*, 307–360.
146. Ajitha AR, Thomas S. Introduction: polymer blends, thermodynamics, miscibility, phase separation, and compatibilization. In *Compatibilization of Polymer Blends*; Elsevier: Oxford, UK, 2020; pp. 1–29.
147. Paul DR. Chapter 12—Interfacial Agents ("Compatibilizers") for Polymer Blends. In *Polymer Blends*; Academic Press: Cambridge, MA, USA, 1978; pp. 35–62.
148. Imre B, Pukánszky B. Compatibilization in bio-based and biodegradable polymer blends. *Eur. Polym. J.* **2013**, *49*, 1215–1233.
149. Hu L, Vuillaume PY. Reactive compatibilization of polymer blends by coupling agents and interchange catalysts. In *Compatibilization of Polymer Blends*; Elsevier: Oxford, UK, 2020; pp. 205–248.
150. Chen K, Li P, Li X, Liao C, Li X, Zuo Y. Effect of silane coupling agent on compatibility interface and properties of wheat straw/polylactic acid composites. *Int. J. Biol. Macromol.* **2021**, *182*, 2108–2116.
151. Rakmae S, Ruksakulpiwat Y, Sutapun W, Suppakarn N. Effect of silane coupling agent treated bovine bone based carbonated hydroxyapatite on in vitro degradation behavior and bioactivity of PLA composites. *Mater. Sci. Eng. C. Mater. Biol. Appl.* **2012**, *32*, 1428–1436.
152. Karakurt I, Ozaltin K, Pistekova H, Vesela D, Michael-Lindhard J, Humpolicek P, et al. Effect of Saccharides Coating on Antibacterial Potential and Drug Loading and Releasing Capability of Plasma Treated Polylactic Acid Films. *Int. J. Mol. Sci.* **2022**, *23*, 8821–8840.
153. Mhiri S, Abid M, Abid S, Prochazka F, Pillon C, Mignard N. Green synthesis of covalent hybrid hydrogels containing PEG/PLA-based thermoreversible networks. *J. Polym. Res.* **2022**, *29*, 328–346.
154. Vachon A, Pépin K, Balampanis E, Veilleux J, Vuillaume PY. Compatibilization of PLA/PEBA Blends via Reactive Extrusion: A Comparison of Different Coupling Agents. *J. Polym. Environ.* **2016**, *25*, 812–827.
155. Oliver-Ortega H, Reixach R, Espinach FX, Mendez JA. Maleic Anhydride Polylactic Acid Coupling Agent Prepared from Solvent Reaction: Synthesis, Characterization and Composite Performance. *Materials* **2022**, *15*, 1161–1178.
156. Meng X, Shi G, Wu C, Chen W, Xin Z, Shi Y, et al. Chain extension and oxidation stabilization of Triphenyl Phosphite (TPP) in PLA. *Polym. Degrad. Stab.* **2016**, *124*, 112–118.
157. Punyodom W, Meepowpan P, Girdthep S, Limwanich W. Influence of tin(II), aluminum(III) and titanium(IV) catalysts on the transesterification of poly(L-lactic acid). *Polym. Bull.* **2022**, *79*, 11409–11429.
158. Zhou L, Zhao G, Jiang W. Effects of Catalytic Transesterification and Composition on the Toughness of Poly(lactic acid)/Poly(propylene carbonate) Blends. *Ind. Eng. Chem. Res.* **2016**, *55*, 5565–5573.
159. Matta AK, Rao RU, Suman KNS, Rambabu V. Preparation and Characterization of Biodegradable PLA/PCL Polymeric Blends. *Procedia Mater. Sci.* **2014**, *6*, 1266–1270.
160. Haneef INHM, Buys YF, Shaffiar NM, Shaharuddin SIS, Nor Khairusshima MK. Miscibility, mechanical, and thermal properties of polylactic acid/polypropylene carbonate (PLA/PPC) blends prepared by melt-mixing method. *Mater. Today Proc.* **2019**, *17*, 534–542.
161. Zhao XP, Liu JC, Li JC, Liang XY, Zhou WY, Pe SX. Strategies and techniques for improving heat resistance and mechanical performances of poly(lactic acid) (PLA) biodegradable materials. *Int. J. Biol. Macromol.* **2022**, *218*, 115–134.
162. Fortelny I, Ujcic A, Fambri L, Slouf M. Phase Structure, Compatibility, and Toughness of PLA/PCL Blends: A Review. *Front. Mater.* **2019**, *6*, 206.
163. Musa L, Krishna Kumar N, Abd Rahim SZ, Mohamad Rasidi MS, Watson Rennie AE, Rahman R, et al. A review on the potential of polylactic acid based thermoplastic elastomer as filament material for fused deposition modelling. *J. Mater. Res. Technol.* **2022**, *20*, 2841–2858.

164. Yuryev Y, Mohanty AK, Misra M. Hydrolytic stability of polycarbonate/poly(lactic acid) blends and its evaluation via poly(lactic) acid median melting point depression. *Polym. Degrad. Stab.* **2016**, *134*, 227–236.
165. Yuryev Y, Mohanty AK, Misra M. Novel biocomposites from biobased PC/PLA blend matrix system for durable applications. *Compos. Part B Eng.* **2017**, *130*, 158–166.
166. Gigante V, Aliotta L, Coltelli MB, Lazzeri A. Upcycling of Poly(Lactic Acid) by Reactive Extrusion with Recycled Polycarbonate: Morphological and Mechanical Properties of Blends. *Polymers* **2022**, *14*, 5058–5072.
167. Ma X, Yu J, Wang N. Compatibility characterization of poly(lactic acid)/poly(propylene carbonate) blends. *J. Polym. Sci. Part B Polym. Phys.* **2006**, *44*, 94–101.
168. Wang Z, Lai XL, Zhang M, Yang W, Yang MB. Synthesis of an Efficient Processing Modifier Silica-*g*-poly(lactic acid)/poly(propylene carbonate) and Its Behavior for Poly(lactic acid)/Poly(propylene carbonate) Blends. *Ind. Eng. Chem. Res.* **2017**, *56*, 14704–14715.
169. Song LX, Li YC, Meng XY, Wang T, Shi Y, Wang YX, et al. Crystallization, Structure and Significantly Improved Mechanical Properties of PLA/PPC Blends Compatibilized with PLA-PPC Copolymers Produced by Reactions Initiated with TBT or TDI. *Polymers* **2021**, *13*, 3245–3262.
170. Wang X, Wu S. Toughening of PLA with PPC. *China Plast. Ind.* **2012**, *40*, 26–28,41.
171. Li JQ, He HZ, Zhu ZW, Xu MH, Gao JF, Gu Q, Tan B. Unique Morphology of Polylactide/Poly(ε-Caprolactone) Blends Extruded by Eccentric Rotor Extruder. *J. Polym. Environ.* **2022**, *30*, 4252–4262.
172. Patrício T, Bártolo P. Thermal Stability of PCL/PLA Blends Produced by Physical Blending Process. *Procedia Eng.* **2013**, *59*, 292–297.
173. Van de Voorde KM, Pokorski JK, Korley LTJ. Exploring Morphological Effects on the Mechanics of Blended Poly(lactic acid)/Poly(ε-caprolactone) Extruded Fibers Fabricated Using Multilayer Coextrusion. *Macromolecules* **2020**, *53*, 5047–5055.
174. Wang B, Ye X, Wang BW, Li XP, Xiao SL, Liu HS. Reactive graphene as highly efficient compatibilizer for cocontinuous poly(lactic acid)/poly(ε-caprolactone) blends toward robust biodegradable nanocomposites. *Compos. Sci. Technol.* **2022**, *221*, 109326.
175. do Patrocinio Dias P, Aparecido Chinelatto M. Effect of Poly(ε-caprolactone-*b*-tetrahydrofuran) Triblock Copolymer Concentration on Morphological, Thermal and Mechanical Properties of Immiscible PLA/PCL Blends. *J. Renew. Mater.* **2019**, 7, 129–138.
176. Wang P, Gao S, Chen XL, Yang L, Cao T, Fan BY, et al. Effect of PCL-*b*-PEG Oligomer Containing Ionic Elements on Phase Interfacial Properties and Aggregated Structure of PLA/PCL Blends. *Macromol. Res.* **2022**, *30*, 438–445.
177. Naser AZ, Deiab I, Darras BM. Poly(lactic acid) (PLA) and polyhydroxyalkanoates (PHAs), green alternatives to petroleum-based plastics: A review. *RSC Adv.* **2021**, *11*, 17151–17196.
178. Vigil Fuentes MA, Thakur S, Wu F, Misra M, Gregori S, Mohanty AK. Study on the 3D printability of poly(3-hydroxybutyrate-co-3-hydroxyvalerate)/poly(lactic acid) blends with chain extender using fused filament fabrication. *Sci. Rep.* **2020**, *10*, 11804.
179. Hu X, Su T, Li P, Wang Z. Blending modification of PBS/PLA and its enzymatic degradation. *Polym. Bull.* **2017**, *75*, 533–546.
180. Jem KJ, Tan B. The development and challenges of poly (lactic acid) and poly (glycolic acid). *Adv. Ind. Eng. Polym. Res.* **2020**, *3*, 60–70.
181. Ramdhanie LI, Aubuchon SR, Boland ED, Knapp DC, Barnes CP, Simpson DG, et al. Thermal and Mechanical Characterization of Electrospun Blends of Poly(lactic acid) and Poly(glycolic acid). *Polym. J.* **2006**, *38*, 1137–1145.
182. Sheth M, Kumar RA, Davé V, Gross RA, McCarthy SP. Biodegradable Polymer Blends of Poly(lactic acid) and Poly(ethylene glycol). *J. Appl. Polym. Sci.* **1997**, *66*, 1495–1505.
183. Nazari T, Garmabi H. Polylactic acid/polyethylene glycol blend fibres prepared via melt electrospinning: effect of polyethylene glycol content. *Micro Nano Lett.* **2014**, *9*, 686–690.
184. Vrandečić NS, Erceg M, Jakić M, Klarić I. Kinetic analysis of thermal degradation of poly(ethylene glycol) and poly(ethylene oxide)s of different molecular weight. *Thermochim. Acta* **2010**, *498*, 71–80.
185. Kong WL, Tong BB, Ye AL, Ma RX, Gou JM, Wang YM, et al. Crystallization behavior and mechanical properties of poly(lactic acid)/poly(ethylene oxide) blends nucleated by a self-assembly nucleator. *J. Therm. Anal. Calorimetry* **2018**, *135*, 3107–3114.
186. Diaz A, Katsarava R, Puiggali J. Synthesis, properties and applications of biodegradable polymers derived from diols and dicarboxylic acids: from polyesters to poly(ester amide)s. *Int. J. Mol. Sci.* **2014**, *15*, 7064–7123.
187. Nifant'ev IE, Bagrov VV, Komarov PD, Ilyin SO, Ivchenko PV. The Use of Branching Agents in the Synthesis of PBAT. *Polymers* **2022**, *14*, 1720–1736.
188. Li RY, Wu LB, Li BG. Poly(L-lactide)/PEG-mb-PBAT blends with highly improved toughness and balanced performance. *Eur. Polym. J.* **2018**, *100*, 178–186.
189. Neng WB, Xie WG, Lu B, Zhen ZC, Zhao JL, Wang GX, et al. Biodegradable thermoplastic copolyester elastomers: Methyl branched PBAmT. *e-Polymers* **2021**, *21*, 336–345.
190. Nifant'ev IE, Bagrov VV, Komarov PD, Ovchinnikova VI, Ivchenko PV. Aryloxy 'biometal' complexes as efficient catalysts for the synthesis of poly(butylene adipate terephthalate). *Mendeleev Commun.* **2022**, *32*, 351–353.
191. Ye SX, Xiang XQ, Wang SJ, Han DM, Xiao M, Meng YZ. Nonisocyanate CO_2-Based Poly(ester-co-urethane)s with Tunable Performances: A Potential Alternative to Improve the Biodegradability of PBAT. *ACS Sustain. Chem. Eng.* **2020**, *8*, 1923–1932.
192. Mahata D, Cherian A, Parab A, Gupta V. In situ functionalization of poly(butylene adipate-co-terephthalate) polyester with a multi-functional macromolecular additive. *Iranian Polym. J.* **2020**, *29*, 1045–1055.

193. Ding Y, Lu B, Wang PL, Wang GX, Ji JH. PLA-PBAT-PLA tri-block copolymers: Effective compatibilizers for promotion of the mechanical and rheological properties of PLA/PBAT blends. *Polym. Degrad. Stab.* **2018**, *147*, 41–48.
194. Sun Z, Zhang B, Bian X, Feng L, Zhang H, Duan R, et al. Synergistic effect of PLA–PBAT–PLA tri-block copolymers with two molecular weights as compatibilizers on the mechanical and rheological properties of PLA/PBAT blends. *RSC Adv.* **2015**, *5*, 73842–73849.
195. Kashani Rahimi S, Aeinehvand R, Kim K, Otaigbe JU. Structure and Biocompatibility of Bioabsorbable Nanocomposites of Aliphatic-Aromatic Copolyester and Cellulose Nanocrystals. *Biomacromolecules* **2017**, *18*, 2179–2194.
196. Wu CS. Antibacterial and static dissipating composites of poly(butylene adipate-co-terephthalate) and multi-walled carbon nanotubes. *Carbon* **2009**, *47*, 3091–3098.
197. Wu CS. Aliphatic-aromatic polyester-polyaniline composites: preparation, characterization, antibacterial activity and conducting properties. *Polym. Int.* **2012**, 61, 1556–1563.
198. Wu CS, Liao HT. Antibacterial activity and antistatic composites of polyester/Ag-SiO_2 prepared by a sol-gel method. *J. Appl. Polym. Sci.* **2011**, *121*, 2193–2201.
199. Wu CS. Utilization of peanut husks as a filler in aliphatic–aromatic polyesters: Preparation, characterization, and biodegradability. *Polym. Degrad. Stab.* **2012**, *97*, 2388–2395.
200. Wu CS. Characterization of cellulose acetate-reinforced aliphatic–aromatic copolyester composites. *Carbohydr. Polym.* **2012**, *87*, 1249–1256.
201. Liu WC, Liu T, Liu H, Xin J, Zhang JW, Muhidinov ZK, et al. Properties of poly(butylene adipate-co-terephthalate) and sunflower head residue biocomposites. *J. Appl. Polym. Sci.* **2017**, *134*, 44644.
202. Wang HT, Wang JM, Wu TM. Synthesis and characterization of biodegradable aliphatic–aromatic nanocomposites fabricated using maleic acid-grafted poly[(butylene adipate)-co-terephthalate] and organically modified layered zinc phenylphosphonate. *Polym. Int.* **2019**, *68*, 1531–1537.
203. Wang HT, Chen EC, Wu TM. Crystallization and Enzymatic Degradation of Maleic Acid-Grafted Poly(butylene adipate-co-terephthalate)/Organically Modified Layered Zinc Phenylphosphonate Nanocomposites. *J. Polym. Environ.* **2020**, *28*, 834–843.
204. Hung YJ, Chiang MY, Wang ET, Wu TM. Synthesis, Characterization, and Physical Properties of Maleic Acid-Grafted Poly(butylene adipate-co-terephthalate)/ Cellulose Nanocrystal Composites. *Polymers* **2022**, *14*, 2742.
205. Niu DY, Xu PW, Sun ZY, Yang WJ, Dong WF, Ji Y, et al. Superior toughened bio-compostable Poly(glycolic acid)-based blends with enhanced melt strength via selective interfacial localization of in-situ grafted copolymers. *Polymer* **2021**, *235*, 124269.
206. Raquez JM, Nabar Y, Narayan R, Dubois P. In situ compatibilization of maleated thermoplastic starch/polyester melt-blends by reactive extrusion. *Polym. Eng. Sci.* **2008**, *48*, 1747–1754.
207. Xiao MM, Pan YF, Xiao HN. Preparation and Properties of Compatibilized Poly(Butylenesadipate-Co-Terephalate)/Thermoplastic Starch Blends. *Appl. Mech. Mater.* **2014**, *556–562*, 15–18.
208. Hwang IT, Jung CH, Kuk IS, Choi JH, Nho YC. Electron beam-induced crosslinking of poly(butylene adipate-co-terephthalate). *Nuclear Instr. Methods Phys. Res. Sect. B Beam Interact. Mater. Atoms* **2010**, *268*, 3386–3389.
209. Choi JH, Jung CH, Hwang IT, Choi JH. Preparation and characterization of crosslinked poly(butylene adipate-co-terephthalate)/polyhedral oligomeric silsesquioxane nanocomposite by electron beam irradiation. *Radiat. Phys. Chem.* **2013**, *82*, 100–105.
210. Malinowski R, Janczak K, Moraczewski K, Raszkowska-Kaczor A. Analysis of swelling degree and gel fraction of polylactide/poly(butylene adipate-co-terephthalate) blends crosslinked by radiation. *Polimery* **2018**, *63*, 25–30.
211. Wang B, Jin Y, Kang K, Yang N, Weng Y, Huang Z, Men S. Investigation on compatibility of PLA/PBAT blends modified by epoxy-terminated branched polymers through chemical micro-crosslinking. *e-Polymers* **2020**, *20*, 39–54.
212. Nishida M, Ichihara H, Watanabe H, Fukuda N, Ito H. Improvement of dynamic tensile properties of Poly(lactic acid)/Poly(butylene adipate-co-terephthalate) polymer alloys using a crosslinking agent and observation of fracture surfaces. *Int. J. Impact Eng.* **2015**, *79*, 117–125.
213. Ai X, Li X, Yu YL, Pan HW, Yang J, Wang DM, et al. The Mechanical, Thermal, Rheological and Morphological Properties of PLA/PBAT Blown Films by Using Bis(tert-butyl dioxy isopropyl) Benzene as Crosslinking Agent. *Polym. Eng. Sci.* **2019**, *59*, 227–236.
214. Wang LF, Rhim JW, Hong SI. Preparation of poly(lactide)/poly(butylene adipate-*co*-terephthalate) blend films using a solvent casting method and their food packaging application. *LWT Food Sci. Technol.* **2016**, *68*, 454–461.
215. Xiao HW, Lu W, Yeh JT. Crystallization behavior of fully biodegradable poly(lactic acid)/poly(butylene adipate-*co*-terephthalate) blends. *J. Appl. Polym. Sci.* **2009**, *112*, 3754–3763.
216. Jalali Dil E, Carreau PJ, Favis BD. Morphology, miscibility and continuity development in poly(lactic acid)/poly(butylene adipate-*co*-terephthalate) blends. *Polymer* **2015**, *68*, 202–212.
217. Deng YX, Yu CY, Wongwiwattana P, Thomas NL. Optimising Ductility of Poly(Lactic Acid)/Poly(Butylene Adipate-*co*-Terephthalate) Blends through Co-continuous Phase Morphology. *J. Polym. Environ.* **2018**, *26*, 3802–3816.
218. Ding Y, Feng WT, Lu B, Wang PL, Wang GX, Ji J. PLA-PEG-PLA tri-block copolymers: Effective compatibilizers for promotion of the interfacial structure and mechanical properties of PLA/PBAT blends. *Polymer* **2018**, *146*, 179–187.
219. Ding Y, Feng WT, Huang D, Lu B, Wang PL, Wang GX, et al. Compatibilization of immiscible PLA-based biodegradable polymer blends using amphiphilic di-block copolymers. *Eur. Polym. J.* **2019**, *118*, 45–52.
220. Sui XY, Zhao XY, Wang ZC, Sun SL. Super-ductile and stiff PBAT/PLA biodegradable composites balanced with random PMMA-*co*-GMA copolymer as compatibilizer. *Polym. Int.* **2022**, *72*, 333–341.

221. Shanks RA. Concepts and classification of compatibilization processes. *Compatibiliz. Polym. Blends.* **2020**, *2*, 31–56.
222. Wu DD, Guo Y, Huang AP, Xu RW, Liu P. Effect of the multi-functional epoxides on the thermal, mechanical and rheological properties of poly(butylene adipate-co-terephthalate)/polylactide blends. *Polym. Bull.* **2020**, *78*, 5567–5591.
223. Wang P, Gao S, Chen XL, Yang L, Wu XS, Feng SJ, et al. Effect of hydroxyl and carboxyl-functionalized carbon nanotubes on phase morphology, mechanical and dielectric properties of poly(lactide)/poly(butylene adipate-co-terephthalate) composites. *Int. J. Biol. Macromol.* **2022**, *206*, 661–669.
224. Han Y, Shi JW, Mao LX, Wang Z, Zhang LQ. Improvement of Compatibility and Mechanical Performances of PLA/PBAT Composites with Epoxidized Soybean Oil as Compatibilizer. *Ind. Eng. Chem. Res.* **2020**, *59*, 21779–21790.
225. Gupta A, Lolic L, Mekonnen TH. Reactive extrusion of highly filled, compatibilized, and sustainable PHBV/PBAT – Hemp residue biocomposite. *Compos. Part A Appl. Sci. Manuf.* **2022**, *156*, 106885.
226. Sousa FM, Costa ARM, Reul LTA, Cavalcanti FB, Carvalho LH, Almeida TG, et al. Rheological and thermal characterization of PCL/PBAT blends. *Polym. Bull.* **2018**, *76*, 1573–1593.
227. Pagno V, Módenes AN, Dragunski DC, Fiorentin-Ferrari LD, Caetano J, Guellis C, et al. Heat treatment of polymeric PBAT/PCL membranes containing activated carbon from Brazil nutshell biomass obtained by electrospinning and applied in drug removal. *J. Environ. Chem. Eng.* **2020**, *8*, 104159.
228. Muthuraj R, Misra M, Mohanty AK. Biodegradable Poly(butylene succinate) and Poly(butylene adipate-co-terephthalate) Blends: Reactive Extrusion and Performance Evaluation. *J. Polym. Environ.* **2014**, *22*, 336–349.
229. Wei XY, Ren L, Sun YN, Zhang XY, Guan XF, Zhang MY, et al. Sustainable composites from biodegradable poly(butylene succinate) modified with thermoplastic starch and poly(butylene adipate-co-terephthalate): preparation and performance. *New J. Chem.* **2021**, *45*, 17384–17397.
230. Jang MO, Kim SB, Nam BU. Transesterification effects on miscibility polycarbonate/poly(butylene adipate-co-terephthalate) blends. *Polym. Bull.* **2011**, *68*, 287–298.
231. Liu ZR, Hu JJ, Gao FX, Cao H, Zhou QH, Wang XH. Biodegradable and resilient poly (propylene carbonate) based foam from high pressure CO_2 foaming. *Polym. Degrad. Stab.* **2019**, *165*, 12–19.
232. Jiang G, Li HL, Wang F. Structure of PBAT/PPC blends prepared by *in-situ* reactive compatibilization and properties of their blowing films. *Mater. Today Commun.* **2021**, *27*, 102215.
233. Mohammadi Nafchi A, Moradpour M, Saeidi M, Alias AK. Thermoplastic starches: Properties, challenges, and prospects. *Starch Stärke* **2013**, *65*, 61–72.
234. Zhai XS, Zhang R, Wang WT, Xue HH. Relationship between phase morphologies and mechanical properties of thermoplastic starch/poly(butylene adipate-co-terephthalate) composite films prepared by extrusion blowing. *Int. J. Biol. Macromol.* **2022**, *224*, 1356–1360.
235. Yimnak K, Thipmanee R, Sane A. Poly(butylene adipate-co-terephthalate)/thermoplastic starch/zeolite 5A films: Effects of compounding sequence and plasticizer content. *Int. J. Biol. Macromol.* **2020**, *164*, 1037–1045.
236. Bai J, Pei HJ, Zhou XP, Xie XL. Reactive compatibilization and properties of low-cost and high-performance PBAT/thermoplastic starch blends. *Eur. Polym. J.* **2021**, *143*, 110198.
237. Leelaphiwat P, Pechprankan C, Siripho P, Bumbudsanpharoke N, Harnkarnsujarit N. Effects of nisin and EDTA on morphology and properties of thermoplastic starch and PBAT biodegradable films for meat packaging. *Food Chem.* **2022**, *369*, 130956.
238. Kargarzadeh H, Galeski A, Pawlak A. PBAT green composites: Effects of kraft lignin particles on the morphological, thermal, crystalline, macro and micromechanical properties. *Polymer* **2020**, *203*, 122748.
239. Xiao LQ, Yao Z, He YB, Han Z, Zhang XJ, Li CC, et al. Antioxidant and antibacterial PBAT/lignin-ZnO nanocomposite films for active food packaging. *Ind. Crops Prod.* **2022**, *187*, 115515.
240. Nunes EdCD, de Souza AG, Rosa DdS. Use of a chain extender as a dispersing agent of the $CaCO_3$ into PBAT matrix. *J. Compos. Mater.* **2019**, 54, 1373–1382.
241. Zhang T, Zhang CL, Yang Y, Yang F, Zhao M, Weng YX. Improved properties of poly(butylene adipate-co-terephthalate)/calcium carbonate films through silane modification. *J. Appl. Polym. Sci.* **2021**, *138*, 50970–50980.
242. Diao X, Zhang C, Weng Y. Properties and Degradability of Poly(Butylene Adipate-Co-Terephthalate)/Calcium Carbonate Films Modified by Polyethylene Glycol. *Polymers* **2022**, 14, 484–496.
243. Helanto K, Talja R, Rojas OJ. Effects of talc, kaolin and calcium carbonate as fillers in biopolymer packaging materials. *J. Polym. Eng.* **2021**, *41*, 746–758.
244. Zhang RQ, Han WJ, Jiang HJ, Wang XF, Wang B, Liu CT, et al. PBAT/MXene monolithic solar vapor generator with high efficiency on seawater evaporation and swage purification. *Desalination* **2022**, *541*, 116015.
245. Bheemaneni G, Saravana S, Kandaswamy R. Processing and Characterization of Poly (butylene adipate-co-terephthalate) / Wollastonite Biocomposites for Medical Applications. *Mater. Today Proc.* **2018**, *5*, 1807–1816.
246. Balbinot GS, Bahlis E, Visioli F, Leitune VCB, Soares RMD, Collares FM. Polybutylene-adipate-terephthalate and niobium-containing bioactive glasses composites: Development of barrier membranes with adjusted properties for guided bone regeneration. *Mater. Sci. Eng. C. Mater. Biol. Appl.* **2021**, *125*, 112115.